UNIVERSITY OF CALGARY

# The role of *mei-2* in *Caenorhabditis elegans* meiosis

by

Martin Anthony Srayko

A DISSERTATION

SUBMITTED TO THE FACULTY OF GRADUATE STUDIES IN

PARTIAL FULFILLMENT OF THE REQUIREMENTS FOR THE

DEGREE OF DOCTOR OF PHILOSOPHY

DEPARTMENT OF BIOCHEMISTRY AND MOLECULAR BIOLOGY

CALGARY, ALBERTA

AUGUST, 2000

# Abstract

The *mei-1* and *mei-2* genes of *C. elegans* are required for the establishment of the oocyte's meiotic spindle. The *mei-1* gene encodes an AAA (ATPase associated with various cellular activities) family member with similarity to the p60 subunit of the sea urchin microtubule-severing protein, katanin. *mei-2* was identified through a combination of genetic mapping and RNA-mediated interference (RNAi). The *mei-2* transcript encodes a 280 amino acid protein containing a region similar to the p80 subunit of katanin. Based on indirect-immunofluorescence experiments, MEI-2 expression was first apparent in the cytoplasm of mature oocytes. In fertilized embryos, MEI-2 antiserum decorated the meiotic spindle poles, condensed meiotic chromatin, condensed sperm pronucleus, and polar bodies from both meiotic divisions. Meiotic spindles were disorganised in all *mei-2* mutants, with the strongest alleles resulting in an amorphous mass of microtubules surrounding the meiotic chromatin. MEI-1 and MEI-2 depend on one another for their subcellular location during meiosis. Furthermore, mutations that cause ectopic MEI-1 staining of the mitotic spindle and chromosomes also cause ectopic MEI-2 staining of the same structures. Therefore, MEI-1 and MEI-2 likely work together during meiotic spindle formation. Yeast two-hybrid experiments

indicate that MEI-1 and MEI-2 can associate with each other. In addition, MEI-1 interacts with MEL-26, a protein implicated in negatively regulating MEI-1 during mitosis. In light of their similarities to katanin p60/p80, MEI-1 and MEI-2 likely form a complex during meiosis that functions to restrict the length of meiotic spindle microtubules. MEL-26 may associate with MEI-1 during mitosis to inactivate or dissociate the putative MEI-1/MEI-2 complex.

# Acknowledgments

I thank my supervisor Dr. Paul Mains for guidance and support throughout the course of this work; my supervisory committee members Dr. Jim McGhee, Dr. Fred Lohka, and Dr. J. B. Rattner for their advice and constructive comments over the years; members of the Mains and McGhee laboratories for stimulating discussions and advice; and Dr. Cairine Logan and Dr. Lynne Quarmby for serving as external examiners.

This work was supported by a studentship award from the Alberta Heritage Foundation for Medical Research.

*for*
*Glenis*

# Table of Contents

# List of Tables

# List of Figures

# List of Abbreviations

| | |
|---|---|
| AAA | ATPase associated with various cellular activities |
| *bli* | blistered |
| cDNA | complementary DNA |
| cM | centimorgans |
| *daf* | dauer formation defective |
| DAPI | 4',6-diamidine-2'-phenylindole dihydrochloride |
| *Df* | chromosomal deficiency |
| *dn* | dominant-negative |
| *Dp* | chromosomal duplication |
| *dpy* | dumpy |
| dsRNA | double stranded RNA |
| *fem* | feminized |
| *gf* | gain-of-function |
| GFP | green fluorescent protein |
| *glp* | germline proliferation defective |
| GST | glutathione S-transferase |
| *him* | high incidence of males |
| HRP | horse radish peroxidase |
| kb | kilobase |
| kDa | kilodalton |
| KRP | kinesin-related protein |
| *let* | lethal |
| *lf* | loss-of-function |
| *lin* | lineage defective |

| | |
|---|---|
| *lon* | long |
| *mec* | mechanosensory defective |
| *mei* | meiosis defective |
| *mel* | maternal-effect lethal |
| PAGE | polyacrylamide gel electrophoresis |
| PBS | phosphate-buffered saline |
| PCR | polymerase chain reaction |
| RNAi | RNA-mediated interference |
| *rol* | roller |
| RT-PCR | reverse transcriptase PCR |
| SDS | sodium dodecyl sulfate |
| SL | spliced leader sequence |
| SPB | spindle pole body |
| *tbb* | tubulin, beta |
| *ts* | temperature-sensitive |
| *unc* | uncoordinated |
| UTR | untranslated region |
| *zyg* | zygote defective |

# Introduction

Sexually reproducing eukaryotes arise from a single diploid cell, the result of fusion between two haploid cells, usually in the form of sperm and egg. This single cell divides mitotically to create a diploid organism that eventually produces haploid gametes via the process of meiosis to complete the reproductive cycle. Although the ability of higher eukaryotic cells to switch between haploid and diploid life is of great importance, we understand very little about the mechanisms by which these events are regulated. An essential result of both meiosis and mitosis is that chromosomes segregate from each other with high fidelity. The segregation of homologous chromosomes occurs during meiosis I and the segregation of sister chromatids occurs during meiosis II and mitosis.

At the heart of chromosome segregation is the bipolar spindle, a specialized microtubule-based structure that provides a structural framework for the forces involved in physically separating chromosomes. Although many aspects of spindle function during meiosis and mitosis are similar, the respective spindles that carry out these processes have some unique features. In most animals, mitotic spindles are organised by two diametrically opposed centrosomes (Schatten, 1994; Merdes and Cleveland, 1997). Microtubules

emanate from the centrosomes in all directions; some contact the inner cell cortex (astral microtubules) and others contact the chromosomes (kinetochore microtubules) or microtubules from the opposite pole (polar microtubules). This arrangement results in the formation of a bipolar spindle that is capable of withstanding the forces exerted by chromosomal movement, as well as those involved in spindle rotation.

For most animals, female meiotic spindles form in the absence of centrosomes (Sawada and Schatten, 1988; Theurkauf and Hawley, 1992; Gard, 1992; Albertson and Thomson, 1993). Instead of nucleating from centrosomes as in mitosis, microtubules initially form around the meiotic chromatin (Tournebize *et al.*, 1997). These microtubules are subsequently organised from the "inside out", likely by chromatin-associated, plus end-directed motor proteins [*e.g.*, chromokinesin (Wang and Adler, 1995), *Xenopus* Xklp1 (Vernos *et al.*, 1995; Walczak *et al.*, 1998) or *Drosophila* Nod (Afshar *et al.*, 1995); see below], which have been implicated in pushing microtubule minus ends away from chromatin. The radially symmetric microtubule array is then focused into two opposing poles, likely by minus end-directed motors with microtubule tethering properties [*e.g.*, Eg5 (Walczak *et al.*, 1998) or *Drosophila* Ncd (Matthies *et al.*, 1996)]. Therefore, chromatin and various motor proteins are important factors in establishing the bipolarity of acentrosomal spindles. However, it should be noted that many microtubule motor proteins, including those mentioned above, have also been implicated in the formation of bipolar

spindles in centrosomal environments (reviewed in Merdes and Cleveland, 1997; also see Walczak *et al.*, 1998). The fact that there are great differences in the morphology, position, and size of meiotic and mitotic spindles suggests that at least some components should be specific. A survey of some of the spindle components involved in the assembly of bipolar spindles is presented below. This thesis contributes to our understanding of how meiotic spindles differ from mitotic spindles, and suggests that the centrosome is not the only factor that distinguishes these two types of spindles.

## Microtubule structure and dynamics

Microtubules are long rigid polymers that form the backbone of the spindle apparatus. They are constructed from globular tubulin molecules, each of which is a heterodimer consisting of α- and β-tubulin subunits. A vast number of different forms of tubulin are possible, from long strings of single αβ repeats (protofilaments), to tubulin sheets, where the α and β tubulin subunits adopt a checkerboard arrangement. Although these conformations form readily *in vitro* and are useful for analysis of molecules that bind to microtubules, the predominant structure *in vivo*, as its name implies, is a tube.

Most naturally occurring microtubules consist of 13 protofilaments, giving a cylinder with a cross-sectional radius of thirteen tubulin subunits (Tilney *et al.*, 1973). In *C. elegans*, the majority of microtubules have only 9-11

protofilaments (Aamodt and Culotti, 1986), although a subset of ciliated neurons contain 13 and the touch receptor neurons contain 15 protofilaments (Chalfie and Thomson, 1982). Within the microtubule, each protofilament is sandwiched between two other protofilaments, all arranged in parallel, with the heterodimeric structure of tubulin accounting for the intrinsic polarity of the microtubule. For example, the protofilament "βα,βα,..." binds to "βα,βα,...", and not "αβ,αβ,...", thus giving the whole microtubule a βα,βα polarity. Although there is considerable debate over which subunit of the pair is the minus end-most subunit, recent evidence favors β (Wolf *et al.*, 1996; Amos and Hirose, 1997).

The polarized structure of microtubules is also reflected in the different rates at which tubulin polymerizes at each end. The fast growing, or "plus" end, can polymerize tubulin at approximately three times the rate of the "minus" end. However, the plus end is subject to the occasional rapid depolymerization (a catastrophe). This process has been termed dynamic instability (Mitchison and Kirschner, 1984) and, as described below, is crucial to the function of microtubule-based structures such as the mitotic spindle.

The structure of a growing microtubule is different from one that is undergoing a catastrophe (reviewed in Hyman and Karsenti, 1996). At the plus end of a growing microtubule, the tube is split open along the longitudinal axis, giving a slightly flared two-dimensional sheet at the tip. This suggests

that microtubules initially form as sheets that eventually close into tubes, with closure lagging behind but traveling in the same direction as the growing tip. Observations of microtubules in *Xenopus* extracts are also consistent with this model (Arnal *et al.*, 2000). Once the seam catches up with the end of the tube, a catastrophe is initiated and tubulin subunits rapidly peel off the end (Simon and Salmon, 1990; Crétien *et al.*, 1995; Tran *et al.*, 1997; Müller-Reichert *et al.*, 1998). It is not understood how this occurs, but it may involve hydrolysis of GTP. GTP binds to the α and β subunit of the tubulin heterodimer. The GTP-β is hydrolyzed to GDP-β after binding to another heterodimer's α subunit. This hydrolysis does not occur concomitantly with the actual binding of tubulin heterodimers, but is delayed. It has been proposed that GTP-tubulin hydrolyzes to GDP-tubulin only upon closure of the tube, thus accounting for the delay (Hyman and Karsenti, 1996). Whether the hydrolysis of GTP causes the tube closure or is a result thereof has yet to be determined. A recent model suggests that closure of the microtubule end results in a metastable intermediate that can either grow or shrink, depending on its GTP state (Arnal *et al.*, 2000). The energy from GTP hydrolysis could be used to maintain lateral interactions between protofilaments within the tube. The tubulin dimer is intrinsically curved, which causes individual protofilaments to bend away from the centre of the tube (Hyman *et al.*, 1995; Tran *et al.*, 1997; Müller-Reichert *et al.*, 1998). This outward physical stress could be the primary force involved in

the collapse of depolymerizing microtubules. The closure reaction may channel potential energy within the tube wall toward an end-directed collapse of the microtubule. The flared tip of a growing microtubule may provide a barrier to this collapse by easing the physical stress on lateral associations between protofilaments.

The growth and shrinkage of microtubules, and the factors that affect this property are crucial for spindle formation. Microtubules growing out from a nucleating centrosome become stabilized if they contact a kinetochore, but rapidly depolymerize and shrink back to their point of origin at some time if they do not make contact (reviewed in Inou'e, 1997; Andersen, 1999). This stabilization does not completely prevent the microtubule from depolymerizing, except that the microtubule is not allowed to retract once captured by the kinetochore and that depolymerization seems to be more regulated. Therefore, the kinetochore allows exchange of tubulin subunits concurrent with microtubule motor movement. This may be accomplished if the motor proteins contact the microtubule at a position somewhat proximal to the very tip of the plus end (Hyman and Karsenti, 1996). During growth, the open protofilament sheet may promote plus end-directed motors to move the chromosome toward this open end resulting in anti-poleward motion. Upon depolymerization, the force produced by the peeling off of subunits may, in addition to minus end-directed motors, propel the chromosome toward the pole.

By allowing microtubules to incorporate tubulin that has been covalently attached to a photoactivatable fluorochrome, it has been possible to determine the fate of tubulin subunits within the seemingly stable kinetochore microtubules (Sawin and Mitchison, 1991). Surprisingly, the incorporated tubulin gradually migrates toward the spindle pole, a phenomenon termed microtubule flux, to distinguish this dynamic behaviour from polymerization-depolymerization. This implies that subunits are continually being added to the plus end and subtracted from the minus end in the kinetochore microtubules. Therefore, it is unlikely that microtubules simply abut the kinetochore or centrosomal surface; each end must be free to exchange tubulin.

Microtubule motors may also couple the depolymerization of microtubules to poleward movement in the absence of ATP (Lombillo *et al.*, 1995). For instance, the energy stored in the tube structure itself (due to GTP hydrolysis) may be harnessed to propel chromosomes upon depolymerization. In order to regulate chromosome movement, depolymerization of microtubules would have to be regulated. Interestingly, a kinetochore-associated microtubule motor protein has been implicated in this process. When this protein, XKCM1 (*Xenopus* kinesin central motor 1) is immuno-depleted, the frequency of microtubule catastrophes is dramatically reduced (Walczak *et al.*, 1996b). The depolymerization by XKCM1 is not coupled to motor movement; rather, the protein can bind directly to either end of the microtubule (Desai *et*

*al.*, 1999). The *in vivo* role of this protein is currently unknown, but it may serve to increase microtubule catastrophes during mitosis (Walczak, 2000).

**Chromatin and centrosomes**

Chromatin lacking kinetochores can also promote microtubule growth by reducing the number of catastrophes and increasing the frequency of catastrophe-to-growth phase switching. Particularly interesting is that this effect of chromatin does not require direct contact, but can act at a distance (Dogterom *et al.*, 1996). Therefore, some substance that is normally associated with or near chromatin may allow probing microtubules to "find" chromosomes. Stathmin/Op18, a microtubule destabilizing agent, may be involved in this effect of chromatin (reviewed in McNally, 1999; Walczak, 2000). Op18 is inactive when phosphorylated, which seems to correlate with the presence of chromatin (Andersen *et al.*, 1997). Although there is some debate as to the specific mechanism of Op18 action, it may act directly by regulating GTP hydrolysis at the plus ends of microtubules, and/or indirectly by sequestering free tubulin subunits (Howell *et al.*, 1999; Wallon *et al.*, 2000).

Even naked DNA can stabilize microtubules to some degree (Heald *et al.*, 1996). In experiments using mitotic egg extracts from *Xenopus* and plasmid-coated magnetic beads, bipolar microtubule arrays form. This indicates that DNA not only stabilizes microtubules but also contributes to their organisation.

A proposed model for this behaviour involves three steps for forming the bipolar array (Heald *et al.*, 1996). At first, microtubules that attach to chromatin become more stable and form a mass of individual polymers. Next, plus end-directed microtubule motors that are attached to the chromatin (or naked DNA) push all minus ends away from the DNA. This action alone establishes a polarization of the microtubule mass. Finally, a minus end-directed motor that is free to cross-link multiple microtubules migrates in the minus direction, thus focusing all minus ends into a point. Although it is not clear how an inherently symmetrical body (the DNA-coated bead) can give rise to a bipolar spindle in this way, it is likely that the bipolar arrangement of two linear chromatids aligned back-to-back could help to direct this process. Some evidence suggests that chromatin may not be essential to the formation of bipolar spindles in an acentrosomal environment. Single chromatids (which are asymmetrical with respect to the kinetochore) in mice oocytes (Kubiak *et al.*, 1992) as well as oocytes devoid of DNA (Brunet *et al.*, 1998) can still occasionally form bipolar spindles. This suggests that other factors present during meiosis can direct the organisation of microtubules into a bipolar spindle.

In most animal cells, the microtubule organising centre is not chromatin, but a structure known as the centrosome (reviewed in Schatten, 1994). This organelle is comprised of a pair of centrioles positioned at right angles to each other, surrounded by a dense filamentous matrix, the pericentriolar material.

An analogous structure in yeast is the spindle pole body (SPB), which, unlike the cytoplasmic centrosome, is embedded in the nuclear membrane (reviewed in Winey and Byers, 1993). Microtubules grow out from the centrosome (and SPB) to form a network that functions as an intracellular roadway for various kinesin-related proteins and dyneins to transport their cargo.

In addition to serving as a hub for intracellular traffic, the centrosome provides two important functions in the assembly of the mitotic spindle. First, it nucleates microtubule formation during mitosis. Second, the centrosome provides the spindle with an organisation such that microtubule plus ends face outward from the centre of the centrosome. This polarity is important for spindle function because it establishes the direction of chromosome movement in concert with the motor proteins that travel along microtubules in a defined direction.

The ability of a centrosome to nucleate microtubules is due, in part, to the γ-tubulin subunit (Joshi *et al.*, 1992; Stearns and Kirschner, 1994). This form of tubulin is found in all centrosomes examined and may initiate microtubule polymerization by binding to the β-tubulin subunit of the tubulin dimer (Wolf *et al.*, 1996). One centrosomal protein that is required to anchor microtubule minus ends to the pericentriolar matrix is pericentrin, a large protein with a central coiled-coil region (Doxsey *et al.*, 1994). Interestingly, this protein is also found at the meiotic spindle pole of oocytes (in mice), despite

the absence of centrioles. Injection of pericentrin antibodies results in a disruption to both mitotic and meiotic spindles, with unfocused poles in meiotic spindles and disorganised asters around centrosomes. γ-tubulin is still present within the centrosomes after the immuno-depletion, indicating that pericentrin contributes to microtubule nucleation downstream of the γ-tubulin-based pathway; whatever anchors γ-tubulin to the centrosomal matrix does not rely on pericentrin.

The absence of centrosomes in meiotic animal cells and plant cells indicates that these structures are not absolutely required to form a functional bipolar spindle. Why do mitotic cells require a centrosome? It may be that centrosomes are more efficient at nucleating microtubules and were selected for as genomes became more complex and competition for cells to divide quickly became more intense. The centrosome may also serve as an important link between the cell cortex and the spindle. For instance, rotation of the spindle in response to cortical changes (as might occur during cell-cell contact) relies on an interaction with the spindle poles in order to exert torque on the spindle.

Although the centrosome and components thereof are important for the nucleation of microtubules, motor proteins also have a prominent role in both the arrangement of microtubules and the movement of cargo (such as chromosomes) along the microtubules. Some of these motor proteins are discussed below.

## Microtubule-dependent motor proteins in spindle assembly

The proteins responsible for motive forces in the assembly and maintenance of the spindle have been placed into two general groups based on sequence similarity. These are the cytoplasmic dyneins and the kinesins. Both of these classes of proteins are generally composed of two heavy chains and a variable number of light chains. Within each heavy chain resides a globular ATP-binding head that interacts with microtubules. The hydrolysis of ATP mediates the motor protein's movement along the microtubule. The actual molecular mechanism of movement by these motors is not well understood, but recent crystallographic analysis of kinesins suggest that the globular heads may walk along microtubules in a "hand-over-hand" fashion (Block, 1996; Amos and Hirose, 1997; Rice *et al.*, 1999).

The first kinesin-related protein (KRP) to be implicated in mitotic spindle formation was identified via genetic analysis in *Aspergillus nidulans* (Enos and Morris, 1990). The mutation, termed *bimC* (blocked in mitosis), resulted in aberrant spindle pole body separation and mitotic spindle assembly. Since its identification, a host of BimC homologues have turned up in a variety of organisms and all are implicated in mitotic function (reviewed in Walczak and Mitchison, 1996a). The BimC family members have a well-conserved N-terminal motor domain but have little or no homology outside this region, with

the exception of a phosphorylation site for cyclin-dependent kinases in some members.

The BimC family members are all likely to be plus end-directed motors, based on *in vitro* analysis of two proteins, *Drosophila* Klp61F (Barton *et al.*, 1995) and *Xenopus* Eg5 (Lockhart and Cross, 1996). The function of the BimC motors is not entirely clear, but they all seem to be involved in separation of duplicated spindle pole bodies (or centrosomes in higher eukaryotes) and bipolar spindle maintenance prior to anaphase (Saunders and Hoyt, 1992). The *S. cerevisiae* Cin8 and Kip1 products are somewhat functionally redundant in separating duplicated spindle pole bodies (Hoyt *et al.*, 1992; Roof *et al.*, 1992).

The most obvious defect in Eg5 immuno-depleted cells is a monoastral array nucleating from a duplicated, but unseparated pair of centrosomes (Sawin *et al.*, 1992). However, close examination of the array suggests fragmentation of pericentriolar material (Blangy *et al.*, 1995); therefore, Eg5 may function in the assembly of the spindle poles as well as spindle pole separation. One mechanism for Eg5 to perform both tasks is by cross-linking adjacent microtubules to each other and/or to the centrosome (Sawin and Mitchison, 1995; Sharp *et al.*, 1999). The presence of these proteins throughout the spindle may reflect promiscuous motoring as a result of their losing hold on some component of the spindle pole. Alternatively, if the BimC members are capable of cross-linking microtubules from opposite poles and pushing them

apart, they may also cross-link two microtubules running in the same direction. It has been proposed that the neck region may swivel to accommodate both of these functions (Sharp *et al.*, 1999).

The prototype member of the Kar3 family of KRPs was identified as a mutation that disrupts nuclear fusion (karyogamy) during mating, thus defining the *kar3* gene (Meluh and Rose, 1990). Family members share a conserved motor domain at the carboxyl-terminus, opposite that for BimC members. In addition to this structural difference, Kar3 kinesins are minus end-directed.

As for many of the BimC members, Kar3 proteins are also located throughout the spindle, with greatest concentration at the spindle pole. Kar3 has a microtubule-binding domain located in the amino-terminus. The ability of Kar3 to bind to microtubules via this region is dependent on the coiled-coil protein Cik1, a putative light-chain subunit for Kar3 (Page *et al.*, 1994). Therefore, Cik1 may promote Kar3-mediated cross-linking of microtubules. Vik1 is another light chain subunit for Kar3. This subunit may localize Kar3 to the spindle pole body and play a role in Kar3-mediated SPB separation (Manning *et al.*, 1999).

Mutations in *kar3* are able to suppress the *cin8 kip1* double mutant (Roof *et al.*, 1992). This suggests that Kar3 may cross-link microtubules between spindle poles like Cin8 and Kip1, and that Kar3-directed force is in opposition to the BimC proteins (Hoyt *et al.*, 1993; Manning *et al.*, 1999). The

reason why a minus end-directed force is required to separate spindle poles in this context is not clear, however. It could be that the separation of the spindle is strictly regulated so that the poles do not completely lose contact with each other by excessive plus end-directed forces during the separation process.

The Drosophila *ncd* (non-claret disjunctional) gene encodes another Kar3 member. *ncd* is required for the formation of spindle poles in both meiosis and early embryonic mitosis, with mutations in *ncd* resulting in frequent non-disjunction of chromosomes (Endow *et al.*, 1994). Furthermore, Ncd serves to aggregate microtubules into a bipolar array during meiosis and to anchor kinetochore microtubules to non-kinetochore microtubules during mitosis at the centrosome (Endow *et al.*, 1994). This latter function likely serves to transfer pole-directed forces generated by the kinetochore to non-kinetochore microtubules, much like the cross-linking behaviour proposed for BimC and Kar3 proteins.

The ability of Ncd to generate torque (spin) on free microtubules *in vitro*, suggests that the protein may rotate around the microtubule as it travels toward the minus end (Walker *et al.*, 1990). This property might be important during meiosis, where a spindle pole must be formed in the absence of centrosomes. Spinning around the microtubule would optimize the chances for contact with an adjacent microtubule; this also implies that upon contact with an adjacent microtubule, it may twist the two polymers together.

Another protein, NuMA (nuclear protein that associates with the mitotic apparatus; Gaglio *et al.*, 1995) is implicated in cross-linking the minus ends of microtubules at the centrosome/microtubule boundary in vertebrate cells. Although NuMA is not a motor protein, it is believed to associate with a minus end-directed motor protein, likely dynein/dynactin (reviewed in Compton, 1998). Therefore NuMA/dynein/dynactin may function much like, but in opposition to, Eg5. NuMa may serve to stabilize microtubule attachment to the centrosome and to distribute forces equally around the spherical spindle pole. Reminiscent of the yeast BimC story, aster assembly *in vitro* is inhibited by immuno-depletion of either NuMA or Eg5, but not both (Gaglio *et al.*, 1996). Therefore, an important aspect of mitotic spindle assembly and function seems to be the balance of opposing microtubule motor-based forces at spindle poles.

Cytoplasmic dyneins are minus end-directed motor proteins that are structurally distinct from kinesins. These motors are involved in organellar positioning, vesicle transport, as well as chromosome movement. In *S. cerevisiae*, dynein is largely responsible for the separation of chromosomes during anaphase B. However, spindle separation occurs in the absence of dynein, indicating that its role in pulling spindle poles apart is relegated to anaphase B. In contrast to yeast, mammalian spindles do not separate when cytoplasmic dynein is immuno-depleted, suggesting that two different modes of spindle pole separation may function in these systems. Furthermore, dynein is required for the association of centrosomes with the nucleus (Gönczy *et al.*,

1999; Robinson *et al.*, 1999). A model where a nuclear membrane-attached dynein pulls on microtubules to separate the centrosomes in *C. elegans* has been suggested (Gönczy *et al.*, 1999). Dynein, dynactin, and NuMA are also thought to maintain spindle pole integrity amidst the forces that arise during mitosis (Compton, 1998). As for chromosome movement in vertebrates, dynein is located at the kinetochore corona, where it is believed to provide the bulk of the minus end-directed force during anaphase in higher eukaryotes (Steuer *et al.*, 1990).

There are at least three different kinesins that associate with chromatin: *Xenopus* Xklp1 (Vernos *et al.*, 1995), chicken chromokinesin (Wang and Adler, 1995), and *Drosophila* Nod (no distributive disjunction; Afshar *et al.*, 1995). All of these proteins contain an amino-terminal motor domain, thus it is believed that they are plus-end directed kinesins (reviewed in Vernos and Karsenti, 1996). All of these proteins have a short carboxyl-terminal tail that contains a set of cysteine residues. These cysteines could form a zinc-finger structure, and there is evidence to support a role for DNA binding by these kinesins. For instance, the Nod protein binds selectively to A-T rich DNA *in vitro* (Afshar *et al.*, 1995).

The function of these kinesins is consistent with a role in chromosome congression during metaphase. For instance, *nod* mutations in *Drosophila* result in nondisjunction of meiotic chromosomes that do not undergo pairing or crossing-over (*i.e.*, univalents). Therefore, *nod* likely opposes the poleward

force generated by the kinetochore in order to prevent premature movement to the poles. Cross-overs can substitute for this function by physically linking oppositely oriented kinetochores, which then provide the stabilizing anti-poleward forces for each other.

## Katanin

There are many factors that influence microtubule length. As mentioned above, some are intrinsic to the microtubule polymer, such as dynamic instability. Others, such as microtubule associated proteins (MAPs) are extrinsic factors implicated in stabilizing the unusually long microtubules found in neurons or the interphase microtubule network.

R. Vale (1991) reported the existence of microtubule-severing activity present in mitotically active *Xenopus* egg extracts. This activity was not found in the interphase extract, suggesting that the component(s) responsible may disassemble interphase microtubules in preparation for mitosis. Furthermore, the severing activity was activated via a post-translational mechanism that correlated with the activity of Cdc2 kinase, as assayed by phosphorylation of histone H1 (Vale, 1991). Subsequent work identified a single heterodimeric protein responsible for the microtubule severing that was named katanin, after the Japanese samurai sword, *katana* (McNally and Vale, 1993).

The katanin heterodimer consists of p60 and p80 subunits (McNally and Vale, 1993). The p60 subunit by itself shows ATP-dependent microtubule-severing activity and belongs to a large family of ATPases known as AAA proteins (ATPases associated with various cellular activities; reviewed in Patel and Latterich, 1998). The p80 subunit is likely involved in subcellular targeting of the p60/p80 complex (Hartman *et al.*, 1998; McNally *et al.*, 2000). p80 contains a WD-40 repeat domain in the N-terminus that is necessary for targeting the heterodimer to centrosomes and seems to attenuate severing activity (McNally *et al.*, 2000). Although the *in vivo* role of katanin is not clear, it is implicated in a wide variety of biological processes. The cell cycle-specific activity of katanin in *Strongylocentrotus purpuratus* (sea urchin) and *Xenopus* extracts could indicate a role for the disassembly of interphase microtubules at the onset of mitosis (Vale, 1991; McNally and Thomas, 1998). Despite the cyclic activity of katanin, it is present at the centrosomes throughout the cell cycle. The location of katanin is distinct from another centrosomal component γ-tubulin, suggesting that katanin may not be a component of the centrosome *per se*. The centrosomal location suggests that katanin may play a role in the mediation of microtubule poleward flux by severing at the minus ends (McNally *et al.*, 1996). Katanin microtubule-severing activity is also implicated in the deflagellation of *Chlamydomonas reinhardtii* (Lohret *et al.*, 1998; Lohret and Quarmby, 1999). The ability of sea urchin katanin to sever the unusual nine outer-doublet microtubules of the flagellar axoneme indicates a

conservation of function that supersedes higher-order structure. Mutations in the *Chlamydomonas* katanin have not been identified, suggesting that other factors may be involved in deflagellation or that katanin may have an unidentified role that is essential for viability (Finst *et al.*, 2000). Katanin has also been found to play a role in the release of microtubules from the centrosome in neurons (Ahmad *et al.*, 1999). In this case, katanin functions to keep microtubules short so that they can be transported to the cell periphery and funnel into the space-restricted axons and dendrites.

The MEI-1 protein of *C. elegans* is also an AAA member (Clark-Maguire and Mains, 1994a) that exhibits a high degree of similarity to sea urchin katanin p60 (Hartman *et al.*, 1998). The similarity is restricted to the AAA domain, which is not a reliable predictor of function for this family of proteins (Patel and Latterich, 1998). However, certain observations are consistent with MEI-1 acting as a microtubule-severing protein. For instance, the meiotic spindle in *C. elegans* is much smaller than the first mitotic spindle. This size-difference suggests that a katanin-like MEI-1 might function to keep microtubules short during meiosis in a cytoplasmic environment that will later support unusually long microtubules. Similarly, ectopic MEI-1(*ct46*gf) severing activity provides a ready explanation for the mitotic spindle phenotypes observed in *mei-1(ct46*gf) mutants (see below).

## Meiosis in *C. elegans*

The reproductive system of the *C. elegans* hermaphrodite is contained within a bilobed tube (Fig.1; reviewed in Hubbard and Greenstein, 2000). The anterior and posterior arms function independently to produce germ cells that arise from mitotically-dividing syncytial nuclei in the distal region. The distal tip cell, located at the end of each lobe, is required to maintain the mitotic proliferation of germ cell nuclei. The product of the *glp-1* gene, a member of the Notch receptor family, is required for germ cells to receive the distal tip cell signal. This signal is encoded by *lag-2*, a homologue of *Drosophila Delta* (Henderson *et al.*, 1994). Through this mechanism, nuclei close to the distal tip cell continue to proliferate mitotically. As nuclei approach the reflexed region of the gonad, they enter meiosis and are encapsulated by surrounding cell membranes of the gonad cortex. Oocytes continue to advance towards the spermatheca and remain in diakinesis of prophase I until fertilization (Fig. 1). As the oocytes pass through the spermatheca, they are fertilized by sperm.

During oocyte maturation, *C. elegans* chromosomes exhibit all of the classically described stages of meiotic prophase: leptotene, zygotene, pachytene, diplotene, and diakinesis. Meiotic chromosomes begin to condense at leptotene. In zygotene, the synaptonemal complex forms between the two pairs of closely associated sister chromatids. It is likely that the synaptonemal complex in *C.*

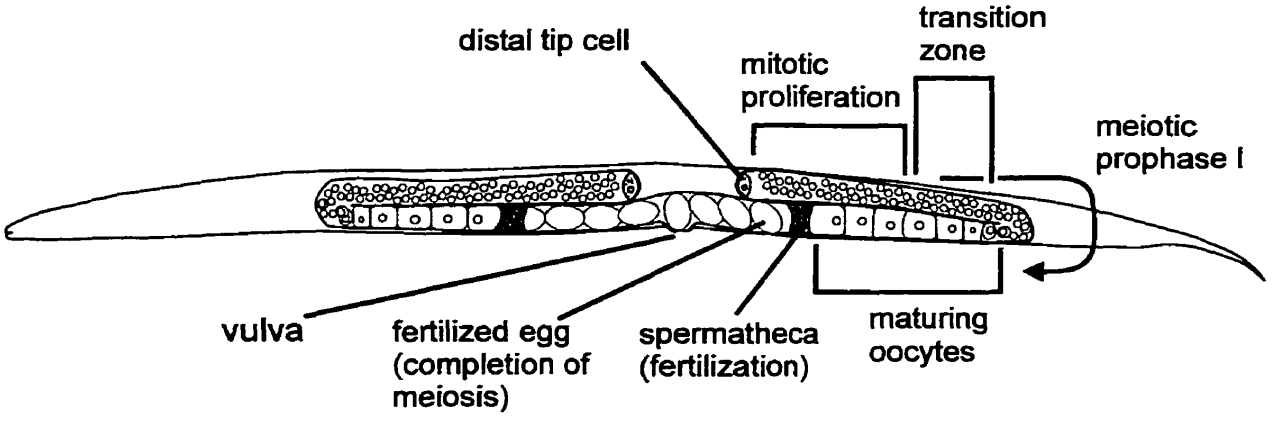


**Figure 1. *C. elegans* oogenesis.**

A schematic diagram of the *C. elegans* gonad is shown. Mitotic proliferation of germ cell nuclei occurs in the distal lobe of both gonad arms. As the nuclei move proximally, they enter meiosis and develop into mature oocytes. These oocytes arrest at diakinesis until they pass through the spermatheca and are fertilized. The fertilized eggs are stored for a short time in the uterus before their deposition via the vulva.

*elegans* serves multiple roles by promoting intimate association of homologues. For instance, the *him-3* gene encodes a component of the synaptonemal complex that is required for synapsis, recombination, and sister chromatid cohesion (Zetka *et al.*, 1999). Leptotene and zygotene stages occur in a region of the gonad known as the transition zone (Crittenden *et al.*, 1994). The completion of synapsis marks the end of zygotene and the beginning of pachytene.

Many genes are involved in the progression of oocytes past pachytene and at least two pathways are involved. First, the RAS/MAP kinase pathway is required for the transition from pachytene to later stages. This is based on the observation that mutations in *let-60* (RAS), *mek-2* (MAP kinase kinase) and *mpk-1* (MAP kinase) result in a pachytene arrest phenotype in both hermaphrodites and males (Church *et al.*, 1995). The source of the signal upstream of this pathway has not been determined, but may involve the receptor tyrosine kinase LET-23, which has a well-established role in RAS-signaling during vulval development (reviewed in Kornfeld, 1997).

Distinct from the RAS pathway are two genes, *gld-1* and *gld-2* (Francis *et al.*, 1995b; Kadyk and Kimble, 1998). The *gld-1* gene is required for the ooctye's progression through meiotic prophase (Francis *et al.*, 1995a). Furthermore, in *gld-1* mutants, meiotic cells enter pachytene but exit and return to mitotic proliferation. The GLD-1 protein has a putative RNA-binding

function and may serve to regulate RNA translation or stability in maturing oocytes (Jones and Schedl, 1995). It has been proposed that GLD-1 may inhibit the translation of cell-cycle factors required for early embryonic divisions (Schedl, 1997). *gld-2* is also essential for progression through meiotic prophase during both oogenesis and spermatogenesis (Kadyk and Kimble, 1998). In addition, *gld-1* and *gld-2* are redundant with respect to the *glp-1*-mediated exit from mitotic proliferation (Kadyk and Kimble, 1998).

By the diplotene stage, chromosomes desynapse but remain attached through chiasmata. These structures are the physical manifestations of recombination events and are first observable in diplotene (Villeneuve, 1994). Chromosomes continue to condense as the oocyte enters diakinesis. The oocytes arrest at this stage until fertilization triggers the formation of the meiotic spindle (see below).

The *C. elegans* hermaphrodite has 12 chromosomes – five pairs of autosomes and a pair of sex chromosomes. The male has only 11 chromosomes because of a single sex chromosome. In meiosis, the bivalents (paired homologues) are oriented in an end-to-end manner (Nigon and Brun, 1955; Herman *et al.*, 1979; Albertson and Thomson, 1993) and are arranged with five bivalents surrounding a sixth, giving a rosette pattern when looking down the spindle axis (Fig. 2A). Cytological analysis revealed that the sister chromatids are aligned side-by-side during metaphase I. Each bivalent is arranged such that homologues abut one another in mirror image (Fig. 2B). After meiosis I,

**Figure 2. The cytology of meiosis in *C. elegans*.**

*A*) During metaphase I and II, condensed chromosomes align on the metaphase plate in a rosette pattern. A schematic representation of metaphase I is shown (axial view). Each bivalent is composed of two homologues, each of which contains two chromatids (shown in white or grey) in meiosis I.

*B*) One bivalent from a heterozygote (A/a) is shown. Homologues disjoin in meiosis I and sister chromatids disjoin in meiosis II. The black circle indicates one end of the chromosome. One half of the products of each meiotic division are extruded as a polar body (pb), such that one haploid genome remains after the completion of meiosis. Figure adapted from (Albertson *et al.*, 1997).

*C*) The orientation and morphology of the meiotic spindle over time is represented schematically. A spindle is drawn next to the anterior cortex. Only 3 paired chromosomes are shown for clarity.

A Chromosome positioning on the metaphase plate

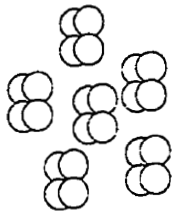

B The segregation of chromosomes in meiosis I and II


Metaphase I Telophase I Prophase II Metaphase II Telophase II

C The morphology and orientation of the meiotic spindle through meiosis

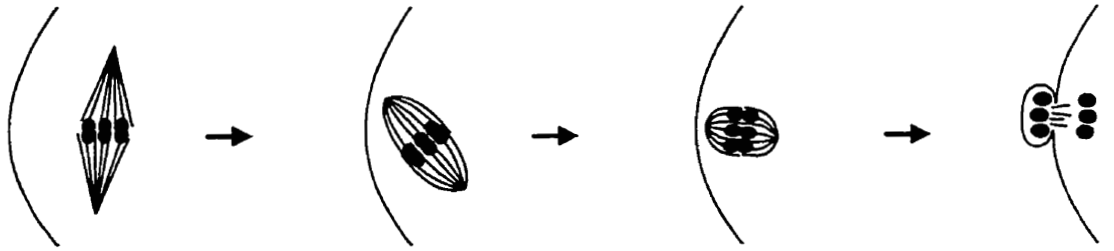

Early Metaphase Late Anaphase Telophase

the sister chromatids align on the metaphase II plate. Again, the orientation is end-to-end. However, the chromosome end that was previously juxtaposed to the homologous chromosome in meiosis I, now faces outwards, toward the spindle pole (Albertson and Thomson, 1993).

## Meiotic spindle morphology in *C. elegans*

After fertilization, the meiotic spindle forms in the anterior of the one-cell embryo. The morphology and orientation of the spindle is dynamic throughout meiosis and has been characterised previously (Albertson and Thomson, 1993). Initially, an amorphous cloud of tubulin surrounds congressed chromosomes. Then, an early metaphase spindle forms parallel to the anterior cortex (Fig. 2C). This spindle measures about 13 μm (pole-to-pole) and is pointed at each end. As metaphase continues, the spindle morphology becomes more barrel-shaped and compressed. In addition, the spindle rotates throughout metaphase, to lie perpendicular to the cortex. This rotation implies that one of the poles establishes a physical connection with the anterior cortex at some stage of meiosis. By anaphase, spindle rotation is complete and the pole-to-pole distance measures about 4 μm. In telophase, chromosomes separate to a maximal distance of 4 μm and tubulin staining is detectable only in the interzone. The chromosomes closest to the cortex become packaged into a polar body and after a brief interphase, the process reiterates in meiosis II.

## The genetics of meiotic and mitotic spindle function in *C. elegans*

*C. elegans* meiotic spindles form as in most higher eukaryotes with microtubules orienting to and emanating from the chromosomes rather than from the centrosomes, which are absent (Albertson and Thomson, 1993). After meiosis is complete, a centrosome-based mitotic spindle forms and specialized components of the previous meiotic spindle must be prevented from interfering with the mitotic process. These two structurally distinct spindles function in the same oocyte cytoplasm within a time span of less than 30 minutes, suggesting a rapid mechanism of turnover or down-regulation for the meiosis-specific components.

A number of genes have been identified that have an essential role in oocyte meiotic and early mitotic spindle function in *C. elegans* (Mains *et al.*, 1990). The *mei-1* gene of *C. elegans* can be mutated to disrupt meiosis (as a loss-of-function *(lf)* mutation) or mitosis (as a dominant gain-of-function *(gf)* mutation) (Mains *et al.*, 1990). *mei-1* is required for meiosis but must be negatively regulated prior to mitosis, otherwise mitotic defects result (Fig 3A). The original mutation was identified in a screen for dominant, *gf*, temperature-sensitive (*ts*) maternal-effect mutations (maternal-effect mutations are those that present a phenotype in the progeny of a homozygous mother, regardless of zygotic genotype). *mei-1(*lf*)* mutations cause recessive meiotic spindle defects that manifest as abnormal (either grossly oversized or absent) polar bodies

**Figure 3. Genetic network controlling meiotic spindle assembly.**

*A)* A proposed pathway for the meiosis-to-mitosis transition in *C. elegans* is shown. Both *mei-1* and *mei-2* are required for meiotic spindle assembly. *mel-26* negatively regulates *mei-1* (based on genetics and immunohistochemistry) and *mei-2* (based on immunohistochemistry). This figure is adapted from Clark-Maguire and Mains (1994b), but altered to reflect new data indicating that both *mei-1* and *mei-2* are negatively regulated by *mel-26* (see Results). *B)* The phenotypes of mutations in genes implicated in meiotic or mitotic function are shown, with those directly implicated in MEI-1 function boxed. Arrowheads indicate polar bodies in the anterior of a two-cell embryo. An enlarged polar body is commonly observed in *mei-1(*lf*)* and *mei-2(*lf*)* mutants. Centrosomes (arrows) are marked to indicate mispositioning and failed rotation of the first mitotic spindle commonly observed in *mei-1(ct46*gf*)* and *mel-26* mutants. Mutations in genes marked by an asterisk result in no obvious phenotype, but are included because of their genetic interaction with the *mei-1* pathway in either meiosis or mitosis.

A

MEIOSIS — MITOSIS

*mei-1*
*mei-2* ⊣ *mel-26*

B

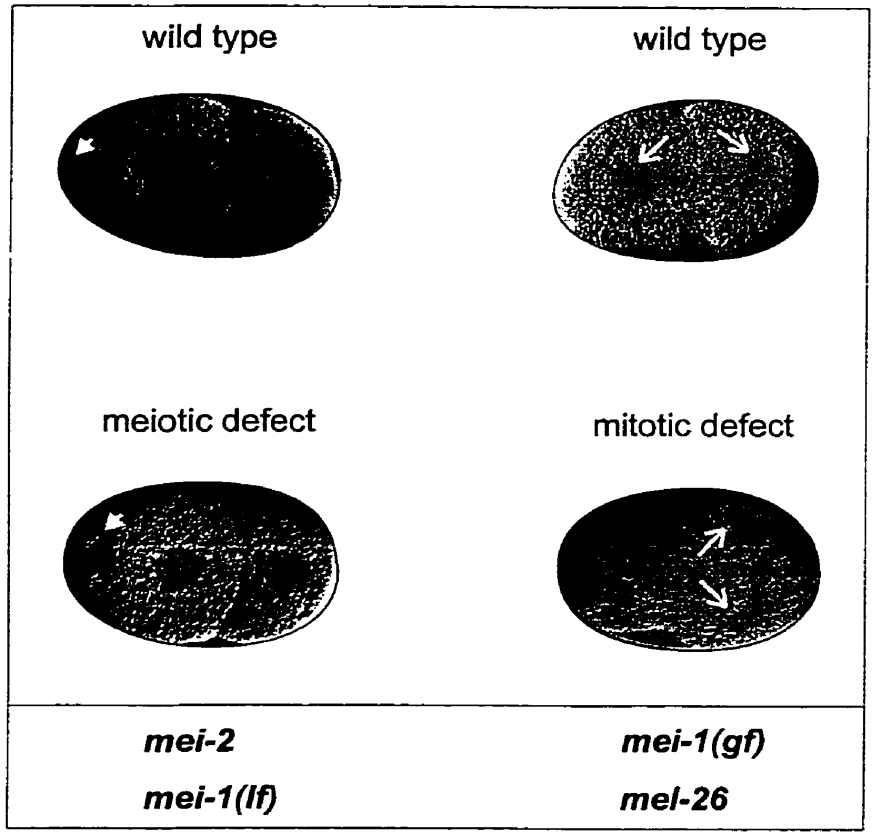


| | |
|---|---|
| ***mei-2*** | ***mei-1(gf)*** |
| ***mei-1(lf)*** | ***mel-26*** |
| *tbb-2** | *zyg-9* |
| *sup(sb27)** | *mel-45* |
| *sup(sb28)** | *tbb-2** |

(Fig. 3B). Furthermore, the meiotic spindle microtubules are disorganised. However, subsequent mitotic spindles in *mei-1(*lf*)* mutants appear to be unaffected with respect to orientation of the spindle and rhythm of cleavage. In contrast to the *lf* mutations, the dominant *ts* mutation *mei-1(ct46*gf*)* results in normal meiosis followed by abnormal mitosis at the restrictive temperature. The mitotic spindles in these mutants are mispositioned toward the posterior of the one-cell embryo and often fail to rotate (Fig. 3B; Mains *et al.*, 1990). Furthermore, the mitotic asters appear smaller (M. R. Dow and P. E. Mains, *pers. comm.*). These phenotypes are reminiscent of the effects of the microtubule depolymerizing drug nocodazole (Strome and Wood, 1983), suggesting that microtubule function may be compromised in the *mei-1(ct46*gf*)* mutant. The two-fold genetic behaviour of *mei-1* suggests that it is essential for meiosis but must be inactivated prior to mitosis. Our interpretation of the *mei-1(ct46*gf*)* mutation is that it can still function within normal parameters during meiosis but has inappropriate activity during mitosis.

Immunolocation of MEI-1 protein indicates close association with the meiotic spindle, meiotic chromatin during telophase, and the condensed sperm pronucleus (Clark-Maguire and Mains, 1994b). In particular, MEI-1 locates to spindle microtubules during meiosis I and II, and is concentrated at the poles, consistent with a role in meiotic spindle assembly. MEI-1 is not detected during subsequent mitosis. However, the *mei-1(ct46*gf*)* mutation does exhibit MEI-1 staining at centrosomes during mitosis (Clark-Maguire and Mains,

1994b). This suggests that the MEI-1(*ct46*gf) protein may not be responding to some form of negative regulation that normally prevents its activity during mitosis. The *mei-1(ct46*gf*)* mutation results in a proline to leucine amino acid change in the N-terminus. The alteration occurs within a region having a high PEST score (abundance of proline, glutamate, serine, and threonine; Rechsteiner and Rogers, 1996). Protein domains exhibiting high PEST scores have been implicated in affecting protein turnover (Rechsteiner and Rogers, 1996). In MEI-1(*ct46*gf*)*, the P to L change reduces the PEST score dramatically, suggesting a possible explanation for the *mei-1(ct46*gf*)* phenotype (P. E. Mains, *pers. comm.;* Dow and Mains, 1998).

MEI-1 belongs to the AAA gene family (Clark-Maguire and Mains, 1994a). This group of ATPases perform functions ranging from proteolysis and membrane function, to cell cycle control (Patel and Latterich, 1998). As mentioned above, the protein to which MEI-1 is most similar is the sea urchin katanin p60 subunit. The similarity does not extend past the AAA domain, weakening arguments for MEI-1 being a microtubule-severing protein. However, many aspects of the *gf* mutation are phenocopied by nocodazole treatment, consistent with *mei-1(ct46*gf*)* resulting in ectopic microtubule severing during mitosis. Furthermore, microtubules form a much smaller spindle in meiosis as compared with the first mitosis, implying a microtubule-severing activity normally limits microtubule growth during meiosis. A relationship between *mei-1* and microtubules is also implied by the discovery

that a mutation in *tbb-2*, a β-tubulin, reduces the activity of *mei-1* in both meiosis and mitosis (T. Clandinin and C. Lu, *pers. comm.*). For example, *tbb-2(sb26)* suppresses *mei-1(ct46*gf*)* mitotic defects and enhances weak *mei-1(ct82)/+* meiotic defects (T. Clandinin, *pers comm.*).

There are two *lf* alleles of *mei-1* in addition to 17 alleles that exhibit antimorphic or dominant-negative (*dn*) properties. These mutations reduce the activity of wild-type MEI-1 and suppress the *mei-1(ct46*gf*)* mutation in a dose-dependent manner. The genetic behaviour of *dn* mutations is often indicative of protein-protein complexes or multimeric forms. Therefore, MEI-1 may physically associate with itself or other proteins during meiosis (Clandinin and Mains, 1993). This is a common feature of many AAA proteins (Patel and Latterich, 1998). For instance, katanin p60 is known to form oligomeric ring structures (Hartman *et al.*, 1998) in the presence of both ATP and microtubules (Hartman and Vale, 1999). The *in vivo* role for this structure is not known, but it may allow simultaneous contact between the severing complex and each of the 13 tubulin dimers within the microtubule protofilament (McNally, 2000).

Extragenic mutations that alleviate (*i.e.* suppressor mutations) or exacerbate (*i.e.* enhancer mutations) an original mutation are often indicative of new genes that participate in the same biological process. By taking advantage of the *mei-1(ct46*gf*)* mutation, a number of suppressor and enhancer mutations have been identified. Although most of the suppressors are intragenic revertants of *mei-1(ct46*gf*)* including null and *dn* alleles, this

approach has uncovered extragenic suppressors and enhancers that are candidates for interacting genes (Mains *et al.*, 1990). Genetic screens of this type could identify a protein that physically interacts with MEI-1, or point to other factors that are required for meiosis, mitosis, or spindle function in general, including any factors that may regulate the activity of MEI-1.

The mitotic defects of *mei-1(ct46*gf) are enhanced by mutations in *mel-45, zyg-9,* and *mel-26*. Recessive *lf* alleles of *zyg-9* and *mel-26,* as well as dominant alleles of *mel-26* and *mel-45,* result in mitotic defects similar to *mei-1(ct46*gf) (Mains *et al.*, 1990; Mitenko *et al.*, 1997; Dow and Mains, 1998). *mel-26,* and *zyg-9* mutations also enhance each other's phenotype (Mains *et al.*, 1990). This suggests that these genes belong to a mitosis-specific pathway. The *mel-45* gene has not been fully characterized, but will be discussed later (see Results and Discussion).

*zyg-9* mutations affect both meiosis and mitosis (Matthews *et al.*, 1998). Meiotic spindles appear slightly disorganised and mitotic spindles are short and fail to rotate. *zyg-9* encodes a putative microtubule-associated protein (Matthews *et al.*, 1998), based on its similarity to the microtubule-associated protein ch-TOGp (Charrasse *et al.*, 1998), a homologue of Xenopus XMAP215 (Gard and Kirschner, 1987). Therefore, ZYG-9 may stabilize microtubules required for the large mitotic spindles in early embryos. *zyg-9*'s genetic interaction with *mei-1* suggests that these two gene products may have opposite effects on the length of microtubules, again consistent with a role for

MEI-1 in severing microtubules. ZYG-9 protein collocates with spindle microtubules in meiosis and is concentrated at the poles. In mitosis, ZYG-9 is present predominantly at the spindle poles. ZYG-9 staining patterns are unaltered in the *mei-1(ct46*gf*)* mutant strain, indicating that the genetic interaction likely reflects a distinct mechanism of action for these two proteins (Matthews *et al.*, 1998).

*mel-26* mutations enhance both *zyg-9* and *mei-1(ct46*gf*)*. However, unlike the *zyg-9* mutations, *mel-26* also interacts with *mei-1(dn)* mutations. *mei-1(dn)* mutations dominantly suppress the mitotic defects of *mel-26* mutations, indicating that decreased *mei-1* can rescue compromised *mel-26*. Furthermore, *mei-1(null) mel-26* double homozygotes exhibit meiotic defects (like *mei-1 lf* homozygotes) but mitotic spindles appear normal (unlike *mel-26* homozygotes). This indicates that *mei-1* is epistatic to *mel-26* and that, in the absence of *mei-1* function, *mel-26* is dispensable (Clark-Maguire and Mains, 1994a). This latter finding strongly suggests that *mei-1* and *mel-26* are part of the same genetic pathway. As in *mei-1(ct46*gf*)* embryos, MEI-1 is found at the centrosomes in *mel-26* mutant embryos. *mel-26* has been recently cloned and encodes a novel protein (Dow and Mains, 1998), with the exception of a conserved BTB (*bric à brac*, *tramtrack*, and *Broad-Complex*) domain implicated in protein-protein interactions (Zollman, *et al.*, 1994). *mel-26* acts as a post-meiotic negative regulator of *mei-1,* and may function to sequester or degrade MEI-1 product prior to mitotic spindle assembly.

The *mei-2* gene was identified as an extragenic, dominant suppressor of *mei-1(ct46*gf) (Mains *et al.*, 1990). All of the *mei-2(*lf) mutations are able to dominantly suppress the mitotic defects of both *mei-1(*gf) and *mel-26(*gf) mutations. The recessive phenotype of *mei-2(ct102)* homozygotes is maternal-effect lethality whereas *mei-2(ct98)* homozygotes produce about 75% viable progeny with excess males due to X-chromosome non-disjunction, likely indicating spindle defects (Mains *et al.*, 1990). Furthermore, all *mei-2* mutations cause recessive meiotic spindle defects indistinguishable from *mei-1(*lf) mutations. In *mei-2* mutant embryos, MEI-1 does not locate to any structures, suggesting a role for *mei-2* in the intracellular localization of MEI-1 (Clark-Maguire and Mains, 1994b).

The null phenotype of *mei-2* is unknown. Loss-of-function mutations are able to suppress *mei-1(*gf) (indeed, this was criteria for their identification) but a chromosomal deletion that removes *mei-2* (and should mimic a complete *lf*) is not able to suppress *mei-1(gf)*. Either the known alleles are not nulls, or the deletion removes another interacting gene.

Epistasis and cytological analysis of these mutations have allowed the construction of a simple genetic pathway to explain the complex interactions (Clark-Maguire and Mains, 1994; Fig. 3A). Together, the genetic analysis indicates that *mei-2(+)* behaves as an activator of *mei-1(+)* in both meiosis (Mains *et al.*, 1990; Clandinin and Mains, 1993; Clark-Maguire and Mains, 1994a) and mitosis in *mei-1(ct46*gf) mutants (Clark-Maguire and Mains,

1994b). Simple models invoke MEI-2 either as an activator of MEI-1 (*e.g.*, a kinase or phosphatase) or as a component of the meiotic spindle that physically associates with MEI-1.

An aim of this thesis was to elucidate the function of the *mei-2* gene and determine how it interacts with the other components of the genetic pathway centred on *mei-1*. Towards this end, *mei-2* was molecularly identified and found to encode a protein that contains a region of similarity to the p80 subunit of the microtubule-severing protein katanin. This region of p80 has been implicated in physically interacting with the p60 subunit (Hartman *et al.*, 1998; McNally *et al.*, 2000). The sequence similarities between MEI-1/MEI-2 and katanin p60/p80 suggest that the *C. elegans* proteins physically interact and sever microtubules during meiosis. Evidence is presented that refines the relationship between *mei-1* and *mei-2*. First, MEI-1 and MEI-2 exhibit similar patterns of subcellular location during wild-type oocyte meiosis and these patterns require the presence of both wild-type proteins. Second, mutations that result in the persistence of MEI-1 into mitosis also result in the persistence of MEI-2 into mitosis. Third, yeast two-hybrid results indicate that MEI-1 and MEI-2 can associate *in vivo*. Furthermore, experiments show that MEL-26 also associates with MEI-1 and a model is proposed to explain the intermolecular associations of these proteins during meiosis and mitosis. Finally, in collaboration with F.J. McNally (University of California, Davis), MEI-1 and MEI-2 were found to exhibit katanin-like microtubule disassembly

in HeLa cells (Srayko *et al.*, 2000). Based on these observations, MEI-1/MEI-2 likely sever microtubules of the meiotic spindle in *C. elegans*. This novel role for a katanin-like protein may explain how meiotic spindles maintain their small size in a cytoplasmic environment that later supports the assembly of a much larger mitotic spindle.

# Materials and Methods

## Nematode strains and culture conditions

*C. elegans* (var. Bristol) was cultured as described by Brenner (1974). Broods were scored by placing an individual L4 hermaphrodite on media with food and transferring it to fresh media approximately every 8 hrs until egg laying was complete.

Unless otherwise stated, all homozygous mutant worms used were derived from the strains shown in Table 1. A description of *C. elegans* genes can be found in Riddle *et al.* (1997). *mei-2(sb31)* was isolated in a screen for suppressors of *mei-1(ct46*gf) (Clandinin and Mains, 1993); *mei-2(sb39)* was isolated in a screen for revertants of *mel-26(ct61)* (Dow and Mains, 1998). These alleles failed to complement *mei-2(ct102)* and mapped to the same region of chromosome I (see Results).

## Nomenclature conventions of *Caenorhabditis elegans*

Generally, *C. elegans* gene names follow the nomenclature outlined in Horvitz *et al.* (1979). All genes are assigned a three-lettered name that describes some aspect of its mutant phenotype or its molecular nature based on

**Table 1. Worm strains used in this study.**

| Strain | Genotype |
|---|---|
| N2 | wild type |
| CB1072 | *unc-29(e1072) I* |
| BW1102 | *dpy-5(e61) mei-2(ct102) unc-29(e1072); sDp2 I;f* |
| HR19 | *dpy-5(e61) mei-2(ct102) daf-8(e1393); sDp2 I;f* |
| HR543 | *mei-2(sb31) unc-29(e1072)/hT2[bli-4(e937) let(h661)] I ; ++/hT2 III* |
| BW1048 | *mei-2(ct98) unc-29(e1072) I* |
| HR827 | *mei-2(sb39) unc-29(e1072) I* |
| JK549 | *fem-3(q20) dpy-20(e1282) IV* |
| HR219 | *fem-1(hc17) IV* |
| BW729 | *mei-1(ct46) unc-29(e1072) I* |
| BW944 | *mei-1(ct46ct101) unc-29(e1072)/unc-13(e1091) lin-11(n566) I; lon-2(e678) X* |
| BW722 | *zyg-9(b244) II* |
| JK892 | *unc36/unc-32(e189) glp-1(q231) III* |
| HR378 | *bli-4(e937) let-607(h402) unc-37(e262); hDp19 I;f* |
| HR245 | *mei-1(ct46ct101) unc-29(e1072) mel-26(ct61)/unc-13(e1091) lin-11(n566) I; lon-2(e678) X* |
| BW737 | *mel-26(ct61) I* |

similarity to well-characterized genes. This three-lettered name is followed by a number. For instance, *dpy-10* is one of many genes that were so labeled because they result in a "Dumpy" phenotype when mutated. When a specific allele is mentioned, it is included parenthetically after the gene name (*e.g.*, *dpy-10(e128)*), where the letter(s) are specific laboratory designations. The Mains laboratory allele designation is "*sb*". For phenotypic description, the gene name is capitalized and non-italicized (*e.g.*, The Dpy-10 worms were scored for viability.). Protein products of a given gene are written in all capitals (*e.g.*, DPY-10 is a collagen.). Predicted genes are assigned a numerical

identifier that indicates the cosmid of origin (*e.g.*, F47G4.4 is a gene on cosmid F47G4). N2 is the canonical wild-type strain.

## Mutagenesis

Ethylmethane-sulfonate (EMS) mutagenesis of young adult hermaphrodites or males was performed as described in Wood (1988). Gamma-irradiation was performed as described (Rosenbluth *et al.*, 1985); the dose administered was approximately 2500 Rads.

## Germline transformation

For germline transformation rescue, cosmids were injected at a concentration of approximately 30-60 ng/μL each, along with pRF4 (Mello *et al.*, 1991), a plasmid containing the marker *rol-6(su1006)* at 100 ng/μL. *rol-6(su1006)* confers a dominant Rol (Rolling) phenotype. All other methodology pertaining to germline transformation was as described in Mello *et al.* (1991).

## RT-PCR

First-strand cDNA was constructed using reagents from the SUPERSCRIPT II (GibcoBRL) kit. 500 ng of polyA$^+$ RNA isolated from wild-type gravid adults was used as template and an EcoRI-dT primer (5'-GCTGCAGAATTCGTCGAC-dT$_{(17)}$-3') was used to prime first-strand synthesis.

Subsequent PCR was performed with forward and reverse primers specific for the *mei-2* coding region, based on Genefinder (Green, 1995) predictions found in ACeDB. All reactions confirmed the predicted structure. In order to determine if *mei-2* was *trans*-spliced to either SL1 or SL2 sequences (Krause and Hirsh, 1987; Huang and Hirsh, 1989), appropriate forward primers specific for each of these leader sequences were used with two different *mei-2* primers. A band of approximately 200 bp was observed upon PCR amplification with primers SL1 and *mei2*R1, and a band of approximately 750 bp was observed with primers SL1 and *mei2*R3 (see Figure 4 for positions and sequences of *mei-2* primers). Both bands were excised and sequenced. No unexpected products were amplified. SL1 is spliced onto the *mei-2* coding sequence immediately before the predicted ATG start codon. Reactions containing SL2 did not amplify any products with any *mei-2* reverse primers. The site of poly-adenylation was determined by performing PCR on the above mentioned cDNA using the EcoRI adapter (reverse) primer (5'-GCTGCAGAATTCGTCGAC-3') and either *mei2*F2 or *mei2*F4 forward primers. Products from each reaction were sequenced. Polyadenylation was found 13 bp downstream of the sequence TATAAA, contained within the *mei-2* 3'-UTR.

RT-PCR was used to clone full-length cDNA of the *C. elegans* genes F47G4.4 and F47G4.5. Primer sequences were designed based on Genefinder predictions. F47G4.4 primers used were F47G4-4BF (forward) and F47G4-4XR

**Figure 4. Location and sequence of primers within *mei-2*.**

Sense primers (drawn above the gene) and antisense primers (drawn below the gene) were designed for multiple experiments discussed in this thesis. Certain primers (1-14) contained added restriction sites for cloning into expression vectors: BamHI (1,3,5,9,10,11); KpnI (2); SmaI (4,6); PstI (7,12); SacI (8,13); SmaI (14).

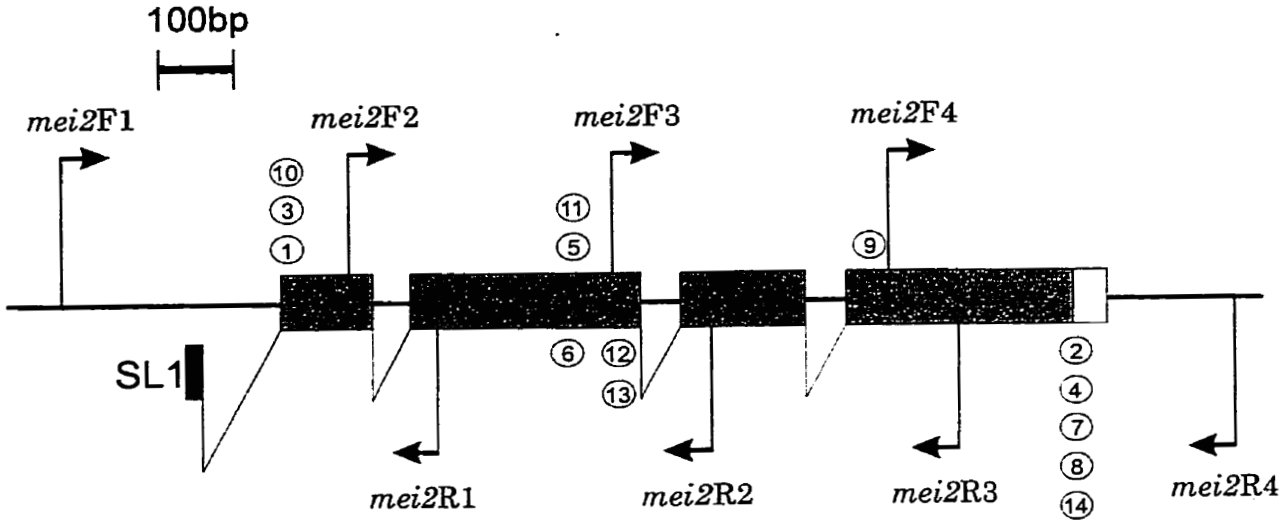


*mei2*F1 5'-CATTGGAATGAGGCAAAAGT-3'
*mei2*F2 5'-GCTGAAAACAGACCAAATAC-3'
*mei2*F3 5'-GAGGAAGTGAATAAAATCGG-3'
*mei2*F4 5'-AAGGCTCTTGCATCAATTAC-3'
*mei2*R1 5'-AACTCCCGATGAAAGTGATG-3'
*mei2*R2 5'-CTGTTCCATGTTACTTGTGA-3'
*mei2*R3 5'-TGTTGCTTTTGCAGCTCGCT-3'
*mei2*R4 5'-TCCATAGACAATGAATCACC-3'

① BamMEI2F 5'-CGGGATCCTCAGGGCTTGACGACCG-3'
② KpnMEI2R 5'-GGGGTACCTCATTACTTATGGCTGGAAAC-3'
③ pGEXBMEI2F 5'-CGGATCCCCTCAGGGCTTGACGACCG-3'
④ SmaMEI2R 5'-GACCCGGGTCATTACTTATGGCTGGAAAC-3'
⑤ MEI2-BamF2 5'-CGGATCCCCGAGGAAGTGAATAAATC-3'
⑥ MEI2-SmaR2 5'-GACCCGGGAGGATTTTGGCAAAGAAC-3'
⑦ MEI2-PstR1 5'-CTGCTGCAGTTACTTATGGCTGGAAAC-3'
⑧ MEI2-SacR1 5'-CTGGAGCTCTTACTTATGGCTGGAAAC-3'
⑨ MEI2-BamF3 5'-CGGATCCCTATCACGAGCGACAATTATG-3'
⑩ MEI2-BamF4 5'-CGGATCCATGTCAGGGCTTGACGACCG-3'
⑪ MEI2-BamF5 5'-CGGATCCCCGAGGAAGTGAATAAAATC-3'
⑫ MEI2-PstR2 5'-CTGCTGCAGGCTCTCTCGCTTCGCACAAAC-3'
⑬ MEI2-SacR2 5'-CTGGAGCTCGCTCTCTCGCTTCGCACAAAC-3'
⑭ MEI2-SalR1 5'-GCGTCGACTTACTTATGGCTGGAAAC-3'

(reverse). F47G4.5 primers were F47G4-5BF (forward) and F47G4-5XR (reverse) (Fig. 5). The full-length cDNAs were used for RNAi experiments and cloning into pFM272, a GST-fusion construct for transient transfection of HeLa cells (F.J. McNally, *pers. comm*; University of California, Davis).

PCR was also used to amplify *mei-1* sequences from a full-length cloned cDNA (pHR8; Clark-Maguire and Mains, 1994a) for cloning into the yeast two-hybrid expression vectors (see below). Primers designed for this purpose and sequencing are shown in Figure 6.

### Sequencing of *mei-2* mutations

For each mutation, approximately 10 homozygous worms were lysed under standard conditions (Williams, 1995). PCR was performed on these mutant templates, using primers specific for the *mei-2* region. PCR products were extracted from gel slices after electrophoretic separation in 1% agarose. The DNA was purified with Prep-a-Gene matrix (BioRAD) and sequenced with ABI (PE Applied Biosystems) technology by Glenis Wiebe at the University Core DNA Services (University of Calgary). At least two independent PCR reactions were sequenced for each mutant.

**Figure 5. Location and sequence of primers within F47G4.4 and F47G4.5.**

Sense primers (drawn above the gene) and antisense primers (drawn below the gene) were designed for multiple experiments discussed in this thesis. Certain primers contained added restriction sites for cloning into expression vectors: BamHI (1,3); XhoI (2,4).

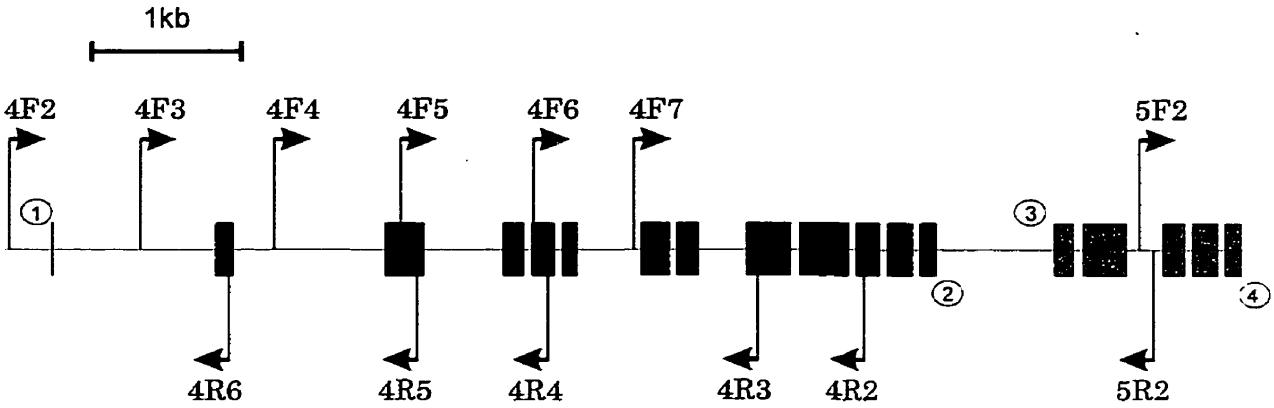


F47G4.4

| | | |
|---|---|---|
| | 4F1 | 5′-GTTGCGAAGAAGGAGAATAG-3′ |
| | 4F2 | 5′-TCATGGTGTTCGGTTTTAGG-3′ |
| | 4F3 | 5′-AGCTTCTGGGGTGGAAAAG-3′ |
| | 4F4 | 5′-GAATTTTGACCAGGCGTTGC-3′ |
| | 4F5 | 5′-TGCGATTCTCAAAGTTGCGG-3′ |
| | 4F6 | 5′-GTCACGCACTAGAGCTTCAC-3′ |
| | 4F7 | 5′-ACATTTCAACGCCAGTTATG-3′ |
| | 4R1 | 5′-CGTAGAGAAACCTGAAAATC-3′ |
| | 4R2 | 5′-GCATCTTGAGCCGTCGGATG-3′ |
| | 4R3 | 5′-TGTGGACCCCGCTGGTTTTG-3′ |
| | 4R4 | 5′-CGCTGGCTTGAATATCATCC-3′ |
| | 4R5 | 5′-CAATCACAATCCGATGACCC-3′ |
| | 4R6 | 5′-GAAGCACTTCGTATGGTCCC-3′ |
| ① | 4BF | 5′-CGGGATCCATGAAAATTGAAGTGGTA-3′ |
| ② | 4XR | 5′-CCGCTCGAGCTAGATCTTCTTTAAAAG-3′ |

F47G4.5

| | | |
|---|---|---|
| | 5F2 | 5′-GGCCATTGACTGGCTTAACA-3′ |
| | 5R2 | 5′-AATCCCACAAGCCACAATTT-3′ |
| ③ | 5BF | 5′-CGGGATCCATGGCACTAACAAGCGTA-3′ |
| ④ | 5XR | 5′-CCGCTCGAGTCAAATGCTCTTCAATCG-3′ |

**Figure 6. Location and sequence of primers within *mei-1*.**

Sense primers (drawn above the gene) and antisense primers (drawn below the gene) were designed for multiple experiments discussed in this thesis. Certain primers contained added restriction sites for cloning into expression vectors: BamHI (1); SalI (2); XhoI (3). A PstI site very near the *mei-1(ct46*gf*)* lesion was used to produce a *mei-1(ct46*gf*)* cDNA for yeast two-hybrid experiments. A primer (4) was designed with the *mei-1(ct46*gf*)* mutation (in bold) for PCR amplification.

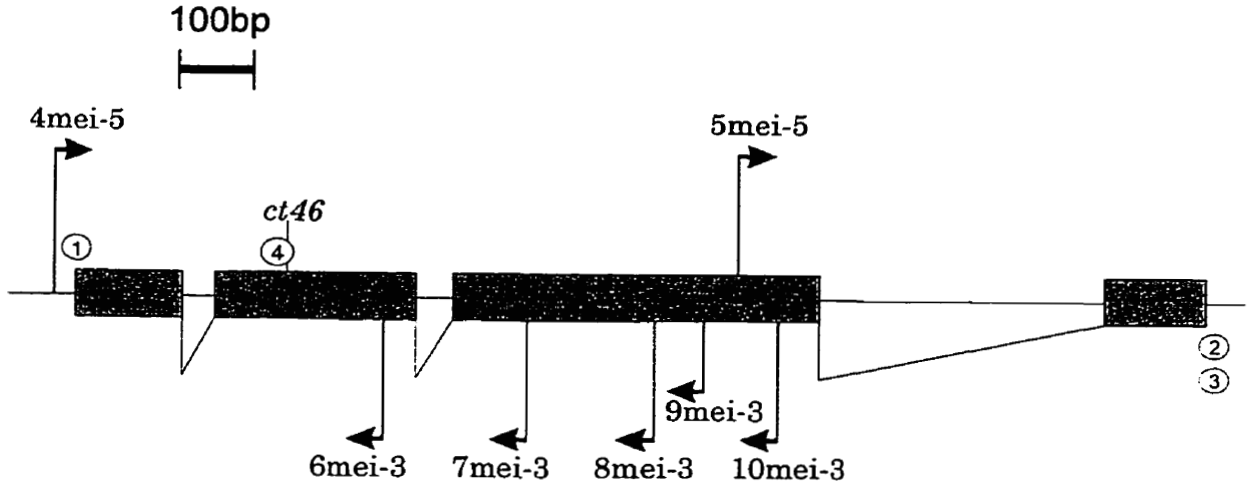


| | |
|---|---|
| 4mei-5 | 5'-GTTCCGTCGTTTCCCTATTCG-3' |
| 5mei-5 | 5'-TCGATGAGGCACTCCGAAGAC-3' |
| 6mei-3 | 5'-TGTGTTGGATTCGCAGGCTTC-3' |
| 7mei-3 | 5'-CTTGCTTCACGTCGTGCATTC-3' |
| 8mei-3 | 5'-ACGCCACTTGCTGGACAGATC-3' |
| 9mei-3 | 5'-TTTAACACGCCGACTCGCTTC-3' |
| 10mei-3 | 5'-TCGGATTTCGGAGTTCCTTCC-3' |

| | |
|---|---|
| ① mei-1BamF1 | 5'-GGGATCCAGAATGGGGATGTGCAGTCA-3' |
| ② mei-1SalR1 | 5'-CTGGTCGACTTACATGGCACCAAAAGAG-3' |
| ③ mei-1XhoR1 | 5'-CTGCTCGAGTTACATGGCACCAAAAGAG-3' |
| ④ ct46PstF | 5'-CACCTGCAGACCTAGATCTTTGGTCC-3' |

## Northern analysis

RNA isolation was carried out on animals that were staged according to the method described in Wood (1988). Adult hermaphrodite strains with temperature-sensitive (*ts*) mutant germlines were also included. When grown at the restrictive temperature, *glp-1(q231)* fail to proliferate their germline (although a few sperm are made in Glp-1 animals; Austin and Kimble, 1987), *fem-3(q20gf)* animals make sperm but no oocytes (Barton *et al.*, 1987), and *fem-1(hc17lf)* animals make oocytes but no sperm (Nelson *et al.*, 1978). Stage-specific poly(A)$^+$ RNA was prepared using the FastTrack mRNA Isolation System (Invitrogen) according to the manufacturer's protocols. Poly(A)$^+$ RNA (3 μg per lane) was fractionated by electrophoresis under denaturing conditions as described (Sambrook *et al.*, 1989), transferred to a Hybond-N$^+$ membrane (Amersham) and hybridized in 5X Denhardt's, 5X SSPE, 0.6% SDS solution with random-primed $^{32}$P-labeled probes (using the Prime-It II Random Primer Labeling Kit, Stratagene). The highest stringency wash was 0.1X SSPE, 0.6% SDS, at 66°C. The *cdc-25.1* probe template was a 2.5 kb EcoRI-SacI genomic fragment that contained the entire coding region. A 1.4 kb XbaI-SpeI genomic fragment which produced a *mei-2*-like RNAi phenotype was used as the *mei-2* probe (see Results, Fig. 19). The blot was simultaneously probed with a ribosomal protein gene (*rp21*, kindly provided by J. Spieth, Indiana University,

Bloomington) to quantify RNA levels. RNA was sized by loading one lane with the G319 Molecular Weight Ladder (Promega), which was removed from the gel and stained with ethidium bromide. Exposure of the blots and signal quantification were performed with the Storm PhosphorImager and ImageQuaNT software (Molecular Dynamics). Images were cropped and processed with Adobe Photoshop and Corel Draw software.

**Antibodies**

Full-length MEI-2 cDNA was obtained by RT-PCR amplification using primers BamMEI-2F and KpnMEI2R (Fig. 4) which contain linkers for insertion into a HIS-tagged fusion vector (QE30) from the QiaExpression kit (Qiagen). Bacterially expressed protein was purified under denaturing conditions (8M urea) by passage through a Ni-NT Agarose column, using manufacturer's protocol. This purified protein was electrophoresed through an SDS-PAGE gel and excised to immunize rabbits (Harlow and Lane, 1988). Antiserum (MS-3F) was affinity purified as follows: an N-terminal portion (residues 2-99) of MEI-2 was fused to GST (glutathione-S-transferase, Promega), bacterially expressed and purified under native conditions. Approximately 2 mg of purified GST-MEI-2(2-99) protein was coupled to cyanogen bromide-activated Sepharose (Pharmacia). Antiserum (500 μL) was applied to the GST-MEI-2(2-99) Sepharose column to produce affinity-purified

antiserum used for all Western blots and immunofluorescence microscopy experiments described herein. Anti-MEI-1 serum (Clark-Maguire and Mains, 1994b) was affinity purified as above with an N-terminal portion (residues 13-217) obtained by inserting an EcoRV - EcoRI *mei-1* cDNA fragment into the GST fusion vector described above (F. Allen, *pers. comm.*). The mouse anti-α-tubulin monoclonal antiserum was described in Piperno and Fuller (1985).

**Immunoblotting**

For all Western analyses, worms were picked into 5 μL of $ddH_2O$ and immediately frozen in a dry ice/ethanol bath. 5 μL of 2X SDS-PAGE loading buffer was added to the frozen worms and the resulting mixture was immediately transferred to a boiling water bath for 10 minutes prior to loading. One hundred gravid adult worms were used for each lane except for the *ct102* lane (genotype: *dpy-5 mei-2(ct102) unc-29*) which contained 125 worms because the *dpy-5* mutation resulted in an approximate 1/4 decrease in the level of signal with the loading control probe, anti-α-tubulin. This was likely due to Dpy-5 worms containing fewer fertilized eggs than wild type. All *mei-2* mutants were linked to *unc-29* and therefore, Unc-29 worms were used for the control lane.

After SDS-PAGE, proteins were electrophoretically transferred to PVDF (Millipore) filters (Sambrook *et al.*, 1989). Filters were blocked in blocking

buffer: 5% skim milk in PBS + 0.1% Tween-20 (PBS-T) overnight at 4°C, washed with PBS-T and incubated 1 hr with the primary antibody in blocking buffer at room temperature. The filters were then washed at least three times for a total of 30 min with PBS-T and incubated with HRP-coupled secondary antibodies (Sheep anti-mouse (Amersham) at 1/2000 dilution or Goat anti-rabbit (Jackson Immunoresearch) at 1/5000 dilution) for 1 hr at room temperature. After a final round of washes for 30 min, the filters were exposed using chemiluminescence (ECL).

**Indirect immunofluorescence microscopy**

Preparation of embryos for immunohistochemistry was performed using the methanol-acetone method of Albertson (1984), and as modified by Kemphues *et al.* (1986). Gonads were released into Egg buffer (Edgar, 1995) by scissoring gravid adults at the head or tail with two 21 gauge needles. Fixation of gonads was performed as above. Affinity purified MEI-2 antiserum (MS-3F) was used at 1/100 dilution. The immunolocation of α-tubulin was performed as described by Clark-Maguire and Mains (1994a). Secondary antibodies (at 1/100 dilution) used were either FITC conjugated Goat anti-rabbit and TRITC conjugated Goat anti-mouse, or Cy3 conjugated Donkey anti-rabbit and Cy2 conjugated Donkey anti-mouse (Jackson Immunoresearch). Stained embryos were immersed in a 1 μg/mL solution of DAPI (4',6-diamidine-2'-phenylindole

dihydrochloride) prior to mounting in a 1 mg/mL solution of p-phenylenediamine in 90% glycerol to reduce fluorescence fading. Photographs were taken with a Zeiss Axioplan fluorescence microscopy camera on Techpan film (Kodak) and developed at ASA100. Photographs in Fig. 25C-E were obtained with a Leica DMRE fluorescence microscope and deconvolved using Vay-Tek software. All images were cropped and processed with Adobe Photoshop and Corel Draw software.

**RNA-mediated interference (RNAi)**

All genomic DNA templates were cloned into the pBluescript SK(+) vector (Stratagene). Transcription with T7 and T3 RNA polymerases (Pharmacia) was performed directly on linearized template according to the manufacturer's instructions. For F47G4.4 and F47G4.5 RNAi, M13 forward and reverse primers were used to amplify the cloned cDNA, followed by transcription from gel-purified template using T3 and T7 reactions with the Ambion MEGAscript system. After transcription, all DNA templates were digested with DNase I, and the resulting RNAs were purified via standard phenol/chloroform extraction followed by ethanol precipitation. To make dsRNA, RNA from both forward and reverse reactions were mixed in a 1:1 ratio (100 ng/μL each), denatured at 95°C, and allowed to reanneal by slow cooling for approximately 10 min. All RNAs were injected into the syncytial gonad of

young N2 adult hermaphrodites, which were allowed to recover at 20°C for several hours. Only healthy survivors of the injection procedure were analyzed further. These injected animals were transferred to individual plates and allowed to lay approximately 20 embryos at 20°C before being picked to a fresh plate. Embryos from animals that laid dead eggs were analyzed further by dissecting and mounting on 5% agar pads for Nomarski photomicroscopy. Embryos were flash-photographed on a Zeiss Axioplan microscope with Techpan film (Kodak) developed at ASA100.

**Yeast two-hybrid protocols**

The yeast experiments were performed using reagents, vectors, and protocols from the CLONTECH Matchmaker GAL4 System 2. Selection for pAS2-1 and/or pACT2 plasmids was accomplished by plating on synthetic dropout media (SD; Bio101), lacking the amino acid tryptophan (-TRP) or leucine (-LEU), or both (-TRP,-LEU). The pAS2-1 vector contains the TRP1 marker, which confers tryptophan prototrophy. The pACT2 vector contains the LEU2 marker, which confers leucine prototrophy. The positive controls were pVA3-1 (a GAL4 DNA-binding domain/murine p53 fusion protein in vector pAS2-1) and pTD1-1 (a GAL4 activation domain/SV40 large T-antigen fusion protein in vector PACT2). pVA3-1 was used to transform yeast strain Y190 (MATa) and pTD1-1 was used to transform yeast strain Y187 (MATα). The

empty pAS2-1 and pACT2 vectors did not produce a positive result (R. Dow, *pers. comm.*). The majority of diploid yeast assayed for 2-hybrid protein-protein interactions were negative. These negative results were useful controls since the plasmid vectors, yeast strains, and subsequent protocols were identical to those that gave positive results. However, in some cases (see Results, Fig. 33), additional negative controls were performed to verify positive results. Basically, a wire loop was used to streak out the same mated cells on single-selection plates (either SD-LEU2 or SD-TRP) to select for only one of the plasmids (Fig. 7). Although there is no negative selection to prevent the inclusion of both plasmids, the vast majority of cells do not mate and therefore have only one plasmid. No positive results were observed with these controls.

All MEI-1, MEI-2, and MEL-26 fusion constructs were cloned into both pACT2 and pAS2-1 vectors. Schematic representations of all fusion fragments are shown in Figure 8. All DNA-binding domain fusions were propagated in Y190 (MATa) and all activation domain fusions were propagated in Y187 (MATα). To test for a physical interaction between two proteins, the appropriate Y190 and Y187 strains were mated as described in Figure 7. After 3-4 days at 30°C, the colonies were assayed for β-galactosidase activity via the colony-lift filter method (Breeden and Nasmyth, 1985) using CLONTECH protocols. Filters were incubated in Z buffer (CLONTECH; which contains

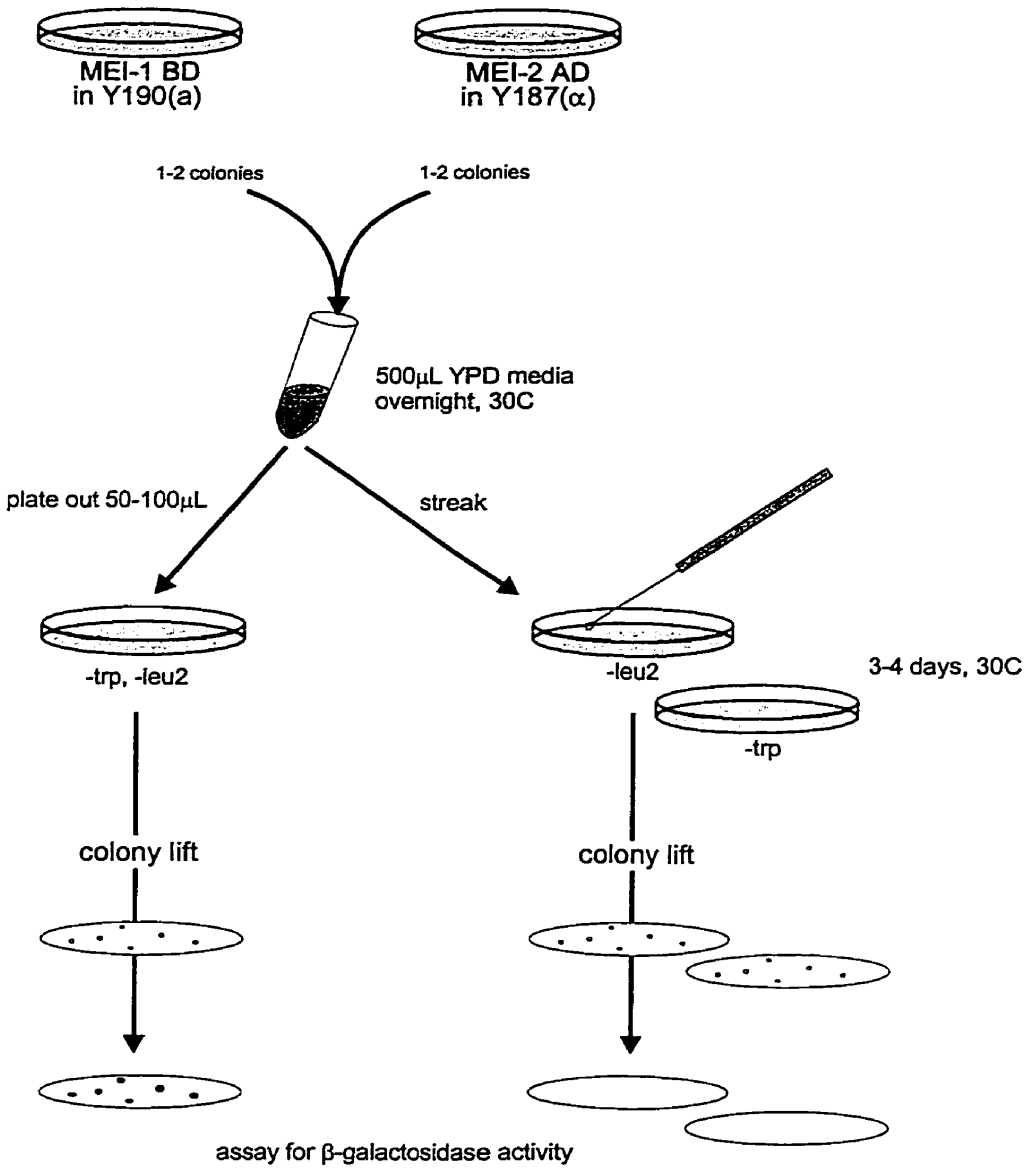


**Figure 7. The yeast two-hybrid mating protocol.**

Clones for yeast two-hybrid analysis were propagated in either Y190 or Y187. To test for protein-protein interactions, the yeast strains were mated and diploid progeny were selected for growth on SD-TRP-LEU2 media. Streaking the culture onto -TRP or -LEU media allowed for concurrent assays on haploid yeast containing only one fusion construct.

**Figure 8. Fragments of MEI-1, MEI-2, and MEL-26 used in yeast two-hybrid experiments.**

A schematic representation of the regions fused to GAL4 DNA-binding domain and activation domain is shown. All fragments were cloned into both pACT-2 and pAS2-1 vectors (CLONTECH). The size (kDa) of each full-length protein and the positions of internal residues are indicated.

*(A)* MEI-2F is the full-length protein, MEI-2A is the N-terminal half and MEI-2B is the C-terminal half. Hatching indicates the region most similar to katanin p80 (see Fig 21B for details). MEI-2F was cloned from cDNA using primers pGEXBMEI2F and MEI2-PstR1 or MEI2-SacR1. MEI-2A was cloned using primers pGEXBMEI2F and MEI2-PstR2 or MEI2-SacR2. MEI-2B was cloned using primers MEI2-BamF5 and MEI2-PstR2 or MEI2-SacR2.

*(B)* MEI-1F is the full-length protein, MEI-1A is N-terminal half and MEI-1B is the C-terminal half. The position of *mei-1(ct46*gf) (a P to L substitution) is indicated. MEI-1F was cloned from cDNA using primers mei-1BamF1 and mei-1XhoR1. MEI-1A and MEI-1B were constructed by M. R. Dow (unpublished). MEI-1(*ct46*gf) was made in multiple steps using the primer ct46PstF, which contains the *ct46* mutation and a neighbouring PstI site.

*(C)* MEL-26F is the full-length protein; subregions are represented by A, B, or C. The BTB (*bric à brac, tramtrack*, and *Broad-Complex* domain; Zollman *et al.*, 1994; Dow and Mains, 1998) is shown (black box). All MEL-26 constructs shown were constructed by M. R. Dow (unpublished).

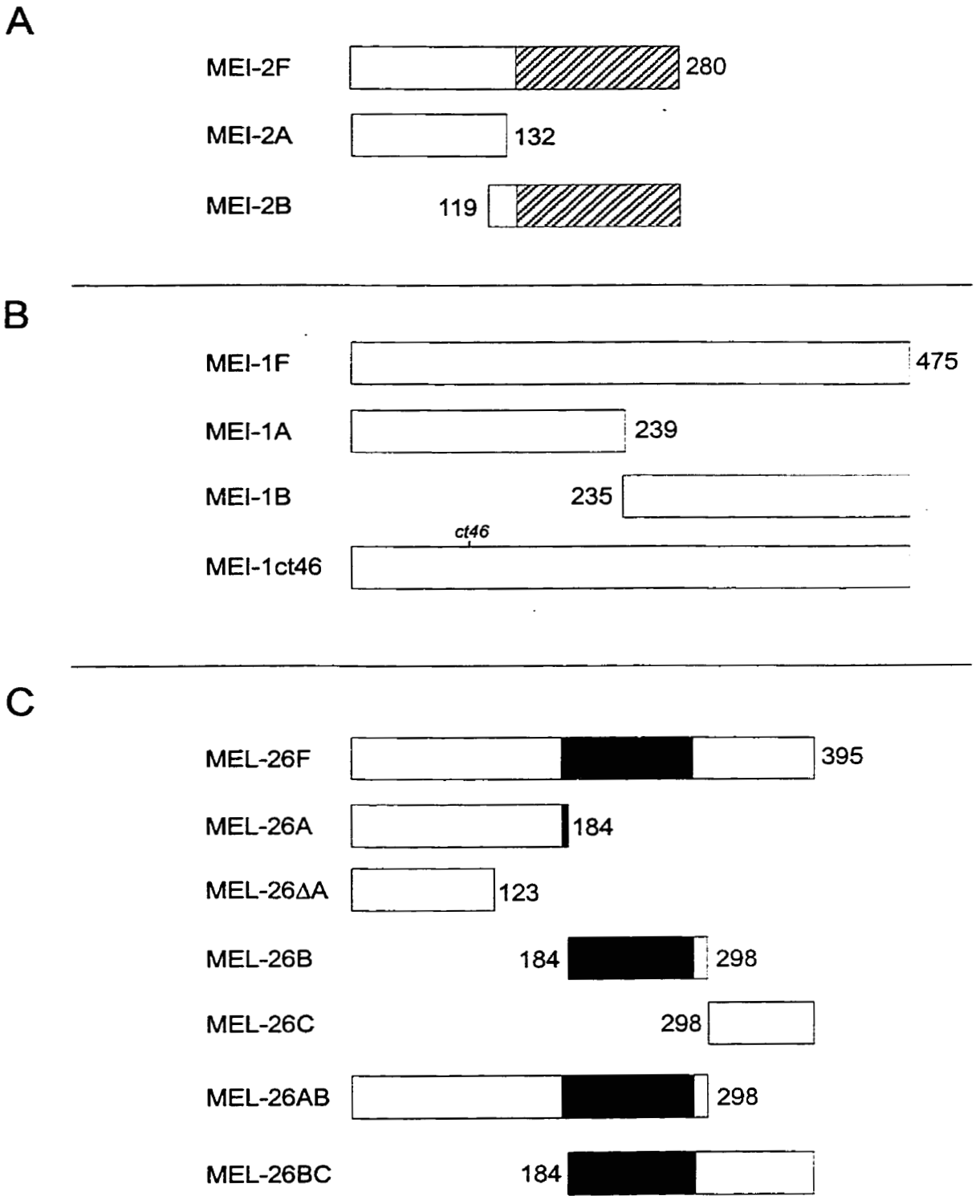
A
MEI-2F
280
MEI-2A
132
MEI-2B
119
B
MEI-1F
475
MEI-1A
239
MEI-1B
235
ct46
MEI-1ct46
C
MEL-26F
395
MEL-26A
184
MEL-26ΔA
123
MEL-26B
184
298
MEL-26C
298
MEL-26AB
298
MEL-26BC
184

X- GAL; 5-bromo-4-chloro-3-indolyl-β-D-galactopyranoside) overnight at room temperature. Filters were dried, scanned and cropped for Figures 30,31,33).

Y190 and Y187 yeast strains are auxotrophic for adenine, due to the mutation *ade2-101*. A red pigment tends to form when growing on media low in adenine. The red colour is likely an oxidized, polymerized derivative of 5-aminoimidazole ribotide, which accumulates in vacuoles (Smirnov *et al.*, 1967; Weisman *et al.*, 1987). The colour of yeast colonies seemed variable and sometimes did not show up well in scanned images, despite being lifted off with the filters. The pink colour did not interfere with the β-galactosidase assay.

# Results

## I. Genetic analysis of *mei-2*

*mei-2* was originally identified as a dominant suppressor of the *mei-1(ct46*gf) mutation approximately twelve years ago. Therefore, much of the genetics of *mei-2* has already been exhaustively studied (Mains *et al.*, 1990; Clandinin and Mains, 1993; Clark-Maguire and Mains, 1994a). However, this early work was performed on two alleles, *mei-2(ct102)* and *mei-2(ct98).* Since then, we have identified two more *mei-2* alleles, and these will be discussed briefly below. A summary of the current state of knowledge on some properties of *mei-2* alleles is presented at the end of this section.

### New alleles of *mei-2*

*sb31* was isolated in a screen for suppressors of *mei-1(ct46*gf). Based on preliminary analysis, *sb31* was thought to be extragenic to *mei-1* and most likely on chromosome I (T. Clandinin, *pers. comm.*). This suggested that the suppressor might be another *mei-2* allele. As an initial test of this idea, the *sb31*-bearing strain was crossed to *mei-2(ct102).* The resulting heterozygote was completely Mel, indicating non-complementation between these mutations

(see Figure 9 for an example of how this analysis was carried out for *sb31* and other *mei-2* candidates).

*sb39* was recovered in a screen for suppressors of *mel-26(ct61)* (M. R. Dow, *pers. comm.*). This mutation was also found to be epistatic to *mel-26(ct61)* such that double homozygotes exhibited meiotic, but not mitotic defects at 25°C (data not shown). This result is consistent with previous observations of *lf* mutations in either *mei-1* or *mei-2*. Complementation analysis with *mei-2(ct102)* demonstrated that *sb39* is also an allele of *mei-2* (data not shown). Further characterization showed that this allele is *ts*, with 85% (978/1146) hatching at 15°C, as compared to 1.1% (8/758) embryos hatching at 25°C. This strong *ts* property makes *mei-2(sb39)* an ideal mutation for identifying suppressors of *mei-2*. In a pilot screen of 5000 F1 progeny from mutagenized *mei-2(sb39)* homozygotes, no suppressors were identified. This indicates that this screen has potential to identify an interacting gene, but may require a relatively large mutagenized population.

**The nature of *mei-2(sb31)***

Geneticists infer biological function from mutant phenotypes. Therefore, it is always necessary to determine the nature of the mutation in question. For example, *mei-1(ct46*gf*)* results in mitotic spindle defects. Knowing nothing about the nature of this mutation, one would conclude that *mei-1* is required

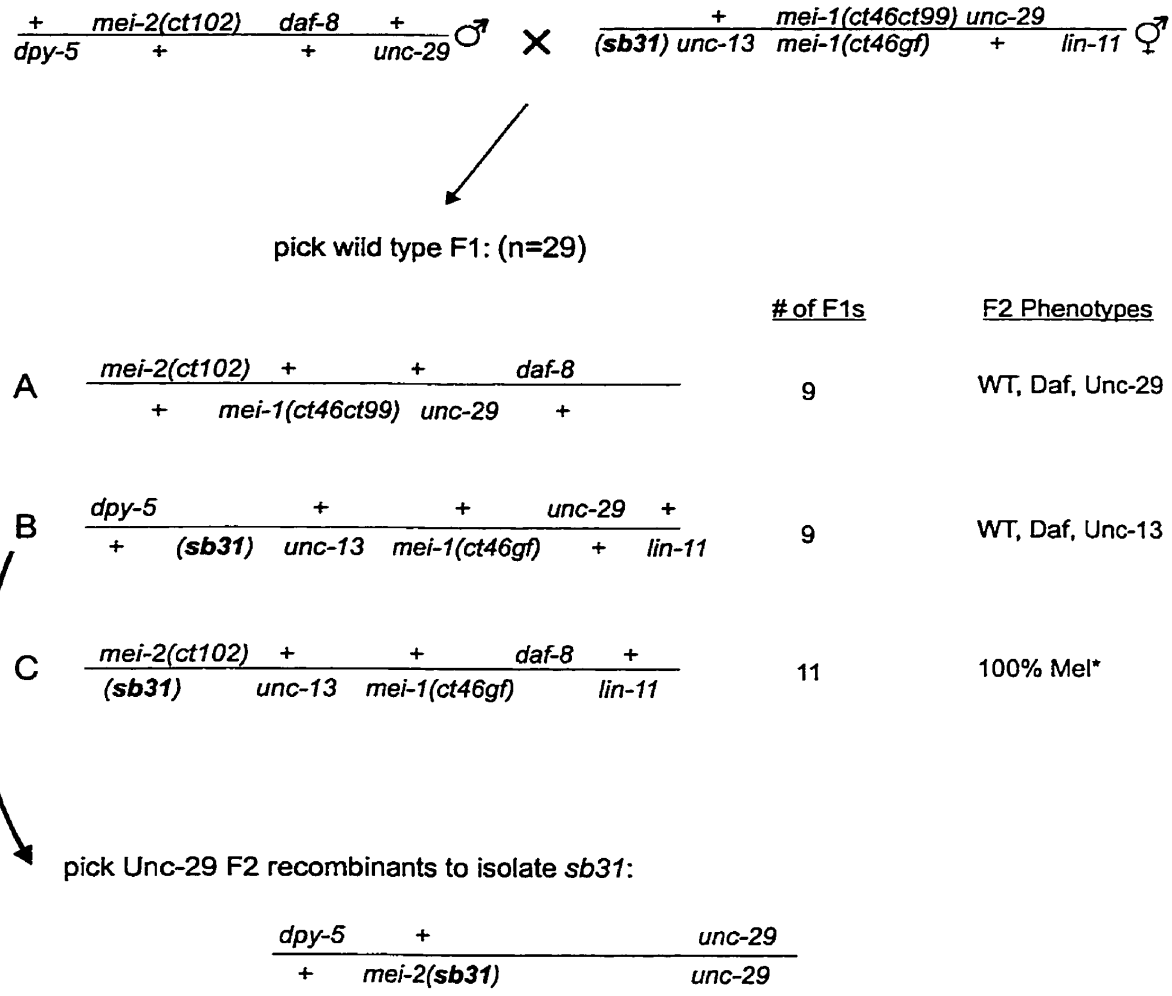


**Figure 9. Complementation testing of candidate *mei-2* alleles.**

A typical strategy to determine if a mutation is allelic to *mei-2* is shown. Males heterozygous for *mei-2(ct102)* were crossed to the strain that contained the suppressor mutation (*sb31*, in bold). All of the expected classes of wild type F1 outcross progeny (*A-C*) were picked to individual plates (Unc-29 progeny were not picked). The genotype of each class was determined by examining the phenotypes of subsequent F2 progeny (shown at right). The number of F1s in each class was also noted (expected 1:1:1 ratio). *Maternal-effect lethality was observed at both 15°C and 25°C.

for mitosis. From careful genetic analysis we know that *mei-1(ct46*gf*)* is, in fact, a *gf* mutation and that *mei-1* is normally required for meiosis, not mitosis (see Introduction). Often, the most reliable way to predict the biological function of a gene is to analyse the null phenotype. Muller's criterion (1932) for the null state requires placement of the gene in question over a deletion that removes the gene. If the *Df/m* phenotype is indistinguishable from *m/m*, then the gene is likely null or nearly null. Previous work showed that *mei-2(ct102)/hDf8* (a relatively small deletion) exhibited 100% maternal-effect lethality, equal in severity to *mei-2(ct102)/mei-2(ct102)* (Table 2, line 1; Mains *et al.*, 1990). This result suggested that *mei-2(ct102)* is a null allele. If *mei-2(sb31)* is also a null allele, it should behave as *mei-2(ct102)*. Indeed, *mei-2(sb31)/hDf8* displayed a 100% Mel phenotype, as did *mei-2(sb31)* homozygotes (Table 2, lines 1-3). In addition, the *mei-2(ct102)/mei-2(sb31)* worms gave exactly the same result as *mei-2(ct102)/hDf8*, further suggesting that at least one of the two alleles is null (Table 2, line 4).

The above experiment indicated that *mei-2(sb31)* was behaving as the deficiency *hDf8*, but these assays may not have been sensitive enough to detect low levels of gene activity. For example, both *mei-2(sb31)* and *mei-2(ct102)* could be very strong hypomorphs or antimorphs (also called dominant-negative, *dn*). The weak allele *mei-2(ct98)* was used to address this problem. *mei-2(ct98)/hDf8* was previously shown to give 42% hatching at 25°C (Table 2, line 5). *mei-2(ct98)/mei-2(ct102)* gave a similar result of 40% hatching

**Table 2. Genetics of *mei-2(sb31)*.**

| Maternal genotype | Embryos hatching 25°C number | percent |
|---|---|---|
| 1. *mei-2(ct102) / hDf8* | - | 0[b,d] |
| 2. *mei-2(sb31) / hDf8* | 0/341 | 0[d] |
| 3. *mei-2(sb31) / mei-2(sb31)* | 0/2000 | 0 |
| 4. *mei-2(ct102) / mei-2(sb31)* | 0/798 | 0 |
| 5. *mei-2(ct98) / hDf8* | - | 42[b,d] |
| 6. *mei-2(ct98) / mei-2(ct102)* | - | 40[b] |
| 7. *mei-2(ct98) / mei-2(sb31)* | 2/674 | 0.3 |
| 8. *mei-2(ct98) / mei-2(sb31)* | 90/577 | 15.6[f] |
| 9. *mei-2(ct98) / mei-2(ct98)* | - | 72[b] |
| 10. + *mei-1(ct46*gf) / + | - | 0.5 |
| 11. + *mei-1(ct46*gf) / *mei-2(ct98)* + | - | 61[a] |
| 12. + *mei-1(ct46*gf) / *mei-2(ct102)* + | 846/1045 | 81 |
| 13. + *mei-1(ct46*gf) / *mei-2(sb31)* + | 1234/1449 | 85 |
| 14. + *mei-1(ct46*gf) / *hDf8* + | - | 1[b,d] |
| 15. *mei-2(sb31)* / + | 552/567 | 97 |
| 16. *mei-2(sb31)* / + / + | 232/256 | 91[e] |
| 17. *mei-2(sb31) / mei-2(sb31)* / + | 629/783 | 80[e] |
| 18. *mei-1(ct46ct82)* / + | - | 98[c] |
| 19. *mei-1(ct46ct82) / mei-1(ct46ct82)* / + | - | 11[c,e] |

[a] Data from Mains *et al.* (1990).
[b] P. E. Mains, *pers. comm.*
[c] Data from Clark-Maguire and Mains (1994a).
[d] Data was corrected for the deficiency homozygotes contributing to 25% lethality
[e] Genotypes include the free duplication, *sDp2 (+)*.
[f] Experiment conducted at 15°C

at 25°C (Table 2, line 6). If *mei-2(sb31)* and *mei-2(ct102)* are equivalent, then *mei-2(ct98)/mei-2(ct102)* and *mei-2(ct98)/mei-2(sb31)* should give the same result. Interestingly, this experiment showed that the two alleles are not equivalent. *mei-2(ct98)/mei-2(sb31)* gave only 0.3% hatching at 25°C (Table 2, line 7). From these results, one could conclude that *mei-2(ct102)* was still behaving as a null (*i.e., hDf8*) but that *mei-2(sb31)* may be a *dn* allele.

Previous work indicated that *hDf8* does not suppress *mei-1(ct46*gf) (P. E. Mains, *pers. comm.;* Table 2, line 14). However, *mei-2(sb31)* was able to suppress *mei-1(ct46*gf), to the same extent as *mei-2(ct102)* (Table 2, lines 10-14). This suggests that removing one copy of *mei-2* (as in *hDf8/+*) is not enough to suppress *mei-1(ct46*gf). For instance, the mutant gene product may antagonize wild-type copies, resulting in less total activity in *dn/+* backgrounds than in *Df/+* backgrounds. If a threshold of *mei-2(+)* activity is required for aberrant *mei-1(ct46*gf) activity, the difference between *mei-2(dn)/+* and *hDf8/+* need not be extreme. Although *dn* alleles are relatively rare, it is not unreasonable for this case, since all *mei-2* alleles were selected as dominant suppressors of aberrant mitotic *mei-1* activity (in either *mei-1(ct46*gf) or *mei-26(ct61)* backgrounds). *mei-2(sb31)* would be the strongest *dn* allele and *mei-2(ct98)* the weakest.

Another explanation for the *mei-2(sb31) – hDf8* paradox is that *hDf8* may remove another gene that genetically interacts with *mei-1*, thereby

providing a false measure for the null state of *mei-2*. Moreover, the putative locus would be a negative regulator of *mei-1*. Removing a negative regulator of *mei-1* would increase *mei-1*'s activity and counteract the removal of the positive regulator, *mei-2*.

The standard test for a dominant-negative allele is to observe its behaviour in a heterozygote; *i.e.*, *m*/+ should be worse than +/+. In cases where the allele is weakly dominant, this test may not be sufficient to detect *dn* activity. For *mei-2(sb31)*/+, approximately 97% of embryos hatch, a value not significantly different from wild type (Table 2, line 15). In order to increase the sensitivity of the assay, *mei-2(sb31)/mei-2(sb31)*/+ animals were constructed by adding the duplication *sDp2*. In this experiment, *m*/*m*/+ worms gave only 80% hatching (Table 2, line 17). *m*/+/+ gave 91% hatching, indicating that *sDp2* contributes only about 9% lethality. The effect of adding the duplication was not as dramatic as has been observed for other *dn* mutations such as *mei-1(ct46ct82)* (Table 2, lines 18, 19). Therefore, *mei-2(sb31)* is likely not a strong *dn* allele. A summary of some of the genetic properties of *mei-2* alleles is shown in Table 3.

### *hDf8* may contain a negative regulator of *mei-1*

Although it remains possible that *mei-2(sb31)* is weakly *dn*, the original assumption that all *mei-2* alleles are recessive *lf* mutations is more likely.

**Table 3. A summary of the genetic properties of *mei-2* alleles.**

| weak | | | | strong |
|---|---|---|---|---|
| *mei-2(ct98)* | < *mei-2(sb39)* < | *mei-2(ct102)* | < *mei-2(sb31)* | |

| Dominant suppression of *mei-1(ct46gf)* | |
|---|---|
| *ct98, sb39, ct102, sb31* | YES |
| *hDf8* | NO |
| *mei-2*(RNAi) | YES |

Furthermore, the simplest explanation for *mei-2(sb31)*'s behaviour is that it is a null or near-null allele. If *mei-2(sb31)* is a null, *hDf8* must remove another gene that negatively regulates *mei-1*. To test this hypothesis, a nested set of duplications (*hDp15, hDp16, hDp54, sDp2* ; McKim and Rose, 1990) were assayed for their ability to suppress *mei-1(ct46*gf). Adding an extra copy of the putative negative regulator should result in some suppression of *mei-1(ct46*gf). Since *hDf*8 is a small deletion, the gene in question should be near *mei-2* (Fig. 10A). Both *hDp15* and *hDp16* lie just outside of the *hDf8* deletion breakpoint and, as expected, did not suppress *mei-1(ct46*gf) (Fig. 10B,C). The *hDp56* endpoint is within *hDf8* but this duplication does not rescue *mei-2* mutations (P. E. Mains, *pers. comm.*). *hDp56* was able to suppress *mei-1(ct46*gf), suggesting that a negative regulator does reside in the region common to both *hDf8* and *hDp56* (Fig 10B,C). The larger duplication *sDp2* also should contain

**Figure 10. A negative regulator of *mei-1* maps near the *mei-2* locus.**

*(A)* The position of the deletion *hDf8* is shown. Chromosomal positions of *mei-1*, *mei-2* are indicated (cM from chromosome centre (0.0); shown above each gene).

*(B)* Four duplications, showing the approximate position of their right breakpoints aligned relative to the map in *A* are shown, with chromosomal position indicated. Note that only *hDp56* enters the zone deleted by *hDf8*. Each duplication was placed in combination with two *mei-1(ct46*gf) chromosomes.

*(C)* The various *mei-1(ct46*gf)/*mei-1(ct46*gf)/*Dp* combinations were scored for percent hatching at 20°C. Only *hDp56* showed an increase in hatching. The putative negative regulator of *mei-1* should reside in the region of overlap between *hDf8* and *hDp56*. This region corresponds to approximately 85 kb (Barnes *et al.*, 1995).

A

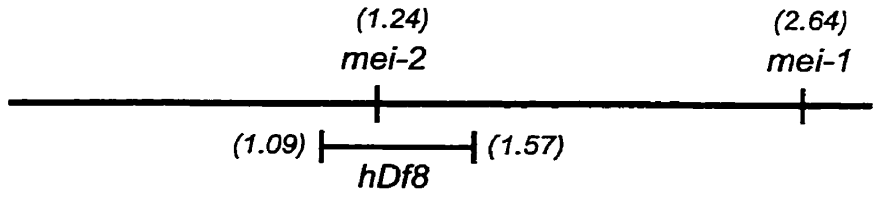


B

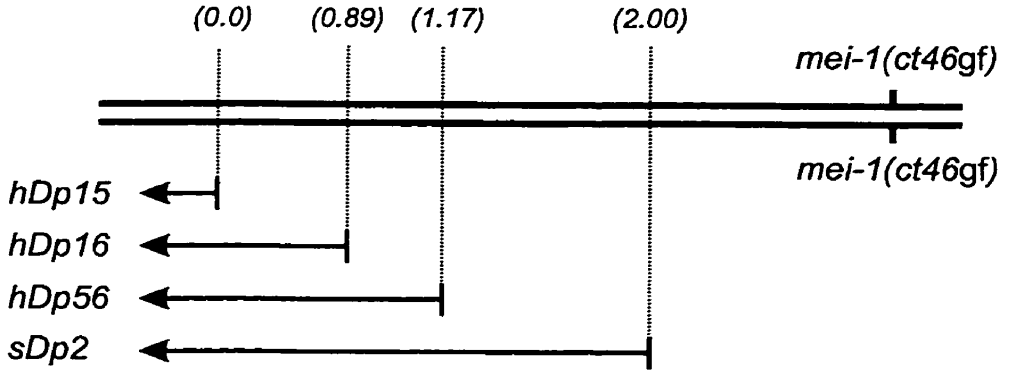


C

| Maternal genotype | Embryos hatching (20°C) number | percent |
|---|---|---|
| *mei-1(ct46gf) / mei-1(ct46gf) / hDp15* | 6/1048 | 5.8 |
| *mei-1(ct46gf) / mei-1(ct46gf) / hDp16* | 62/1159 | 5.3 |
| *mei-1(ct46gf) / mei-1(ct46gf) / hDp56* | 151/941 | 16.0 |
| *mei-1(ct46gf) / mei-1(ct46gf) / sDp2* | 74/1295 | 5.7 |

the putative negative regulator, but it did not suppress *mei-1(ct46*gf*)*. This can be explained by the fact that *sDp2* contains both *mei-2* (which is an activator of *mei-1*) and the negative regulator. This putative negative regulator may be responsible for the slight dominant-negative properties apparent in the *mei-2(sb31)/mei-2(sb31)/+* strain (see above). In these experiments, 3 copies of the negative regulator may reduce *mei-1*'s activity enough to cause the lethality observed.

## II. Cloning *mei-2*

*mei-2* was previously genetically mapped to chromosome I, 0.016 centimorgans (cM) to the left of *let-607* (P. E. Mains, *pers. comm.*). Barnes *et al.* (1995) estimate a metric of 1062 kb per cM within the gene cluster of chromosome I, which places *mei-2* approximately 17 kb to the left of *let-607*. *let-607* was rescued by cosmids F57B10 and F48A9, thus defining the right-most physical boundary for *mei-2* (Fig. 11; P. E. Mains, *pers. comm.*). The chromosomal duplication *hDp54* (McKim and Rose, 1990) failed to complement the *mei-2(ct102)* mutation and this duplication's right endpoint was physically mapped to C01B6 (and two other overlapping cosmids, T09G11, and T01E9) by a SalI polymorphism (S. Clark-Maguire, *pers. comm.*).

The identification of *mei-2* was paramount to our understanding of meiotic spindle assembly in *C. elegans*. Therefore, various different strategies

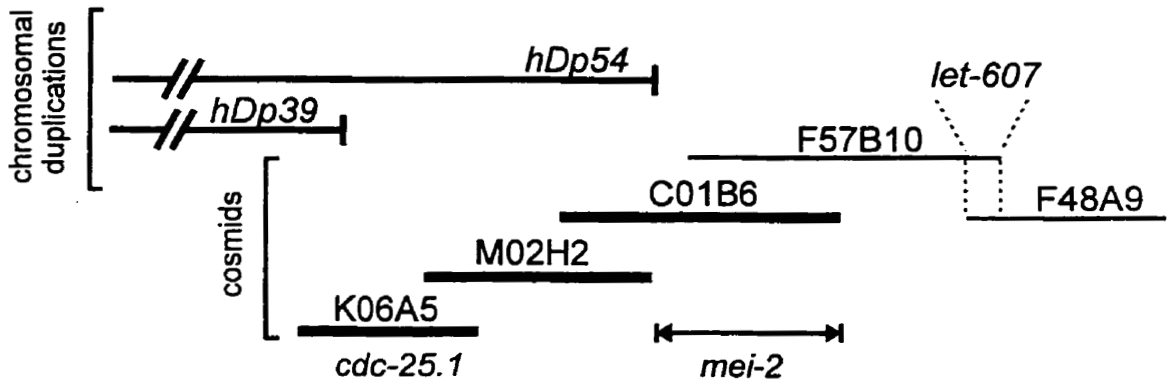


**Figure 11. Genetic and physical mapping of *mei-2*.**

*mei-2* was genetically mapped 0.016 cM (corresponding to approximately 17 kb; Barnes *et al.*, 1995) to the left of *let-607*, a gene that was rescued with cosmids F57B10 and F48A9 (P. E. Mains, *pers. comm.*). The duplications *hDp39* and *hDp54* do not rescue *mei-2* mutations. The endpoint of *hDp54* was mapped to cosmid C01B6, thus placing *mei-2* to its right (S. Clark-Maguire, *pers. comm.*). Cosmids that rescued the *mei-2(ct102)* mutation when co-injected are shown in bold (see text for details).

were employed to undertake the cloning of this gene. First, transformation rescue experiments were performed. Second, restriction fragment-length polymorphism (RFLP) analysis was conducted on the two mutant strains available at that time. Third, genetic screens for null mutations were undertaken, with the purpose of generating a deletion mutation in *mei-2* that would be more likely to produce an RFLP. Finally, RNAi (RNA-mediated interference) was used on various candidate genes to ultimately identify *mei-2*. Although the last technique proved successful, each of the above experiments will be dealt with briefly below.

## Transformation rescue

Cosmid clones from the *mei-2* region were first injected individually into *mei-2(ct102)* homozygotes. No single cosmid from the genetically defined region rescued the *mei-2* mutation. In order to increase the likelihood of rescue, multiple cosmids were co-injected. Recombination can occur between homologous regions of extrachromosomal DNA, thus reconstituting genes broken during cosmid cloning procedures (Mello *et al.*, 1991). + *mei-2(ct102)* + *daf-8/dpy-5* + *unc-29* + males were crossed into independent transgenic lines shown in Table 4, and Rol Daf (at 25°C) progeny were downshifted to allow exit from the dauer larval stage (due to the *ts daf-8* mutation) and scored for maternal-effect lethality. Using this method, rescue of *mei-2* was achieved

**Table 4. Cosmid combinations tested for *mei-2(ct102)* rescue.**

| Cosmids | Concentration | Rescue/lines | Rescue[a] |
|---|---|---|---|
| 1. K06A5 + M02H2 + C01B6 | 30[b]:100[c] | 2/3 | + |
| 2. F14G7 + M02H2 + C01B6 | 30:100 | 2/2 | + |
| 3. K06A5 + M02H2 | 30:100 | 0/2 | - |
| 4. K06A5 + M02H2 | 60:100 | 0/1 | - |
| 5. M02H2 + C01B6 | 30:100 | 0/2 | - |
| 6. M02H2 + C01B6 | 30:100 | 0/2 | - |
| 7. K06A5 + C01B6 | 30:100 | 0/3 | - |
| 8. M02H2 | 30:100 | 0/1 | - |
| 9. C01B6 | 30:100 | 0/1 | - |
| 10. K06A5 + M02H2 + C01B6 + FTR[d] | 30:60 | 0/2 | - |
| 11. C01B6 + FTR[d] | 30:100 | 0/1 | - |

[a] Rescue was determined by comparing to a sibling control group; >2000 embryos were counted for each group of cosmids assayed. *e.g.*, a total of 52/6608 embryos survived from transgenic worms in line 2 versus 1/2676 in control group.

[b] Represents the concentration (ng/μL) of each cosmid in the injection cocktail

[c] Represents the concentration (ng/μL) of plasmid pRF4 (*rol-6*) in the injection cocktail

[d] FTR represents cosmids F57B10, T01E9, R137, which are contiguous to the right of C01B6

with three cosmids K06A5 (or F14G7), M02H2, and C01B6. Four out of five lines showed maternal rescue of *mei-2* (survival of 52/6608 progeny, or 0.8%, compared to 1/2676 (0.04%) for Daf, Non-Rol sibling control group). Unfortunately, no single cosmid or pairwise combination of cosmids from this region rescued *mei-2(ct102)*. The reason for this is unclear but may stem from poor expression typical of maternally-expressed transgenes (Kelly *et al.*, 1997).

## Restriction fragment length polymorphism analysis

Although transgenic rescue did not identify *mei-2,* it did suggest that *mei-2* was within the three cosmids that gave weak rescue. Therefore, RFLP analysis was performed on *mei-2* mutant strains using the cosmids K06A5, M02H2, and C01B6 as probe template (see Fig. 12). When this work was conducted, only two alleles of *mei-2* were known, *mei-2(ct98)* and *mei-2(ct102).* Ten different restriction enzymes were used to digest genomic DNA isolated from each of the two *mei-2* mutant strains (Fig. 12). Southern blots of each mutant's DNA were probed with $^{32}$P- labeled cosmids (Fig. 12). If either of these *mei-2* mutants were the result of a nucleic acid alteration that fortuitously altered a restriction enzyme site, a corresponding change in digestion pattern would be observed. However, no polymorphisms were identified in either of these mutant strains.

## A genetic screen to induce deletion alleles of *mei-2*

To increase the chances of finding *mei-2* via RFLP analysis, a genetic screen was developed to create null alleles of *mei-2.* Gamma radiation was used to mutagenize *mei-2(sb31)/mei-2(ct98)* heteroallelic worms. Based on the results for *hDf8,* a deletion that removes *mei-2(sb31)* and extends left, to include the putative negative regulator, should result in an increase in

**Figure 12. RFLP analysis of *mei-2(ct98)* and *mei-2(ct 102)*.**

Genomic DNAs from *mei-2(ct98)* homozygotes (left lane of each pair) and a *mei-2(ct102)* strain balanced by *sDp2* (right lane of each pair) were digested with: S = SacI/SstI; Sal = SalI; RI = EcoRI; RV = EcoRV; H = HindIII; D = DraI; B = BglII; C = ClaI; X = XhoI; and Sp = SpeI. *mei-2(ct98)* DNA was loaded in the first of each pair of lanes. Digested DNA was Southern blotted and probed with $^{32}$P-labeled cosmids (indicated on right). For many of the restriction-digested DNAs, a large-sized band was present in *mei-2(ct102)* lanes, but not *mei-2(ct98)* lanes. Subclones of these cosmids were used as probes on double-digested genomic DNA to reveal that these high molecular weight bands were probably artefacts associated with partially-digested *mei-2(ct102)* DNA (not shown).

probe

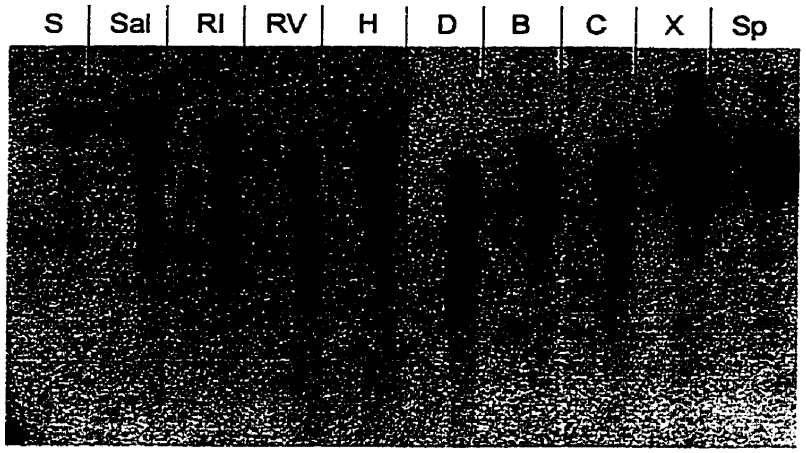


K06A5

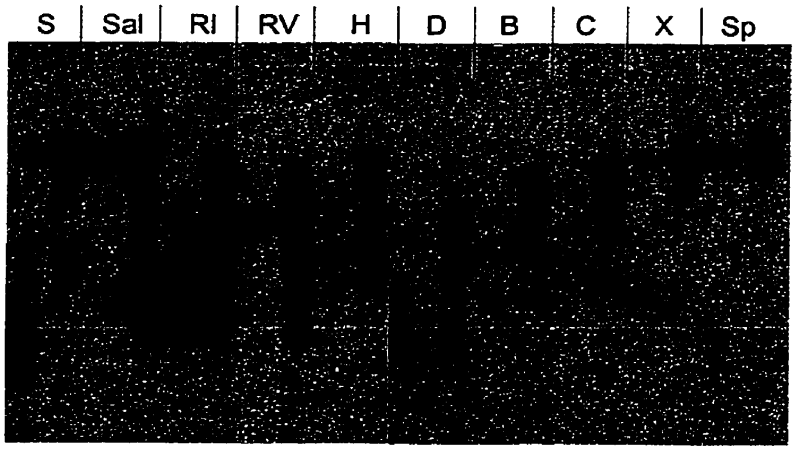


M02H2

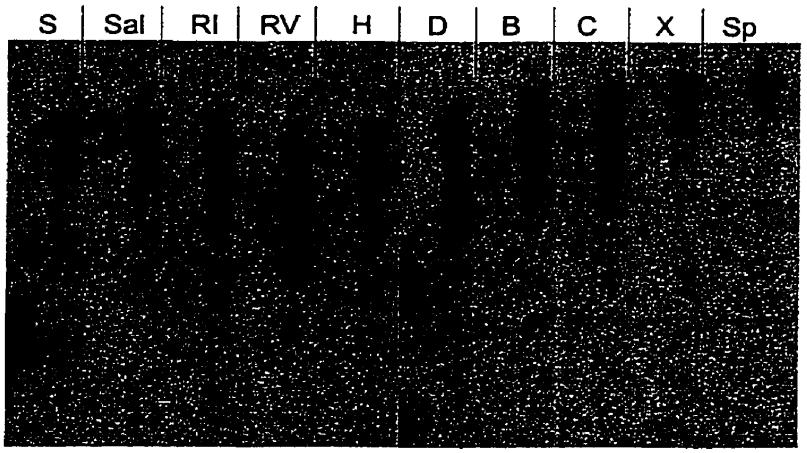


C01B6

hatching (Fig. 13). Such a mutation would be relatively easy to identify by RFLP analysis. However, after screening 14,795 mutagenized chromosomes, no candidates were recovered. The frequency of *lf* or null alleles (based on analysis of a different locus) created by gamma mutagenesis in *C. elegans* is about 1/2000 (Greenwald and Horvitz, 1980). Therefore, this screen may be flawed for reasons unknown.

### An RNAi approach to identify *mei-2*

The technique of RNA-mediated interference (RNAi; Fire *et al.*, 1991; Guo and Kemphues, 1995; Fire *et al.*, 1998; Montgomery *et al.*, 1998) was used to identify *mei-2*. Briefly, RNA is transcribed from a cDNA or genomic clone and injected into the syncytial gonad of a young adult hermaphrodite and the progeny of this animal are assayed for a phenotype. This technique has proven very effective for phenocopying a given gene's null or *lf* phenotype. Throughout the course of this work, the Genome Sequencing Consortium was actively sequencing the *mei-2* region. BLAST (Altschul *et al.*, 1990; Altschul *et al.*, 1997) searches were regularly conducted to look for possible candidates of *mei-2* (Table 5). Two criteria were considered when assessing candidates: 1) MEI-2 should function during female meiosis, 2) MEI-2 may directly interact with the MEI-1 protein; it is expected that MEI-1 attaches either directly or through other proteins to the meiotic spindle apparatus. Due to the diverse

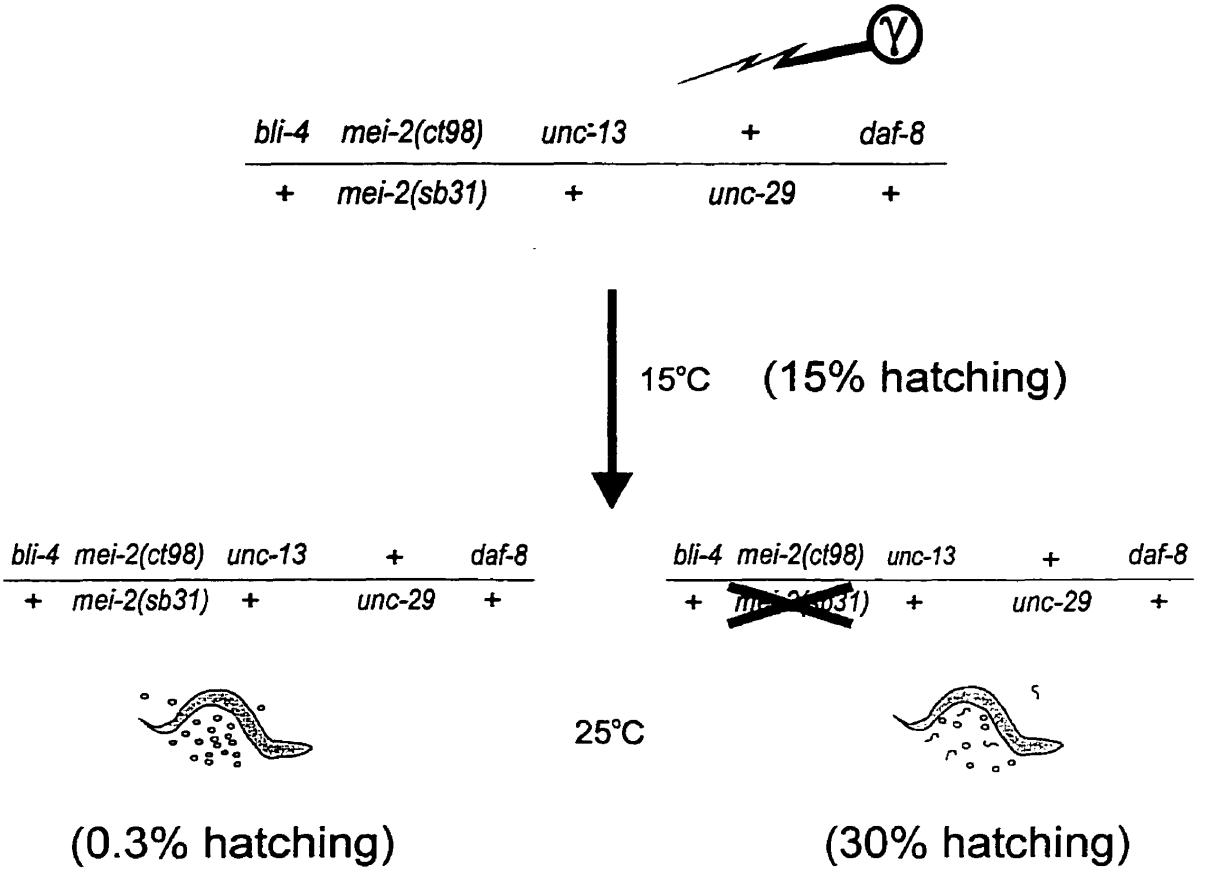


**Figure 13. A genetic screen for *mei-2* null alleles.**

A screen to identify null alleles of *mei-2* was performed by taking advantage of the genetic properties of *mei-2(ct98)*, *mei-2(sb31)*, and the deletion *hDf8* (see Table 2). *mei-2(ct98)/mei-2(sb31)* animals were grown at 15°C and gamma-irradiated (2500 Rads). Wild-type F1 progeny were shifted to the restrictive temperature of 25°C at the L4 (pre-adult) stage. Removal of the *mei-2(sb31)* mutation and the putative negative regulator to the left of *mei-2* was expected to increase hatching to approximately 30% (including potential homozygous lethality of the deletion).

**Table 5. A summary of predicted genes in the *mei-2* region.**

| Cosmid and predicted genes[a] | P-value[d] |
|---|---|
| **K06A5** | |
| 1. Ras-related protein ORA1 | $9.5e^{-80}$ |
| 2. Glutamic acid -rich protein | $3.8e^{-06}$ |
| 3. Acyl-CoA dehydrogenase, short branch | $9.7e^{-161}$ |
| 4. M-phase inducer phosphatase *cdc25* (*C.elegans*) | $7.4e^{-34}$ |
| 5. *C. elegans* predicted gene | $8.4e^{-14}$ |
| 6. G-protein beta 3 subunit | $1.9e^{-07}$ |
| **C55B7**[b] | |
| 7. Sulfate transporter | $1.6e^{-14}$ |
| 8. Lariat debranching enzyme | $1.3e^{-46}$ |
| 9. Vitellogenin | $6.8e^{-11}$ |
| 10. RNA binding protein | $1.3e^{-05}$ |
| 11. Acyl-CoA dehydrogenase, short chain | $2.9e^{-134}$ |
| 12. Similar to Casein kinase | $8.3e^{-50}$ |
| 13. Alpha-1,3(6)-Mannosylglycoprotein | $3.9e^{-39}$ |
| 14. ATP-dependent RNA helicase (*glh-2*?) | $6.7e^{-13}$ |
| **T10E9**[c] (Unfinished) | |
| 15. *C. elegans* predicted gene | $5.3e^{-14}$ |
| 16. NADH dehydrogenase | $2.1e^{-85}$ |
| 17. Acyl-CoA dehydrogenase, short chain | $4.8e^{-31}$ |
| 18. programmed cell death suppressor | $3.4e^{-66}$ |
| 19. trehelase I | $1.0e^{-290}$ |
| 20. DNA repair protein (break in contiguous sequence) | $5.0e^{-38}$ |
| 21. Associated to Golgi apparatus | 0.00043 |
| 22. Synaptonemal complex protein 1 (SCP1) | 0.010 |
| 23. 2,3 Bisphosphoglycerate-mutase | $3.2e^{-100}$ |

[a] *circa* September, 1997
[b] Canonical for M02H2
[c] Canonical for C01B6
[d] Probability that the sequence is similar to query by chance

family of proteins to which MEI-1 belongs, it was not possible to make predictions *a priori* about the specific molecular characteristics of such a protein. In truth, an argument could be made for many of the predicted genes in Table 5 to encode *mei-2*. However, some genes were empirically ruled out; for example, *glh-2* (germline helicase) was already characterized and did not give any RNAi phenotypes similar to *mei-2* (K. Bennet, *pers. comm.*).

Initially, two putative genes were chosen as good candidates for *mei-2* because their homologues had potential meiotic function. One predicted gene, a *C. elegans* member of the *cdc25* phosphatase gene family, was located on K06A5 (Table 5, line 4). Characterized cdc25 homologues, such as *S. pombe* cdc25 (Russell and Nurse, 1986) and *Drosophila string* (Edgar and O'Farrell, 1989; Edgar and O'Farrell, 1990) are involved in regulation of the mitotic cell cycle; mutations in these genes lead to arrest in G2 phase. A *Drosophila* homologue, *twine*, has been shown to be required specifically during meiosis (Courtot *et al.*, 1992; Alphey *et al.*, 1992; White-Cooper *et al.*, 1993). The other potential candidate gene initially showed similarity to a rat coiled-coil-related protein that associates specifically with male meiotic chromosomes, SCP1 (synaptonemal complex protein 1; Meuwissen *et al.*, 1992; Table 5, line 22). Although the initial scores were very low (much of the sequence was not complete), later searches returned higher scores for the human centromere-associated motor protein, CENP-E (Yen *et al.*, 1992). Both the Cdc25

homologue and the CENP-E homologue were considered reasonable candidates for *mei-2*.

If *mei-2* is a cell-cycle regulator such as Drosophila *twine*, there are some predictions that can be made about the possible *in vivo* function of this gene. For instance, *mei-2* would not be expected to have any structural function by associating with the MEI-1 product. Instead, it may directly or indirectly activate the MEI-1 product. Cdc25 homologues activate the Cdc2 kinase by removing a phosphate at Tyr15 and most probably Tyr14 (for a review of Cdc25, see Hoffmann and Karsenti, 1994). Although the targets of Cdc2 are not well established, MEI-1 is likely not a direct substrate as it does not contain the phosphorylation consensus sequence Z-S/T-P-X-Z, where X is polar and Z is generally basic. One possibility is that *mei-2* mutations delay cell-cycle progression without directly affecting MEI-1 or any structural components *per se*. By delaying meiosis, MEI-1 may eventually be degraded by other factors (perhaps involving MEL-26) before fulfilling its role as spindle component, causing meiotic defects. In this way, the *mei-1(*gf*)* mutation may be suppressed by the *mei-2(*lf*)* mutations; meiosis is sufficiently prolonged such that excess *mei-1* activity would be reduced by factors that are not affected by the same delay in cell cycle progression. To test this hypothesis, *mei-2(ct102)/mei-2(ct102)*, *mei-2(ct102)*/+ and +/+ embryos were observed with Nomarski photomicroscopy and time-lapse video-recorded. Four embryos from

each group were scored for time spent in meiosis. As shown in Figure 14, no differences were observed between these groups.

Dr. Andy Golden's group (National Cancer Institute, Frederick, MD) was studying the roles of all four *C. elegans* Cdc25 homologues, encoded by *cdc-25.1*, *cdc-25.2*, *cdc-25.3*, and *cdc-25.4* (Ashcroft *et al.*, 1998). A collaborative effort was initiated to study the *mei-2* candidate, *cdc-25.1*. Towards the goal of determining whether this gene is *mei-2*, a developmental Northern was probed with the *cdc-25.1* gene and RNAi was employed to determine the loss-of-function phenotype of *cdc-25.1*.

**Northern blot analysis of *cdc-25.1***

If *cdc-25.1* is *mei-2*, its expression should be enhanced in the female germline since all *mei-2* mutations are maternal-effect lethal. A Northern probed with a 2.5 kb genomic EcoRI-SacI clone containing the entire *cdc-25.1* gene revealed a single transcript of approximately 2.3 kb, consistent with the size of a previously isolated cDNA (Ashcroft *et al.*, 1998). *cdc-25.1* expression was high in gravid worms (adults containing many fertilized eggs), slightly lower in L1 larval stage and almost absent in the L2/L3 larval stages (Fig. 15).

At the L4 larval stage, expression levels were about as high as in L1. In order to determine if *cdc-25.1* was expressed specifically in the female germline, I also probed RNA isolated from mutant strains lacking oocytes (*fem-*

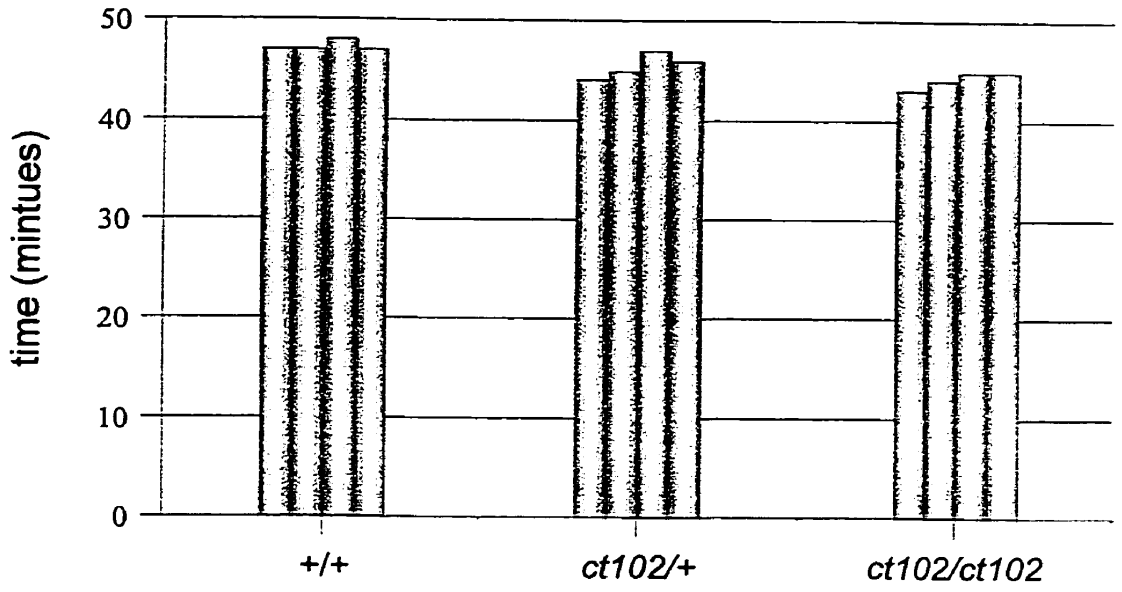


**Figure 14. *mei-2(ct102)* does not result in prolonged meiosis.**

Adult hermaphrodites representing each of the three genotypes listed, were mounted in a 0.1% tetramisole / 0.01% tricaine solution (to paralyze body wall muscles). Oocytes were followed before and after fertilization with Nomarski optics and time-lapse video-recorded. The time from oocyte nuclear envelope breakdown to the completion of the first mitotic cleavage *in utero* was recorded at 25°C.

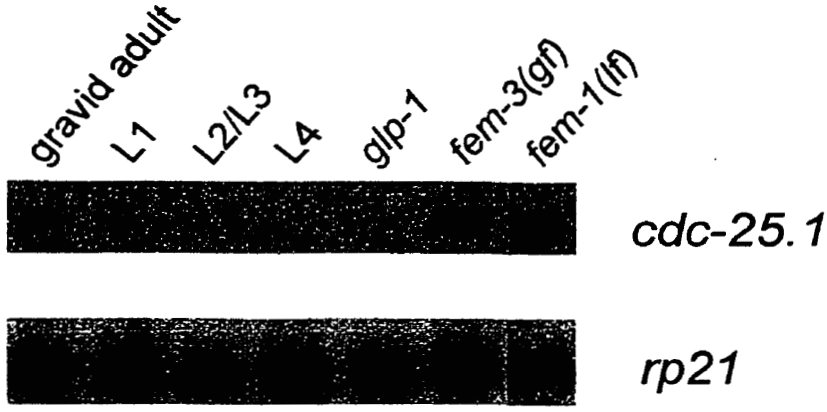


**Figure 15. Northern blot analysis of *cdc-25.1* mRNA.**

Poly $A^+$ RNA was loaded into each lane and probed with a genomic clone containing *cdc-25.1* (see Materials and Methods). RNA was harvested from gravid wild-type hermaphrodites, larval stages L1, L2/L3, L4, *glp-1* hermaphrodites (lacking a germline), *fem-3* adults (which produce sperm, but not oocytes), and *fem-1* adults (which do not produce sperm, and tend to bloat with unfertilized oocytes). As a loading control, the blot was simultaneously probed with *rp21*, a ribosomal protein gene.

*3(q20*gf); Barton *et al.*, 1987), lacking sperm (*fem-1(hc17)*; Nelson *et al.*, 1978) or lacking both due to the loss of mitotic germ cell proliferation (*glp-1(q231)*; Austin and Kimble, 1987). Expression was almost absent in *glp-1*, suggesting that *cdc-25.1* mRNA is specifically expressed in the germline. A strong signal was observed in the *fem-1(hc17)* lane, indicating high expression in female germline; however, *cdc-25.1* was also expressed in *fem-3(q20*gf) mutants, which produce only sperm. Therefore, *cdc-25.1* mRNA is enriched in worms that contain mitotically dividing germ cells. Expression in L4 larvae may also be explained by the above generalization, since germline proliferation is rapid at this stage. The relatively high amounts of *cdc-25.1* mRNA in L1 larvae may reflect a requirement for *cdc-25.1* in late embryonic or early larval cell divisions.

**Analysis of *cdc-25.1*(RNAi) embryos**

The goal of this project was to determine if any of the *cdc-25.1*(RNAi) phenotypes resemble *mei-2* phenotypes. RNA transcribed from the EcoRI-SacI genomic subclone described above was injected into wild-type adult worms. Most of the progeny died as a result of the RNA injection, indicating a clear requirement for *cdc-25.1* in early embryogenesis. Some progeny survived until hatching but most of these were morphologically abnormal and did not develop into adults. Those embryos that did survive to adulthood were sterile (Ashcroft

*et al.*, 1999). Three predominant phenotypes were consistently observed: 1) embryos with abnormal cell sizes and multiple nuclei within some cells (Fig. 16A), 2) fragmentation of the maternal pronucleus (Fig. 16B,C), and 3) large cytoplasts (some of which were found at the anterior; Fig. 16D). Certain aspects of *cdc-25.1* phenotypes were very similar to *mei-2* phenotypes. In particular, *mei-2* mutants often give rise to aneuploid embryos like those shown in Figure 16A. Also, the meiotic spindle defects in *mei-2* mutants frequently lead to fragmented maternal pronuclei. However, the large cytoplasts in *cdc-25.1*(RNAi) were similar but never identical to the large polar bodies produced by *mei-2* mutants. Furthermore, these cytoplasts did not always contain DNA (as assayed by DAPI staining; not shown) suggesting that their genesis may be different from that which gives rise to abnormal polar bodies in *mei-2* mutants, which always contain DNA.

To determine whether the cytoplasts and multiple pronuclei could have resulted from defects in meiosis, the morphology of the meiotic spindles were examined by immunostaining with antibodies directed against α-tubulin and MEI-1. No abnormalities were found in the morphology of the meiotic spindles (Fig. 17*A-F*). However, many of the spindles were displaced from the anterior (Fig. 17*G,H*).

The distance of the meiotic spindle from the anterior was plotted as a percent of egg-length (Fig. 18A). The data clearly show that meiotic spindles in

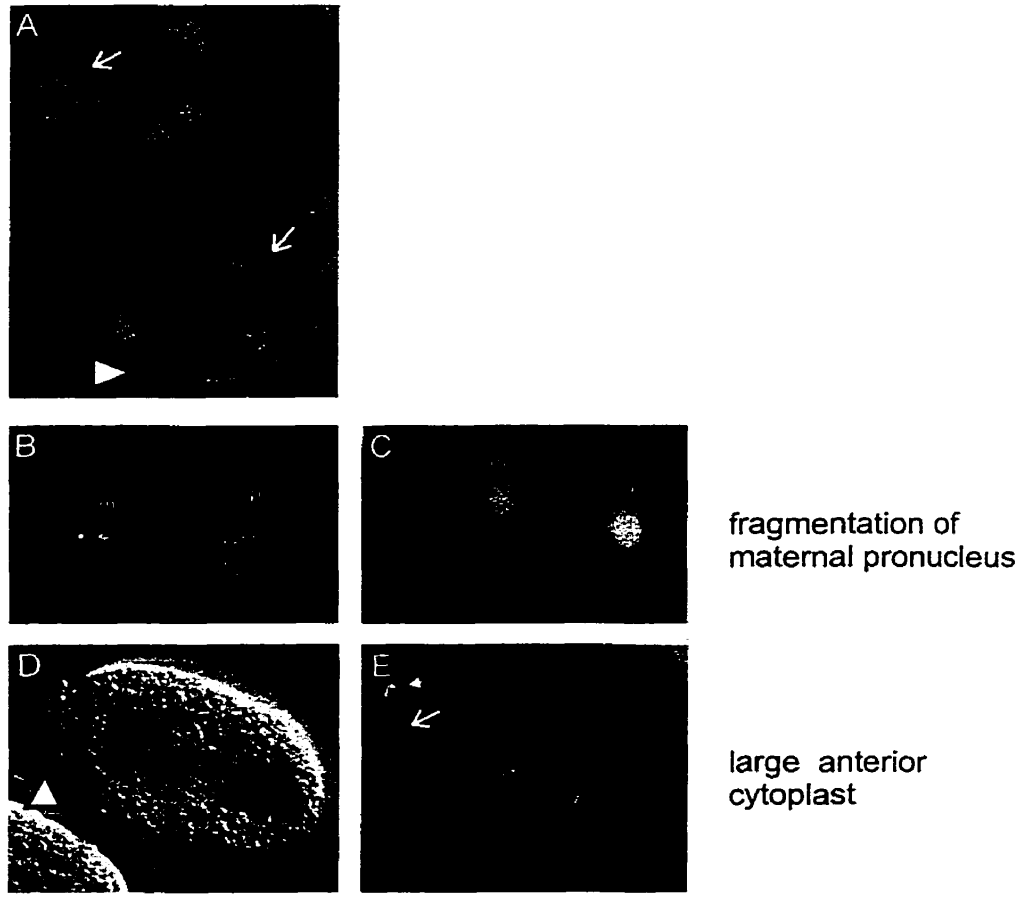


**Figure 16. Phenotypes of *cdc-25.1*(RNAi) embryos**

Representative phenotypes of *cdc-25.1*(RNAi) embryos are shown with Nomarski optics with DAPI *(A,C,E)* or without DAPI *(D)*, or just immunofluorescence of DAPI to visualize chromatin *(B)*. *(A)* Early embryos containing many cells displayed aneuploidy, with multiple nuclei present in some cells (arrows). Cytoplasts often contained no DNA (arrowhead). *(B,C)* Fragmentation of the maternal pronucleus (m) was frequently observed. These smaller nuclear fragments still migrated to meet the paternal pronucleus (p), as shown in *(C)* (two small nuclei on the right of the paternal pronucleus). *(D,E)* Occasionally, a large cytoplast (arrowhead) that contained DNA (open arrow) was observed in the anterior, which may represent a large polar body. A normal-sized polar body is visible above this cytoplast (closed arrow).

**Figure 17. Meiotic spindle morphology is normal in *cdc-25.1*(RNAi) embryos.**

An embryo from an uninjected wild-type worm was stained with DAPI *(A)* and labeled with antibodies against tubulin *(B)* and MEI-1 *(C)*, as described in Materials and Methods. An embryo from a *cdc-25.1* RNA-injected hermaphrodite was stained with DAPI *(D)* and labeled with antibodies against tubulin *(E)* and MEI-1 *(F)*. *(G,H)* Meiotic spindles were often found near the midline of embryos, rather than at the anterior. Chromatin is stained with DAPI. The anaphase I spindle in (*H*) is oriented parallel to the cortex and the focal plane is in the middle of the embryo. Polar body extrusion will probably fail since the segregated chromosomes will not be near the cortex.

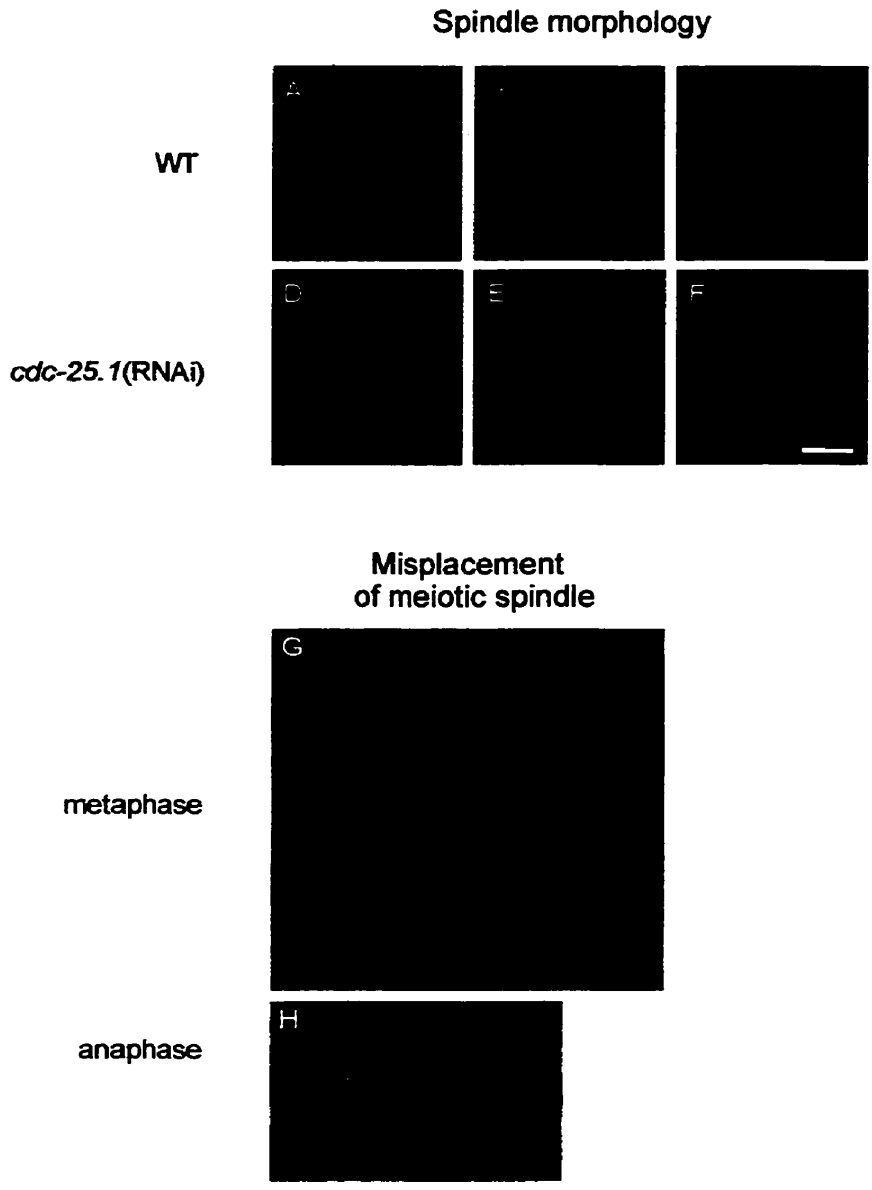
Spindle morphology
WT
cdc-25.1(RNAi)
A
D
E
F
Misplacement
of meiotic spindle
metaphase
anaphase
G
H

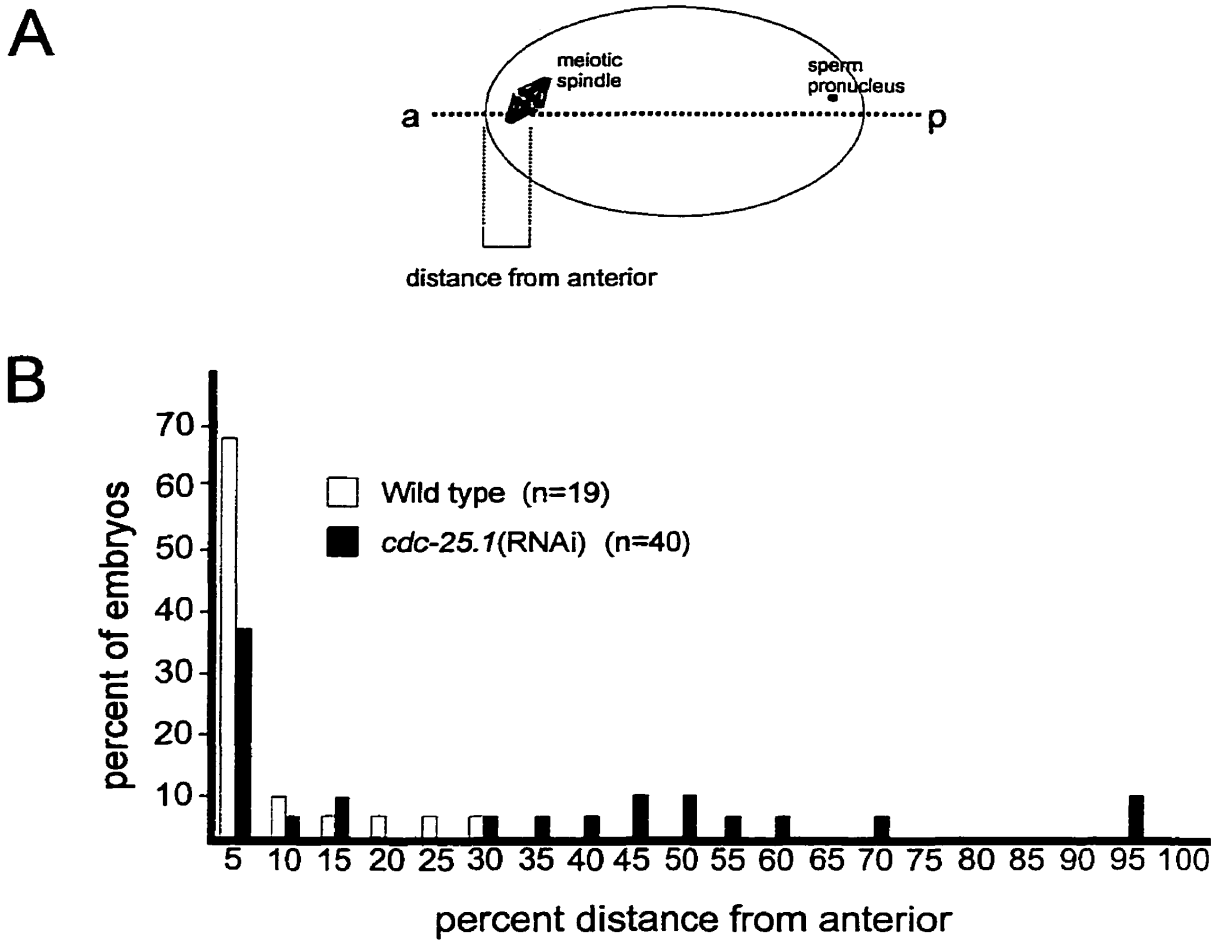


**Figure 18. *cdc-25.1*(RNAi) results in meiotic spindle mispositioning**

Wild type and *cdc-25.1(RNAi)* embryos were dissected from their respective parents, fixed, and stained with DAPI and labeled with antibodies against tubulin. *(A)* The positions of the meiotic spindles were measured from the anterior (the position of the condensed sperm pronucleus marks the future posterior; Goldstein and Hird, 1996). *(B)* The meiotic spindles of *cdc-25.1(RNAi)* embryos were more broadly distributed along the anterior–posterior axis than were those of wild-type embryos.

*cdc-25.1*(RNAi) embryos are displaced from the anterior, as compared to wild type. Could this be the cause of aneuploidy in the later embryos, as shown in Figure 16? Meiotic spindles in *cdc25.1(*RNAi) embryos are often oriented parallel, rather than orthogonal to the cortex (*e.g.*, see Fig. 17H). Polar body extrusion probably does not occur in such embryos, thus explaining at least one source of aneuploidy. Furthermore, the meiotic failure in these embryos likely is not due to a meiotic spindle defect, *per se*. Rather, this phenomenon probably is the result of a defect in spindle attachment to the anterior cortex. Why are these spindles displaced from the anterior?

Videomicroscopy of *cdc-25.1*(RNAi) embryos was employed to better understand the phenotypes documented above. In many of the RNAi embryos, the cortical membrane of fertilized eggs was extremely active (not shown; Ashcroft *et al.*, 1999). These observations indicated that abnormally dynamic cortical activity in *cdc-25.1*(RNAi) embryos is the most-likely cause of mispositioned meiotic spindles, which would also lead to enlarged polar bodies/cytoplasts and multiple pro-nuclei.

Although some of the *cdc-25.1* phenotypes were somewhat similar to *mei-2* mutants, the data was far from conclusive. As a final test, the *cdc-25.1* gene was sequenced in *mei-2(ct98)* and *mei-2(ct102)* mutants (N. Ashcroft, *pers. comm.*). No mutations were found, leading us to conclude that *cdc-25.1* is not *mei-2*.

**RNAi identifies *mei-2***

F57B10.4 (Genbank #AAB96721), a gene predicted by Genefinder (Green, 1995; *C. elegans* Sequencing Consortium, 1998), showed similarity to the human centromere-associated motor protein, CENP-E (Yen *et al.*, 1992), and weak similarity to a rat coiled-coil-related protein that associates specifically with male meiotic chromosomes, SCP1 (synaptonemal complex protein 1; Meuwissen *et al.*, 1992). A 4.8 kb XbaI genomic clone containing F57B10.4 was used as a template for *in vitro* transcription (Fig. 19). When RNA from this clone was injected into wild-type hermaphrodites, F1 embryos often had grossly enlarged polar bodies, a phenotype identical to *mei-2* mutant embryos (Fig. 19A). A smaller gene, F57B10.12, was also predicted within this genomic clone, in the opposite orientation to the putative CENP-E-like gene. RNA from a 1.4 kb XbaI-SpeI subclone that only contained F57B10.12 produced the *mei-2* phenotype, whereas RNA from a second 1.3 kb SacI-EcoRI subclone that contained only F57B10.4 gave no obvious phenotype (Fig. 19B).

Additional support for F57B10.12 encoding *mei-2* came from an experiment where the RNA was injected into *mei-1(ct46*gf*)* homozygotes. *mei-2(*lf*)* alleles dominantly suppress the mitotic defects of *mei-1(ct46*gf*)* (Mains *et al.*, 1990). However, *mei-2* is epistatic to *mei-1*, such that *mei-2(ct102) mei-1(ct46*gf*)* double homozygotes are completely meiotic-defective (P. E. Mains, unpublished). *mei-2*(RNAi) might suppress *mei-1(ct46*gf*)* if some oocytes

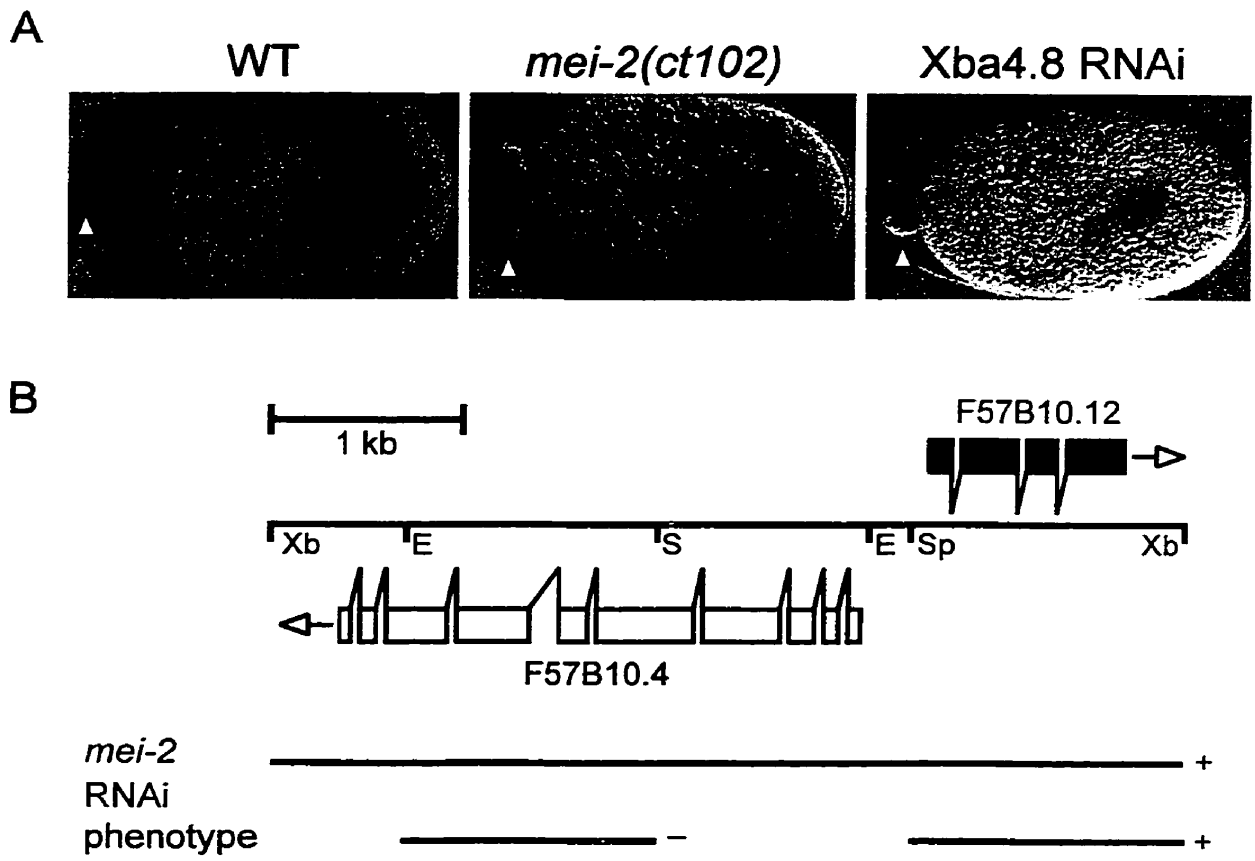


**Figure 19. Identification of the *mei-2* gene using RNAi.**

*A*) Embryos from hermaphrodites injected with RNA transcribed from a 4.8 kb XbaI subclone of cosmid F57B10 (shown in *B*) exhibited the *mei-2*-like phenotype. Note the large polar body in the anterior, compared with wild type (WT) (arrows). *B*) In order to identify the *mei-2* gene, RNA was transcribed from three genomic subclones of cosmid F57B10, as indicated at the bottom of the figure. RNA transcribed from a SacI-EcoRI subclone containing a gene with similarity to CENP-E (F57B10.4, white boxes) did not produce any obvious phenotype when injected into adult hermaphrodites. A SpeI-XbaI subclone containing *mei-2* (F57B10.12, dark boxes) did produce the *mei-2* phenotype, identical to the entire XbaI 4.8 kb subclone. Xb = XbaI; Sp = SpeI; E = EcoRI; S = SacI.

have reduced, but not absent *mei-2* activity. I observed a range [0/145 (0%) – 72/121 (60%)] of embryos surviving from *mei-1(ct46*gf) F57B10.12(RNAi) hermaphrodites at the restrictive temperature of 25°C, compared with no survivors [0/573 - (0%)] in *mei-1(ct46*gf) controls. Furthermore, one *mei-1(ct46*gf) F57B10.12(RNAi) line was maintained for three generations at 25°C, indicating transient heritability (Tabara *et al.*, 1998) of the RNAi-induced suppression. Together, these experiments showed that F57B10.12(RNAi) affected a gene that not only produced a *mei-2*-like phenotype, but also behaved as a *lf* suppressor of *mei-1(ct46*gf).

## III. Molecular characterization of *mei-2*

### Gene structure and identification of *mei-2* mutations

RT-PCR was used to confirm the Genefinder (Green, 1995) predicted structure of the *mei-2* gene (Fig. 20). Primers to exons of the *mei-2* gene were used in multiple RT-PCR reactions and only expected products were amplified. *mei-2* was also found to be *trans*-spliced to the SL1 leader sequence (Krause and Hirsh, 1987); no product was detected using the SL2 leader sequence (Huang and Hirsh, 1989) as a primer. An oligo-dT primer was used in conjunction with two different *mei-2*-specific forward primers (*mei-2*F3 and *mei-2*F4) to reveal the site of poly-adenylation. The signal sequence UAUAAA

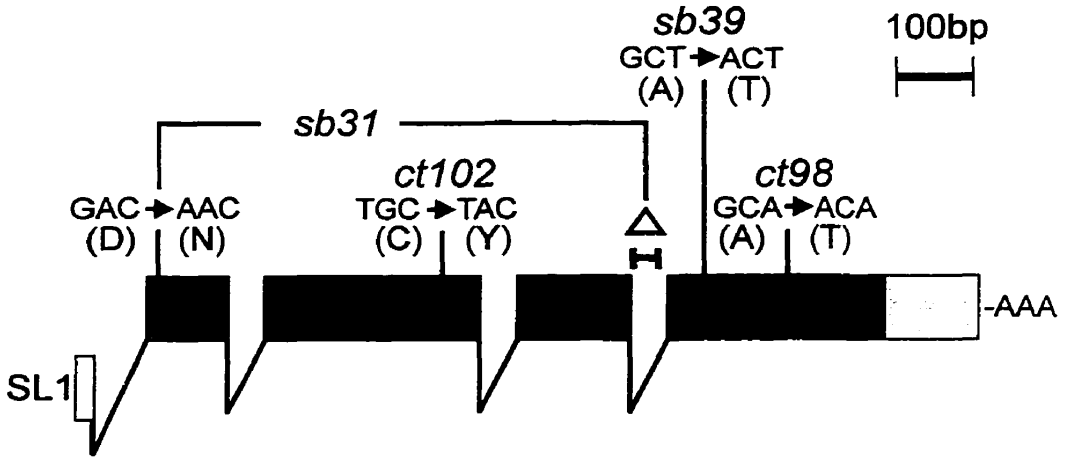


**Figure 20. Molecular structure of the *mei-2* gene.**

The *mei-2* structure, as predicted by Genefinder and confirmed by RT-PCR, is shown. *mei-2* is *trans*-spliced to the leader sequence SL1(white box) and encodes 4 exons (black boxes). The 3' UTR is 122 nucleotides long (grey box). The DNA sequence alterations responsible for each of the four *mei-2* mutations are also shown. *mei-2(sb31)* contains two lesions, one point mutation and a 35 bp deletion (Δ) that results in an in-frame insertion of four amino acids.

was found 13 nucleotides upstream of the site of poly-adenylation, which corresponded to nucleotide position 16,365 of cosmid F57B10. This sequence closely resembles the consensus sequence AAUAAA (Krause, 1995; Blumenthal and Steward, 1997).

All four *mei-2* mutations were identified within the coding region (Fig. 20). Three mutations (*ct98, ct102,* and *sb39*) were the result of G to A transitions, as expected from the ethyl methanesulfonate (EMS) mutagenesis (Anderson, 1995). *mei-2(ct98)*, the weakest *mei-2* mutation was an A237T amino acid substitution. *mei-2(sb39)*, a strong *ts* mutation resulted from an A201T amino acid substitution. The non-conditional Mel mutation, *mei-2(ct102)*, was a C117Y substitution. Another non-conditional Mel, *mei-2(sb31)*, contained two lesions, a G to A transition resulting in a D6N substitution and a 35 bp deletion that removed one nucleotide from the 3' end of exon 3 and the splice donor sequence of the third intron. This deletion results in the insertion of four amino acids (FCNS) derived from the unspliced sequence remaining from intron 3, which is in-frame with exon 4 (see below).

The *mei-2* gene is predicted to encode a 280 amino acid protein. A BLAST (Altschul *et al.*, 1990; Altschul *et al.*, 1997) search for proteins similar to MEI-2 revealed two predicted *C. elegans* genes of unknown function, F47G4.4 (Genbank CAB16313) and F47G4.5 (Genbank CAB16311). In addition, MEI-2 showed 29% identity and 52% similarity over 96 amino acids to *Strongylocentrotus purpuratus* katanin p80 subunit. This region of

similarity is restricted to the carboxyl-terminal half of both proteins (amino acids 144-240 for MEI-2 and 559-654 for katanin p80).

Likewise, all four proteins share a well-conserved region within the C-terminus (Fig. 21). F47G4.4 was more similar to katanin p80 than the other *C. elegans* proteins, with two additional regions of homology, shown schematically in Fig. 21A. The alignment of all four proteins is shown in Fig 21B, along with the positions of *mei-2* mutations, which disrupted amino acids that are conserved among the *C. elegans* proteins. Two motifs are present within the MEI-2 sequence. One is a prokaryotic membrane lipoprotein lipid attachment site (reviewed in Hayashi and Wu, 1990) found at amino acids 107-117. The function of this motif in eukaryotes has not been determined. The other is a tyrosine kinase phosphorylation site (Hunter, 1982; Patschinsky *et al.*, 1982), at amino acids 249-255 (the putative phosphorylated Y target is indicated in Fig. 21B). Both of these motifs are also present in the homologues F47G4.4 and F47G4.5, but not in katanin p80.

## Expression of *mei-2* mRNA and protein

*mei-2* mutations exhibit strict maternal-effect lethality (Mains *et al.*, 1990). Therefore, the *mei-2* product is likely provided by the female germline. To test this idea, the levels of *mei-2* mRNA and protein were measured at different stages of development and in various germline-defective mutants. A

**Figure 21. Comparison of MEI-2 and related proteins.**

*A*) Schematic representations of full-length MEI-2, F47G4.4, F47G4.5, and katanin p80 proteins are shown. The region of similarity as determined by BLAST searching with MEI-2 sequence is represented by black boxes containing amino acid coordinates. Percent identity (and similarity in brackets) to MEI-2 are shown below each protein. Two regions of homology between F47G4.4 and katanin p80, as determined from a BLAST search with F47G4.4 are also depicted (28% identity / 51% similarity for the N-terminal region, and 23% identity / 37% similarity for the middle region, grey boxes). *B*) Pileup results for MEI-2, F47G4.4, F47G4.5, and katanin p80 are shown. Full-length MEI-2 protein sequence is aligned with the C-terminal portion of *C. elegans* F47G4.4, most of *C. elegans* F47G4.5, and the C-terminus of *S. purpuratus* katanin p80. Identical amino acids (black boxes) and similar amino acids (grey boxes) to MEI-2 are indicated. Also shown are the positions and nature of molecular lesions found in each *mei-2* mutant. (∇ represents the insertion of four amino acids (FCNS) caused by the 35 bp deletion in *mei-2(sb31)* (see Fig. 20). The putative tyrosine phosphorylation site is indicated with a "P". Alignment of sequences was performed with the Genetics Computer Group (Madison, WI) Pileup program and the freeware program, Boxshade.

A

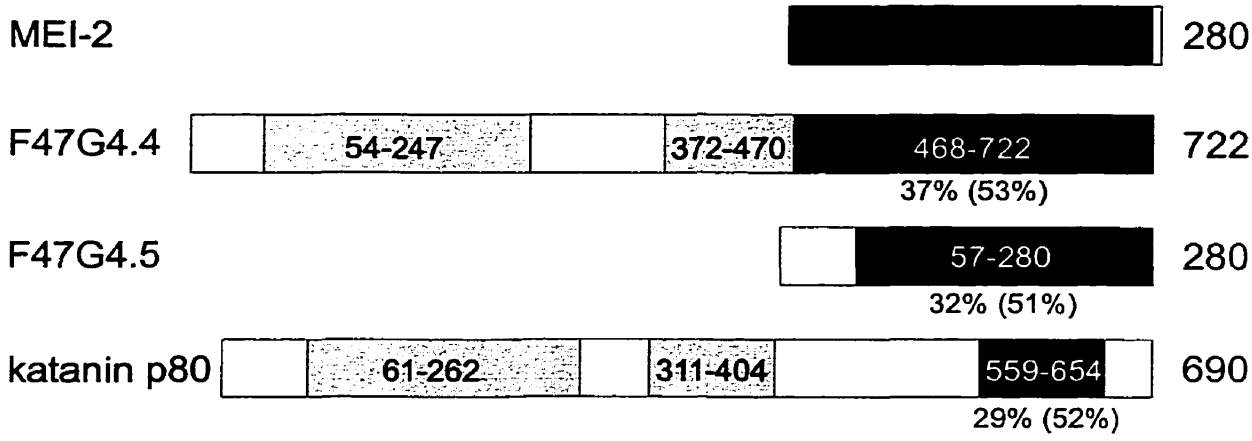
MEI-2
280
F47G4.4
54-247
372-470
468-722
722
37% (53%)
F47G4.5
57-280
280
32% (51%)
katanin p80
61-262
311-404
559-654
690
29% (52%)

B

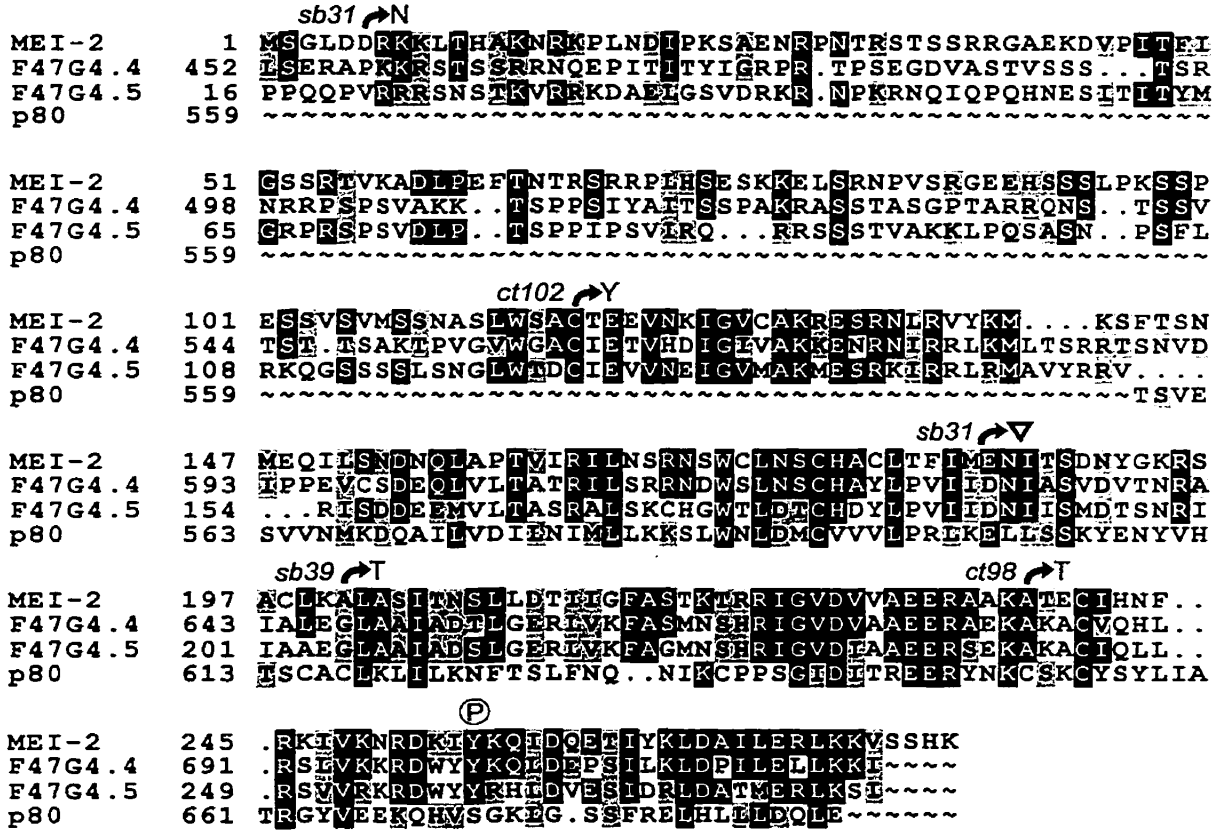
sb31 N
MEI-2 1 MSGLDDRKKLTHAKNRKPLNDIPKSAENRPNTRSTSSRRGAEKDVPITEI
F47G4.4 452 LSERAPKKRSTSSRRNQEPITITYIGRPR.TPSEGDVASTVSSS...TSR
F47G4.5 16 PPQQPVRRRSNSTKVRRKDAEIGSVDRKR.NPKRNQIQPQHNESITITYM
p80 559 ~~~~~~~~~~~~~~~~~~~~~~~~~~~~~~~~~~~~~~~~~~~~~~~~~~~~~
MEI-2 51 GSSRTVKADLPEFTNTRSRRPLHSESKKELSRNPVSRGEEHSSSLPKSSP
F47G4.4 498 NRRPSPSVAKK..TSPPSIYAITSSPAKRASSTASGPTARRQNS..TSSV
F47G4.5 65 GRPRSPSVDLP..TSPPIPSVIRQ...RRSSSTVAKKLPQSASN..PSFL
p80 559 ~~~~~~~~~~~~~~~~~~~~~~~~~~~~~~~~~~~~~~~~~~~~~~~~~~~~~
ct102 Y
MEI-2 101 ESSVSVMSSNASLWSACTEEVNKIGVCAKRESRNLRVYKM....KSFTSN
F47G4.4 544 TST.TSAKTPVGVWGACIETVHDIGLVAKKENRNIRRLKMLTSRRTSNVD
F47G4.5 108 RKQGSSSSLSNGLWTDCIEVVNEIGVMAKMESRKIRRLRMAVYRRV....
p80 559 ~~~~~~~~~~~~~~~~~~~~~~~~~~~~~~~~~~~~~~~~~~~~~~~~~~TSVE
sb31 V
MEI-2 147 MEQILSNDNQLAPTVIRILNSRNSWCLNSCHACLTFIMENITSDNYGKRS
F47G4.4 593 IPPEVCSDEQLVLTATRILSRRNDWSLNSCHAYLPVIIDNIASVDVTNRA
F47G4.5 154 ...RISDDEEMVLTASRALSKCHGWTLDTCHDYLPVIIDNIISMDTSNRI
p80 563 SVVNMKDQAILVDIENIMLLKKSLWNLDMCVVVLPRIKELLSSKYENYVH
sb39 T
ct98 T
MEI-2 197 ACLKALASITNSLLDTTIGFASTKTRRIGVDVVAEERAAKATECIHNF..
F47G4.4 643 IALEGLAAIADTLGERIVKFASMNSHRIGVDVAAEERAEKAKACVQHL..
F47G4.5 201 IAAEGLAAIADSLGERIVKFAGMNSHRIGVDIAAEERSEKAKACIQLL..
p80 613 TSCACLKLILKNFTSLFNQ..NIKCPPSGIDITREERYNKCSKCYSYLIA
P
MEI-2 245 .RKIVKNRDKTYKQIDQETIYKLDAILERLKKVSSHK
F47G4.4 691 .RSIVKKRDWYYKQLDEPSILKLDPILELLKKI~~~~
F47G4.5 249 .RSVVRKRDWYYRHLDVESIDRLDATMERLKSL~~~~
p80 661 TRGYVEEKQHVSGKIG.SSFRELHLLLDQLE~~~~~~

Northern blot probed with the 1.4 kb genomic XbaI-SpeI clone containing the *mei-2* gene revealed a single transcript of 950 bp, consistent with the results from RT-PCR analysis (Fig. 22). *mei-2* expression was highest in the gravid adult stage, but the transcript was also present at low levels in L1 and L4 larval stages. In order to determine if *mei-2* was expressed specifically in the female germline, we also probed RNA isolated from mutant strains lacking oocytes (*fem-3(q20*gf); Barton *et al.*, 1987), lacking sperm (*fem-1(hc17);* Nelson *et al.*, 1978) or lacking both due to the loss of mitotic germ cell proliferation (*glp-1(q231);* Austin and Kimble, 1987). Expression was severely reduced, but not absent in *glp-1*, suggesting that the majority of *mei-2* expression was indeed derived from germline tissue. A strong signal was observed in the *fem-1(hc17)* lane, indicating strong expression in female germline; however, *mei-2* was also expressed in *fem-3(q20)* mutants, which produce only sperm. Since *mei-2* mutants result in a strict maternal-effect lethal phenotype, transcription in male germline was unexpected (see below).

Antibodies produced to a full-length bacterially-expressed MEI-2 protein were affinity purified with an N-terminal portion of MEI-2 (Materials and Methods) and used to probe Western blots of wild-type and mutant worm lysates. A single band of approximately 33 kDa was observed, consistent with the predicted size for MEI-2 (Fig 23A). This band was greatly reduced in *fem-3(q20*gf) (sperm-only mutant), indicating maternal expression of the protein (Fig. 23B), despite the presence of *mei-2* transcript in both male and female

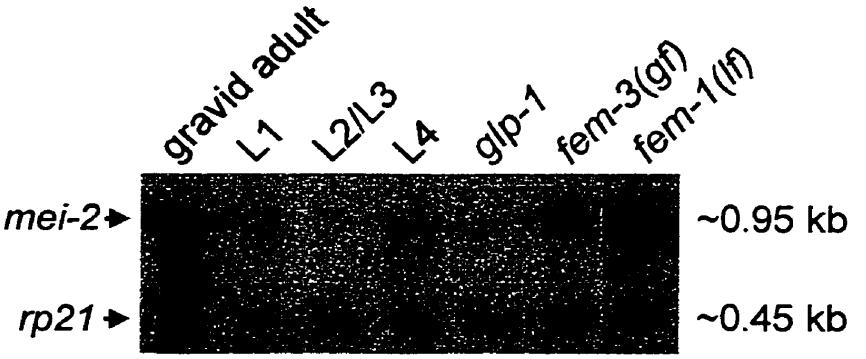


**Figure 22. Northern blot analysis of *mei-2* mRNA.**

Poly A$^+$ RNA was loaded into each lane and probed with a genomic clone containing *mei-2* (see Materials and Methods). RNA was harvested from gravid wild-type hermaphrodites, larval stages L1, L2/L3, L4, *glp-1* hermaphrodites (lacking a germline), *fem-3* adults (which produce sperm, but not oocytes), and *fem-1* adults (which do not produce sperm, and tend to bloat with unfertilized oocytes). As a loading control, the blot was simultaneously probed with *rp21*, a ribosomal protein gene.

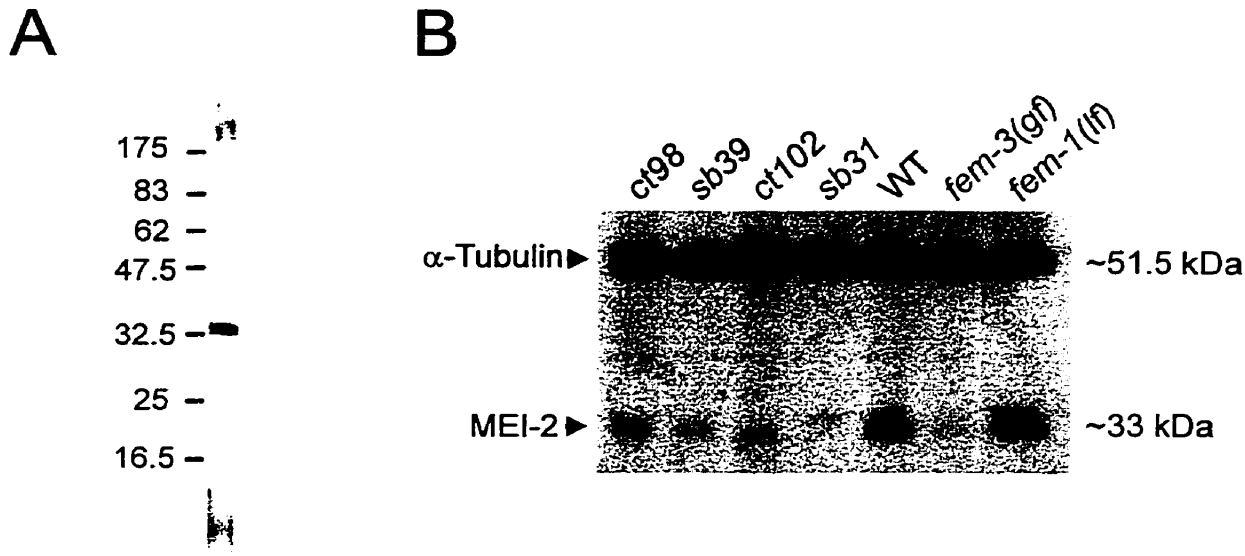


**Figure 23. Western blot analysis of MEI-2.**

*A)* Total wild-type worm homogenate probed with anti-MEI-2 serum indicates a single band of the expected size.

*B)* Homogenates prepared from *mei-2* mutant hermaphrodites, wild type, *fem-3(*gf*)* (which produce sperm, but not oocytes), and *fem-1* (which do not produce sperm and tend to bloat with unfertilized oocytes) were probed with anti-MEI-2 serum. The molecular weight of MEI-2 was estimated to be approximately 33 kDa using a protein molecular weight marker that was removed from the blot prior to probing. Note the slightly retarded migration of MEI-2*(sb31)* protein, consistent with the net insertion of 4 amino acids. As a loading control, the blot was simultaneously probed with anti-α-tubulin.

germlines as observed in Figure 22. As expected, MEI-2 expression was high in the *fem-1(hc17)* (oocytes-only) mutant worm lysate. Immunoreactivity with each *mei-2* mutant was consistently lower than with wild type (especially for *sb31*), suggesting decreased accumulation of mutant forms of MEI-2. The MEI-2(*sb31*) protein consistently migrated slightly slower (approximately 0.5 kDa larger than wild type), confirming the prediction that this mutation results in a net increase of four amino acids. This altered migration of MEI-2*(sb31)* also confirmed the specificity of this antiserum for MEI-2 on Western blots.

**Immunolocation of MEI-2 in wild-type embryos**

To determine the subcellular location of the MEI-2 protein, affinity purified MEI-2 antiserum was applied to dissected wild-type worms and embryos. MEI-2 was detected throughout the cytoplasm of the last few mature oocytes within the proximal gonad (Fig. 24A). In fertilized embryos, anti-MEI-2 decorated the condensed chromatin and spindle poles of meiosis I and meiosis II, as well as the condensed sperm pronucleus and polar bodies (Fig. 24B). A detailed examination using deconvolution immunofluorescence microscopy of meiotic spindles revealed MEI-2 at both equatorial and axial faces of the chromatin (Fig. 25C,F). Spindle pole staining by anti-MEI-2 seemed to extend beyond the region of the α-tubulin staining (Fig. 25B) and a considerable amount of MEI-2 was diffusely distributed around the spindle microtubules.

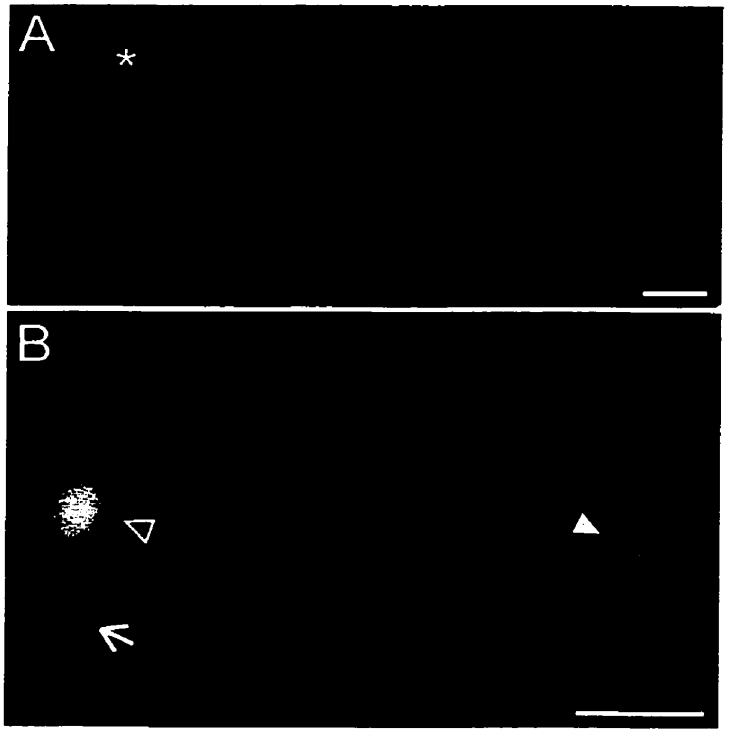


**Figure 24. Immunolocation of MEI-2.**

*A)* MEI-2 expression was first apparent in the proximal gonad of adult hermaphrodites. Typically, the last 2-3 oocytes in this region stained with anti-MEI-2. MEI-2 was not observed in the distal portion of the gonad (*), where mitotic proliferation of germ cells occurs. A dotted line indicates the outline of one gonad arm (as determined by Nomarski microscopy and DAPI immunofluorescence, not shown).

*B)* An embryo undergoing meiosis II is shown. MEI-2 antiserum decorated the meiotic spindle and condensed meiotic chromatin (clear arrowhead), the polar body from meiosis I (arrow) and the condensed sperm pronucleus (white arrowhead). Anti-MEI-2 also stained the meiosis I spindle and polar body from meiosis II (not shown). Scale bars in *A* and *B;* 10 μm.

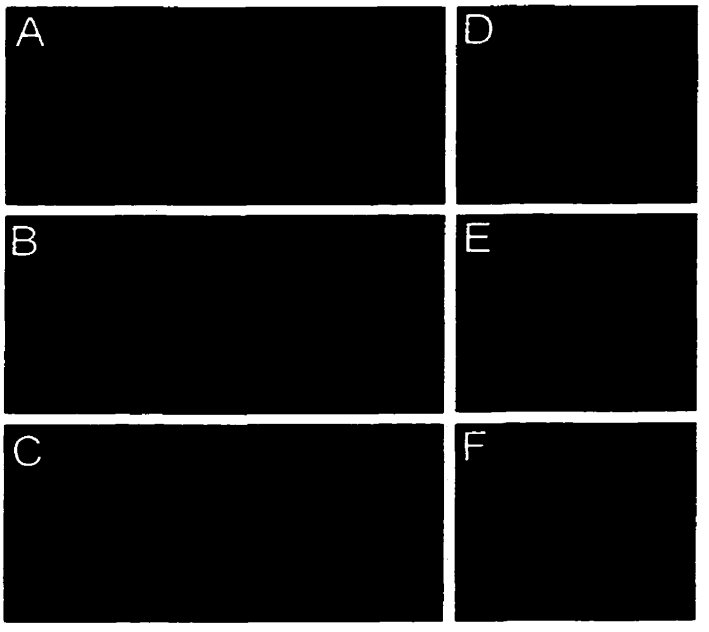


**Figure 25. Deconvolution image of a meiotic spindle in metaphase.**

Two deconvolution images of meiotic spindles are shown, *A-C* is a side-view; *D-F* is an axial view focused through the chromosomes on the metaphase plate. Staining was with *A,D*) DAPI, to visualize chromatin, *B,E*) anti-α-tubulin, and *C,F*) anti-MEI-2. The MEI-2 staining patterns were also documented in the absence of DAPI and α-tubulin staining (data not shown), to ensure that the observed patterns did not result from artefacts of multi-channel fluorescence microscopy.

With the exception of the polar body staining, anti-MEI-2 was not detectable after the completion of meiosis (see below; Fig. 28C). MEI-2 was not observed in the male meiotic spindles or in total male worm lysates via Western blot analysis (not shown), consistent with *mei-2*'s strict maternal requirement.

*mei-2* mutant embryos were also stained with antibodies to MEI-2 (Fig. 26). In all *mei-2* mutants, female meiotic chromosomes condensed normally and were located near the zygote anterior, indicating that MEI-2 does not play a major role in chromosome condensation. However, strong *mei-2* mutants displayed paired chromosomes that were not aligned on a metaphase plate. Embryos mutant for the genetically weak allele *mei-2(ct98)* had slightly disorganised spindles, but still exhibited MEI-2 staining in a pattern similar to wild type (Fig 26E,F). All staining (including oocyte cytoplasm, chromatin, polar bodies, and sperm pronucleus) was identical to wild type, albeit at reduced intensity (data not shown). The stronger *ts* allele, *mei-2(sb39)* displayed less organised spindle structure than *mei-2(ct98)*, but also exhibited chromatin staining with anti-MEI-2 (Fig. 26H,I). The strong, non-conditional mutant *mei-2(ct102)*, displayed severely disorganised meiotic spindles that lacked bipolarity, and all MEI-2 staining was absent (Fig 26K,L). This was also observed for *mei-2(sb31)* (Fig. 26N,O). These results indicate that MEI-2 is required for meiotic spindle microtubule organisation and that strong *mei-2* mutations disrupt the localization of MEI-2 and/or reduce the amount of MEI-2 below the limit of detection via immunohistochemistry.

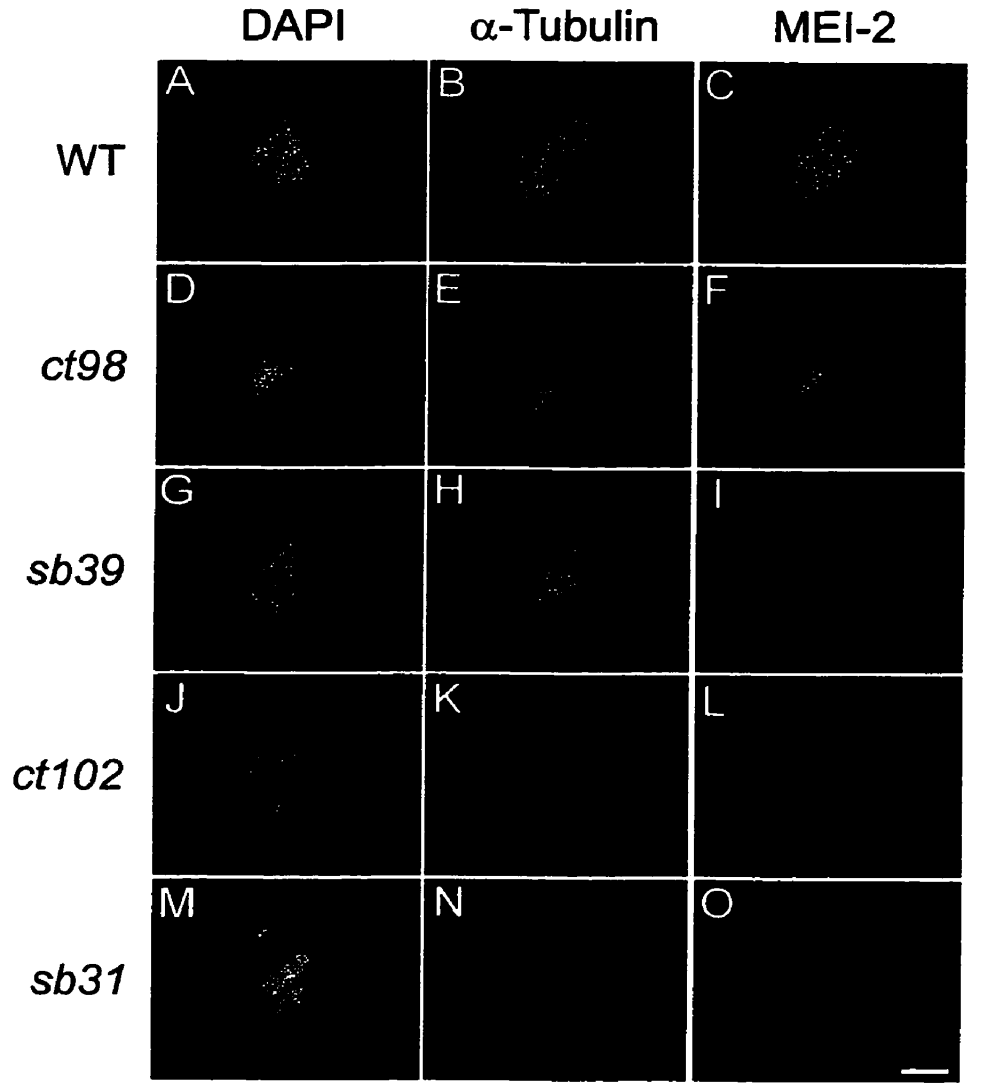


**Figure 26. MEI-2 immunolocation in *mei-2* mutants.**

Meiotic spindles from wild-type (WT; *A-C*) and *mei-2* mutant embryos (*D-O*) were fixed and stained with DAPI (*A,D,G,J,M*) anti-α-tubulin (*B,E,H,K,N*) and anti-MEI-2 (*C,F,I,L,O*). WT = wild type; *ct98*, *sb39*, *ct102*, and *sb31* are *mei-2* alleles (top-down is in order of increasing genetic severity). The *ts* alleles *mei-2(ct98)* and *mei-2(sb39)* were grown at the restrictive temperature of 25°C. Scale bar; 2 μm.

**MEI-2 localization requires MEI-1**

In order to determine if MEI-2 protein localization was dependent on *mei-1* activity, MEI-2 staining was observed in three mutant backgrounds: *mei-1(ct82)* - a dominant-negative, *mei-1(ct101)* - a null mutant, and *mei-1(ct46gf)*. Meiotic spindles fail to form in *mei-1(ct82)* and *mei-1(ct101)* mutants. Furthermore, chromatin, spindle poles, polar bodies, and the sperm pronucleus failed to stain with anti-MEI-2 (Fig. 27). Thus, *mei-1*(+) is required for the localization of MEI-2, even to non-spindle structures. *mei-1(ct46gf)* results in ectopic MEI-1 staining of mitotic spindles and the centre of the centrosomes (Clark-Maguire and Mains, 1994b). Interestingly, ectopic MEI-2(+) staining was also observed during mitosis in the *mei-1(ct46gf)* mutant background (Fig. 28D-I). Specifically, anti-MEI-2 was detected within the microtubule-free zone at the centre of the centrosomes and with condensed mitotic chromatin from metaphase to anaphase. *mel-26(ct61)*, a post-meiotic negative regulator of *mei-1*, causes mitotic defects identical to *mei-1(ct46gf)* as a result of ectopic MEI-1(+) persistence into mitosis (Clark-Maguire and Mains, 1994b; Dow and Mains, 1998). The ectopic MEI-2 staining pattern observed in *mei-1(ct46gf)* embryos was also observed in *mel-26(ct61)* embryos (not shown). I used anti-MEI-2 to immunostain *mei-1(ct101) mel-26(ct61)* double mutant embryos (which show meiotic, but not mitotic, defects; Clark-Maguire and Mains, 1994b). No MEI-2 staining was observed in either meiosis or mitosis,

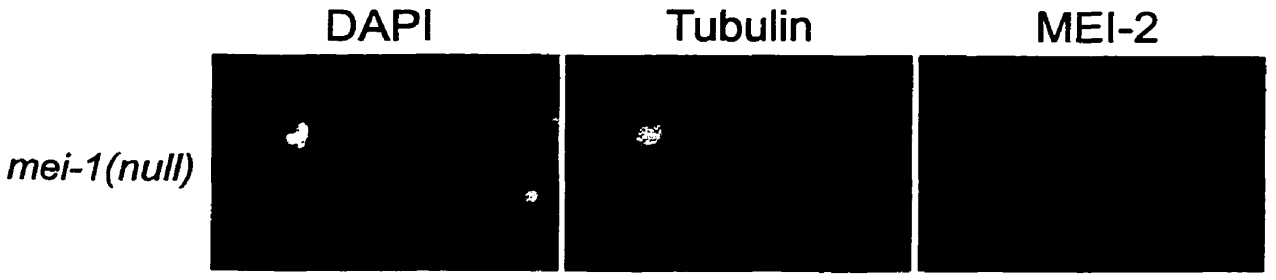


**Figure 27. MEI-2 localization requires MEI-1.**

Homozygous *mei-1(ct101)* embryos from strain HR245 (genotype: *mei-1(ct101) unc-29(e1072) mel-26(ct61)/unc-13(e1091) lin-11(n566) ; lon-2(e678)* were immunostained with anti-MEI-2 serum. Note the absence of MEI-2 at the disorganised meiotic spindle (left) as well as the condensed sperm pronucleus (right). *mei-1(ct101) unc-29(e1072) mel-26(ct61)* homozygotes display meiotic defects identical *to mei-1(ct101)* homozygotes. MEI-2 staining was also absent from all structures in both single mutant *mei-1(ct101)* and *mei-1(ct82)* homozygotes (not shown).

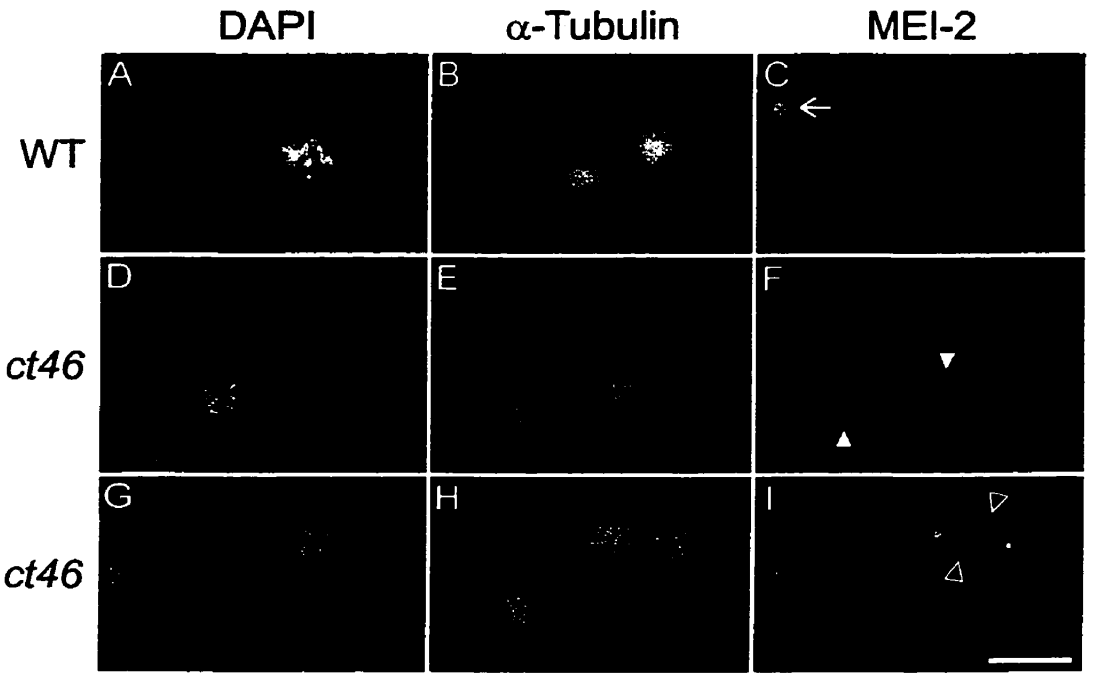


**Figure 28. Ectopic MEI-2 at mitotic chromatin and centrosomes in *mei-1(ct46gf)* mutant embryos.**

Wild-type (WT; *A-C*) and *mei-1(ct46gf)* (*D-I*) mutant embryos were fixed and stained with DAPI (*A,D,G*) anti-α-tubulin (*B,E,H*) and anti-MEI-2 (*C,F,I*). All meiotic staining of MEI-2 appeared normal in both wild-type and *mei-1(ct46gf)* embryos (not shown). Wild-type embryo at prometaphase of first mitosis (*A-C*) showed no MEI-2 staining other than the polar bodies (arrow). During prometaphase (*D-F*), centrosomal staining was apparent in *mei-1(ct46gf)* (white arrowheads). Chromatin also stained with anti-MEI-2 during metaphase (for instance, see Fig. 29B) and throughout anaphase (*I*; clear arrowheads). The centrosomal and mitotic chromatin staining pattern reiterated for several divisions. Scale bar; 10 μm.

indicating that the mislocalization of MEI-2 in *mel-26(ct61)* embryos also depends on the presence of wild-type MEI-1 (not shown).

The Mains laboratory reported previously that MEI-1 locates to the female meiotic spindle microtubules, polar bodies, the condensed sperm pronucleus, and the condensed chromatin during telophase (Clark-Maguire and Mains, 1994b). However, antibodies to MEI-2 also stain meiotic metaphase chromatin, which we did not observe previously with anti-MEI-1. The original MEI-1 experiments were performed with crude antisera, so I reexamined MEI-1's intracellular distribution with affinity-purified antiserum. With the new reagent, I observed staining of meiotic chromatin in wild-type embryos, and mitotic chromatin staining in *mei-1(ct46*gf*)* in a pattern identical to MEI-2 (Fig. 29), along with all previously reported staining patterns. This indicated that MEI-1 and MEI-2 have an identical intracellular distribution. Although there are quantitative differences between MEI-1 and MEI-2 immunoreactivity at meiotic chromatin (generally, MEI-1 staining of chromatin appears less intense than MEI-2), their staining patterns are qualitatively similar.

*zyg-9* mutations exacerbate the mitotic defects associated with *mei-1(ct46*gf*)* and *mel-26(ct61)* (Kemphues *et al.*, 1986; Mains *et al.*, 1990; Matthews *et al.*, 1998). These mutations specifically enhance *mei-1(ct46*gf*)* but do not genetically interact with *mei-1(*lf*)* or any *mei-2* mutations. Similar to what was previously reported for anti-MEI-1 staining in a *zyg-9(b244)* background (Clark-Maguire and Mains, 1994b), I was unable to detect any

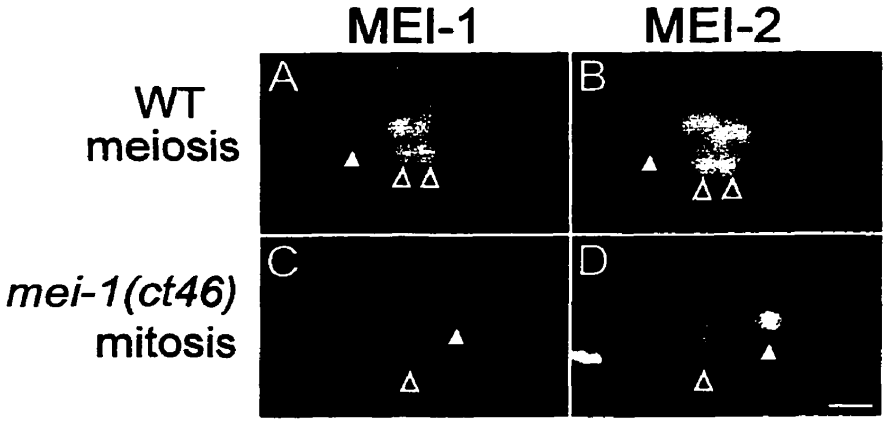


**Figure 29. Subcellular distribution of MEI-1 and MEI-2 is similar in wild-type and *mei-1(ct46*gf) embryos.**

Spindles from wild type (WT) and *mei-1(ct46*gf*)* mutant embryos were fixed and immunostained with anti-MEI-1 (*A* and *C*) and anti-MEI-2 (*B* and *D*). In wild type (*A* and *B*), MEI-1 and MEI-2 were found at meiotic spindle poles (out of focal plane, white arrowheads and chromatin (clear arrowheads). In *mei-1(ct46*gf*)* (*C* and *D*), MEI-1 and MEI-2 were found at centrosomes (white arrowheads) and chromatin (clear arrowheads). Embryos in *C* and *D* have approximately 10 cells; a close-up of one metaphase spindle from each embryo is shown. Scale bar; 2 μm.

differences in the staining patterns of MEI-2 in *zyg-9(b244)* mutant embryos (data not shown). Therefore, the mitotic-defect enhancement by *zyg-9* is likely not due to increasing amounts of MEI-2 protein in mitosis.

Similar to *zyg-9(b244)*, *mel-45(sb51)* is a mutation that exhibits a *mei-1(ct46*gf)-like phenotype and enhances the *mei-1(ct46*gf) mutation. *mel-45* mutant embryos did not reveal any obvious alteration in the distribution of either MEI-1 or MEI-2 via indirect immunofluorescence (data not shown). Therefore, the molecular basis for the enhancement between *mei-1(ct46*gf) and *mel-45(sb51)* probably is not analogous to the basis for the enhancement between *mel-26* mutants and *mei-1(ct46*gf).

In order to determine if the location of MEI-2 depends on meiotic spindle microtubules, embryos were treated with the microtubule depolymerizing drug nocodazole. Not surprisingly, I found a correlation between the presence of microtubules and MEI-2 staining at the spindle poles (data not shown). However, MEI-2 staining of chromatin persisted (albeit, at lower intensity than in untreated embryos) even after most of the meiotic spindle microtubules had disappeared, as assessed by anti-α-tubulin staining. In contrast, ectopic mitotic MEI-2 chromatin staining in *mei-1(ct46*gf) embryos appeared more sensitive to nocodazole treatment, but MEI-2 staining appeared to persist at centrosomes. These results suggest that MEI-2 is at least partly dependent on microtubules for localization, but short microtubules (surrounding centrosomes

in *mei-1(ct46gf)* and meiotic chromatin in wild type) are likely sufficient for the localization of some product.

**MEI-1/MEI-2 disassemble microtubules in HeLa cells**

If MEI-1 and MEI-2 are functional homologues of p60 and p80 katanin respectively, then these proteins should associate physically with each other as do p60 and p80 katanin. Furthermore, MEI-1 and MEI-2 might sever microtubules like katanin, with MEI-2 acting as a potentiator of MEI-1. To test these ideas, a collaboration with Dr. Frank McNally (University of California, Davis) was pursued. The McNally lab developed a convenient assay for microtubule severing that involves the transient transfection of HeLa cells with either GFP- (green fluorescent protein) or GST- (glutathione-S-transferase) fusion constructs (McNally *et al.*, 2000). I constructed GST-fusions with MEI-2, F47G4.4, F47G4.5, and MEL-26. McNally's group cotransfected HeLa cells with these fusions along with a GFP-MEI-1 construct to show that MEI-1 and MEI-2 can form a complex similar to the p60/p80 katanin dimer (Srayko *et al.*, 2000). MEI-1 also associated with F47G4.4 and F47G4.5, suggesting that these proteins may represent alternate dimerization partners for MEI-1 in *C. elegans*.

We also showed that MEI-1 disassembles the interphase network of microtubules and that this activity increases dramatically in the presence of

MEI-2. This is consistent with genetic evidence for MEI-2 being an activator of MEI-1. If the two MEI-2 homologues represent alternate binding partners for MEI-1, they might also stimulate MEI-1's microtubule disassembly activity. Cotransfections involving these fusion proteins indicated that they were as effective as MEI-2 in potentiating MEI-1 activity (Srayko *et al.*, 2000).

## IV. Analysis of F47G4.4 and F47G4.5

To assess the function of F47G4.4 and F47G4.5, dsRNA from full-length cDNA clones of each gene were made (see Materials and Methods). The RNAs were then injected into both wild type and CB1211, a strain that contains the *him-8(e1489)* mutation. The latter strain produces approximately 10% males due to non-disjunction of the X chromosomes during meiosis, allowing an analysis of the effect of RNAi on males, without having to outcross injected hermaphrodites. For both F47G4.4 and F47G4.5, approximately 15% of embryos from injected animals died (Table 6, lines 1-4). However the uninjected control gave about 5% lethality (Table 6, line 8), suggesting that the effect of RNA was about 10% lethality. Of the affected embryos, most did not hatch and the few that did were morphologically abnormal, slow growing, and failed to reach adulthood (not shown). Male progeny from *him-8*-injected worms were morphologically normal. There was no increase in the penetrance or severity of the RNAi-induced lethality when both dsRNAs were co-injected

**Table 6. RNAi of F47G4.4 and F47G4.5.**

| RNA injected | Host | Embryos hatching Number | Percent |
|---|---|---|---|
| 1. F47G4.4 | N2 | 607/701 | 86.6 |
| 2. F47G4.4 | *him-8* | 366/497 | 73.7 |
| 3. F47G4.5 | N2 | 573/668 | 85.8 |
| 4. F47G4.5 | *him-8* | 674/790 | 85.4 |
| 5. F47G4.4 & F47G4.5 | N2[a] | 688/747 | 92.1 |
| 6. F47G4.4 & F47G4.5 | N2[b] | 1144/1243 | 92.0 |
| 7. F47G4.4 & F47G4.5 | N2[c] | 555/645 | 86.0 |
| 8. uninjected | N2[c] | 289/304 | 95.1 |

[a] Injected worms were incubated at 15°C.
[b] Injected worms were incubated at 20°C.
[c] Injected worms were incubated at 25°C.

into wild type (Table 6, lines 5-7). Therefore, the dsRNAi may not have effectively disrupted F47G4.4 and F47G4.5, or these two genes may be functionally redundant with other *C. elegans* genes. Since strong *mei-2* mutations have fully penetrant recessive phenotypes on their own, it is unlikely that *mei-2* is redundant with F47G4.4 or F47G4.5.

### F47G4.4 encodes *mel-45*

The discovery of two *mei-2* homologues in *C. elegans* prompted an investigation into the possibility that these genes may also function in spindle assembly. These two proteins also physically interact with MEI-1 in HeLa

cells, suggesting that they may form alternate dimerization partners for MEI-1 (Srayko *et al.*, 2000). Unfortunately, the RNAi experiments described above did not produce an obvious phenotype that could be reliably characterized.

*mel-45(sb51)* was isolated in a *ts* screen for maternal-effect dominant mutations and exhibits a mitotic phenotype similar to *mei-1(ct46*gf*), mel-26,* and *zyg-9* mutants (Mitenko *et al.*, 1997). This mutation was also found to enhance the *mei-1(ct46*gf*)* mutation (P. E. Mains, *pers. comm.*). *mel-45* was mapped to the far right end of chromosome I, between *unc-59* and *unc-101* (P. E. Mains, *pers. comm.*). This is also where both *mei-2* homologues, F47G4.4 and F47G4.5, reside. Based on the phenotype and genetic interactions described above, *mel-45* could be encoded by either of these genes.

In order to test this idea, I sequenced both genes from *mel-45(sb51)* worms using primers indicated in Figure 5 (Materials and Methods). One sequence alteration was found in the ninth intron of F47G4.4. This putative mutation changes the splice acceptor sequence "TTCCAG" to "TTCTAG" (Fig. 30). Splicing to this acceptor sequence may be compromised in the *mel-45(sb51)* mutants. One possible outcome is that splicing of this intron occurs at the next available acceptor sequence, in which case exon 10 would be deleted (Fig. 30). Future experiments, such as RT-PCR analysis to look for differentially spliced products in the *mel-45(sb51)* mutant, may address this issue.

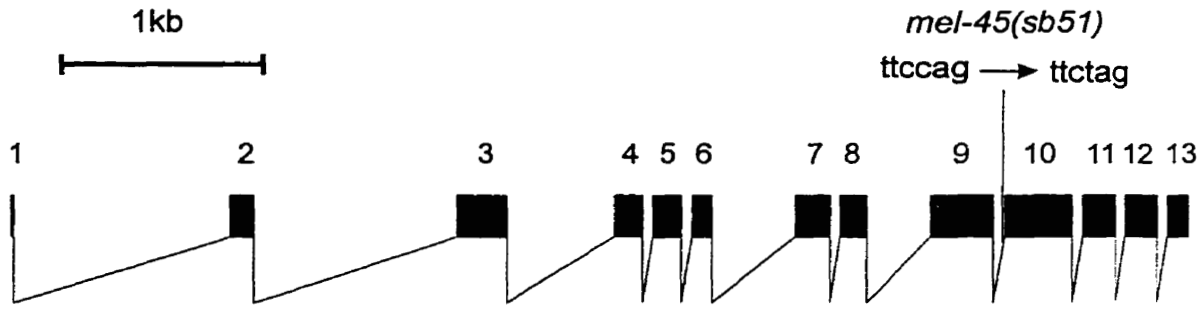


**Figure 30. *mel-45(sb51)* results in a putative splice-acceptor mutation within the F47G4.4 gene.**

The gene structure of F47G4.4 is shown, along with the sequence alteration found in *mel-45(sb51)* homozygous worms. This lesion is predicted to disrupt a splice-acceptor sequence (shown above the gene) and may result in altered splicing of this gene (see text). Exon numbers are also shown above the gene.

## V. Yeast two-hybrid experiments

Genetic evidence, immunostaining data, and the HeLa cell assay suggested that MEI-1 and MEI-2 proteins physically associate. In order to confirm this and also to test for interactions with MEL-26, the post-meiotic negative regulator of MEI-1, a yeast two-hybrid analysis was performed. Various subclones were also constructed to determine possible interaction domains within these proteins (see Figure 8, Materials and Methods, for a description of the subclones).

### MEI-1, MEI-2, and MEL-26 self-associate in yeast

The *mei-1(ct46*gf*)* mutation results in a proline-lysine substitution in the N-terminal region of the protein (residue 99) (Clark-Maguire and Mains, 1994a). To investigate the effect of this mutation on intermolecular interactions, I constructed MEI-1*(ct46*gf*)* fusion proteins for the yeast two-hybrid assay. As shown in Figure 31A, MEI-1(+) interacts with both MEI-1(+) and with MEI-1(*ct46*gf). MEI-1(*ct46*gf) also interacts with MEI-1(*ct46*gf), suggesting that this mutation does not alter the ability of the MEI-1 protein to interact with itself. This is consistent with interpretations derived from genetic analysis: 1) that MEI-1(*ct46*gf) should have near-normal activity during meiosis and 2) that MEI-1(*ct46*gf) antagonizes wild-type product (Clandinin and Mains, 1993).

**Figure 31. Yeast two-hybrid interactions involving MEI-1 and MEI-2.**

Results from MEI-1 and MEI-2 intermolecular association assays in yeast are shown. Yeast strains Y190 were mated with Y187 to assay physical interactions between different MEI-1 (*A*) and MEI-2 (*B*) fusion proteins (see Materials and Methods and Figure 8 for details on fusion constructs). Blue colour indicates a possible interaction between the two fusion proteins present in the progeny of the mated yeast. A "+" is also shown for each filter that gave any blue colour. [a]The original pACT2*mei-1*F construct did not exhibit a positive result with any of the pAS2 constructs, suggesting a possible problem with the expression of this particular clone. This construct was remade and gave a positive result with MEI-1F, but was not retested with any of the other constructs. [b]pAS2*mei-2*B could not be propagated in Y190 for reasons unknown.

A

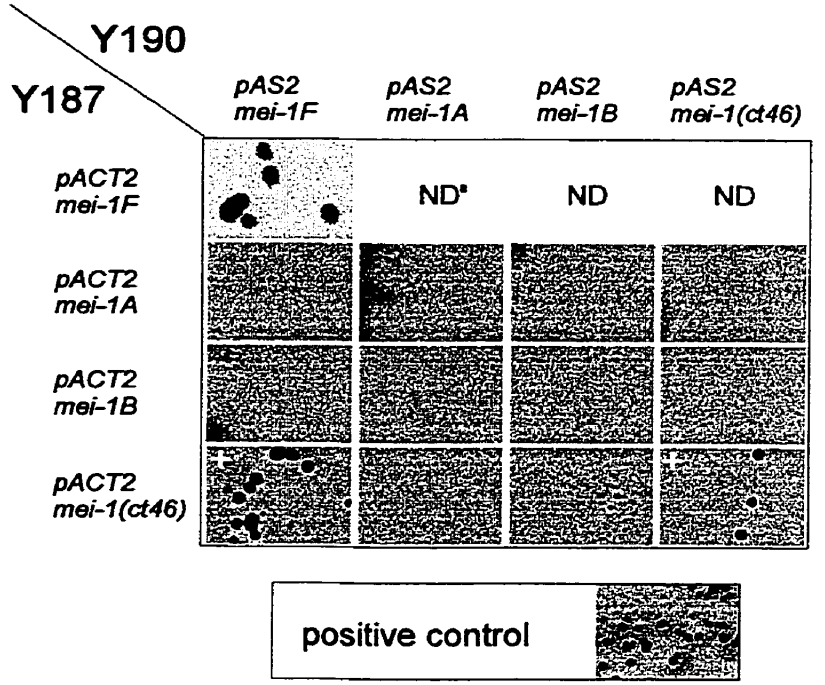
Y190
Y187
pAS2 mei-1F
pAS2 mei-1A
pAS2 mei-1B
pAS2 mei-1(ct46)
pACT2 mei-1F
pACT2 mei-1A
pACT2 mei-1B
pACT2 mei-1(ct46)
ND[a]
ND
ND
positive control

B

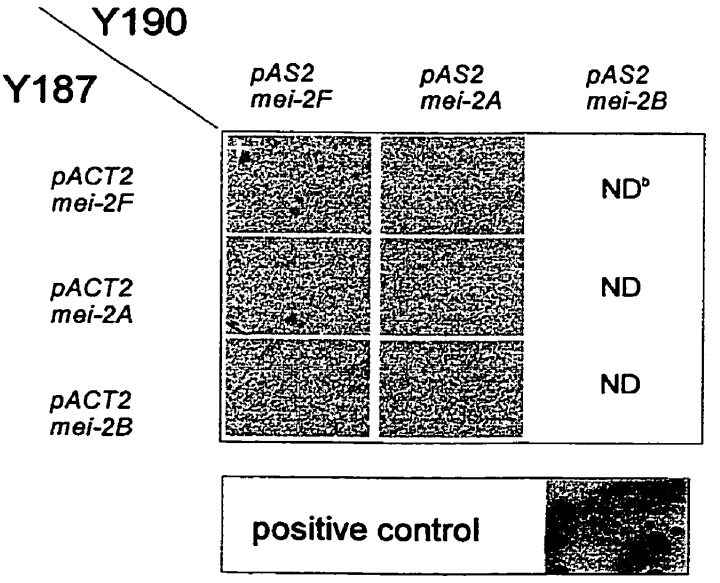
Y190
Y187
pAS2 mei-2F
pAS2 mei-2A
pAS2 mei-2B
pACT2 mei-2F
pACT2 mei-2A
pACT2 mei-2B
ND[b]
ND
ND
positive control

MEI-2 was found to interact weakly with MEI-2 (Fig. 31B). However, a sub-domain responsible for this interaction was not identified in either N-terminal (MEI-2A) or C-terminal (MEI-2B) halves of the protein.

The MEL-26 fusion proteins also showed self-association in yeast (Fig. 32). Furthermore, the N-terminal region MEL-26AB was found to interact with the full-length protein (MEL-26F) (Fig. 32 and 33B). This region was further subdivided and found to contain two separate regions that can interact with full-length MEL-26 (Fig 32 and 33B,C). Based on this analysis, MEL-26A and MEl-26BC (or possibly B alone, see below) may play an important role in the ability of MEL-26 to self-associate in yeast. It was not possible to determine which region the MEL-26A portion binds, since this fragment only interacted with full-length protein. MEL-26 BC associated with MEL-26AB, suggesting that the region involved in all of the MEL-26BC interactions may be MEL-26B. In support of this, MEL-26B and MEL-26BC did give a weak positive result (see Fig. 32).

**MEI-1, MEI-2, and MEL-26 intermolecular associations**

All of the MEI-2 and MEL-26 activation domain fusions in the Y187 strains were combined with each of the four MEI-1 DNA binding domain fusions in the Y190 strains (Fig. 34). MEI-1 was found to interact with MEI-2F and MEL-26F, suggesting that these proteins associate in *C. elegans*.

**Figure 32. Yeast two-hybrid interactions involving MEL-26.**

Results from MEL-26 intermolecular association assays in yeast are shown. Yeast strains Y190 were mated with Y187 to assay physical interactions between different MEL-26 fusion proteins (see Materials and Methods, and Figure 8 for details on fusion constructs). Blue colour indicates a possible interaction between the two fusion proteins present in the progeny of the mated yeast. A "+" is also shown for each filter that gave any blue colour.

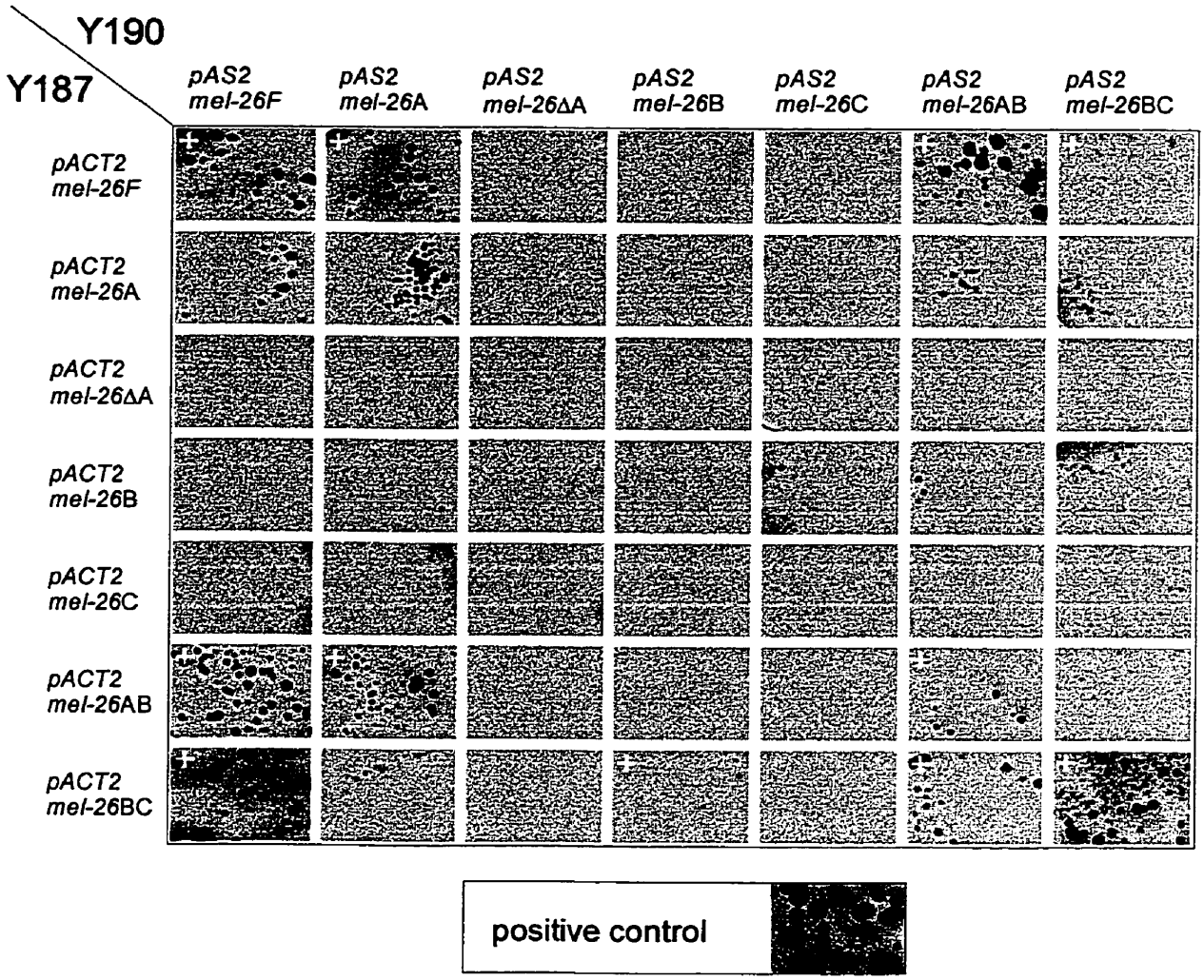
Y190
Y187
pAS2 mel-26F
pAS2 mel-26A
pAS2 mel-26ΔA
pAS2 mel-26B
pAS2 mel-26C
pAS2 mel-26AB
pAS2 mel-26BC
pACT2 mel-26F
pACT2 mel-26A
pACT2 mel-26ΔA
pACT2 mel-26B
pACT2 mel-26C
pACT2 mel-26AB
pACT2 mel-26BC
positive control

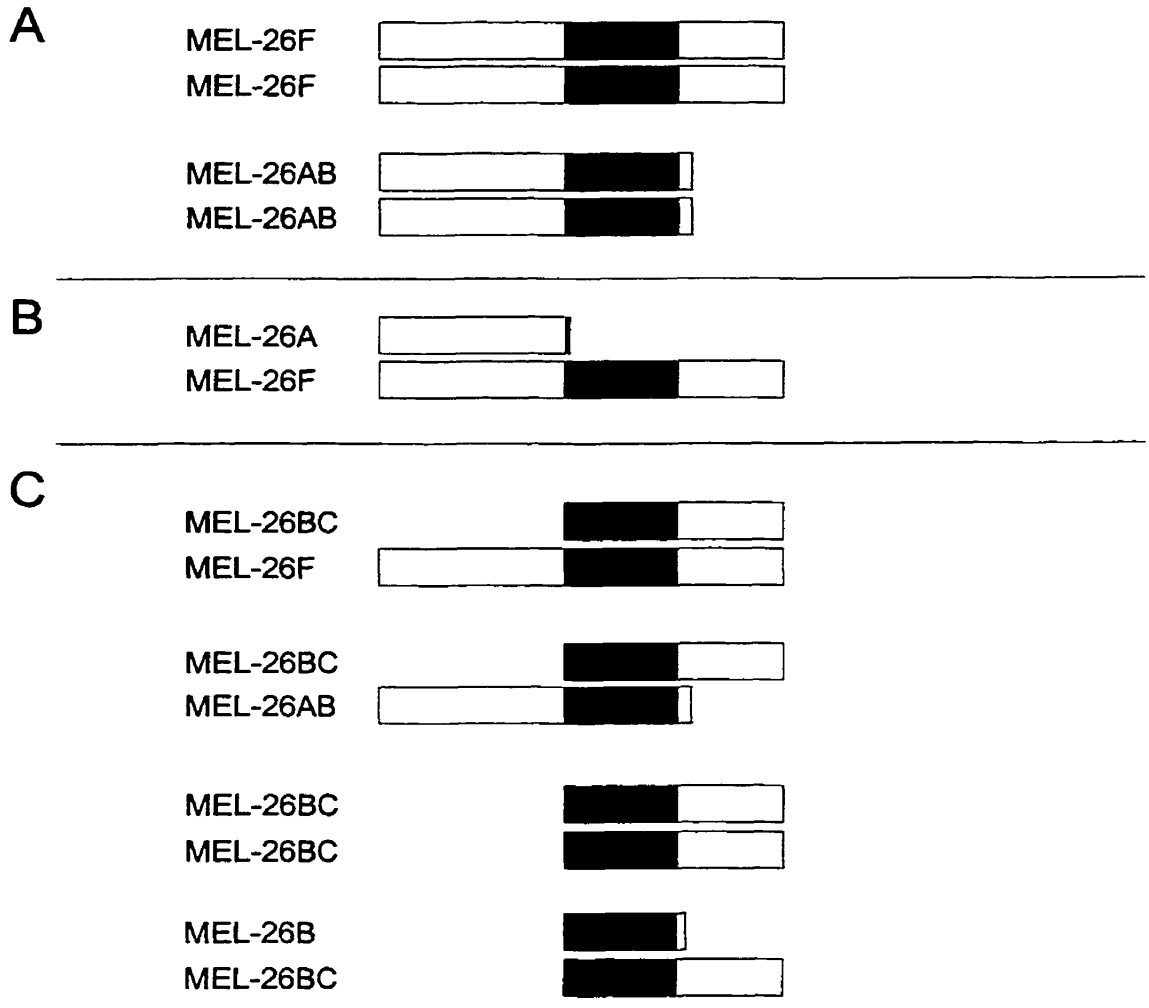


**Figure 33. A summary of MEL-26 yeast two-hybrid interactions.**

*A*) Full-length MEL-26 interacts with itself and MEL-26AB interacts with itself. *B*) The N-terminal region, MEL-26A is capable of binding to full-length MEL-26. *C*) MEL-26BC interacts with regions that contain MEL-26BC but also with MEL-26AB, suggesting a role for MEL-26B region in all of these interactions. A weak positive result was also observed with MEL-26B and Mel-26BC, indicating that the B region alone may be responsible for all of these interactions. Black shading indicates the BTB domain (Dow and Mains, 1998).

**Figure 34. Yeast two-hybrid interactions between MEI-1, MEI-2, and MEL-26.**

Results from MEI-1, MEI-2, and MEL-26 association assays in yeast are shown. Yeast strains Y190 (containing the MEI-1 fusion proteins) were mated with Y187 (containing the MEL-26 and MEI-2 fusion proteins) to assay physical interactions between these proteins (see Materials and Methods, and Figure 8 for details on fusion constructs). Blue colour indicates a possible interaction between the two fusion proteins present in the progeny of the mated yeast. A "+" is also shown for each filter that gave any blue colour. "Ø" indicates additional negative controls (see Materials and Methods, and Figure 7) performed by assaying haploid yeast containing either pAS2 or pACT2 (containing the fusion protein) vectors by themselves.

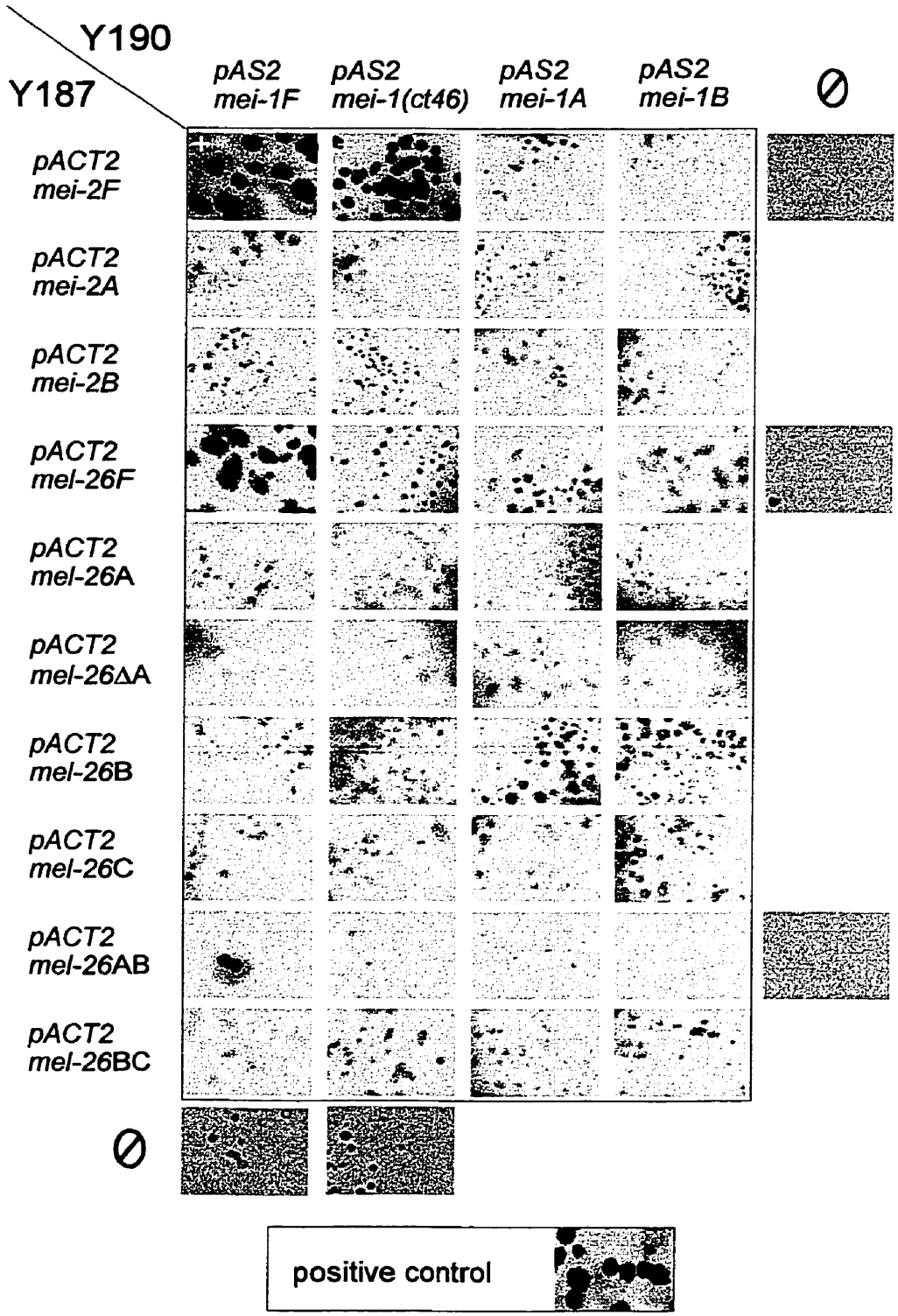
Y190
Y187
pAS2 mei-1F
pAS2 mei-1(ct46)
pAS2 mei-1A
pAS2 mei-1B
∅
pACT2 mei-2F
pACT2 mei-2A
pACT2 mei-2B
pACT2 mel-26F
pACT2 mel-26A
pACT2 mel-26ΔA
pACT2 mel-26B
pACT2 mel-26C
pACT2 mel-26AB
pACT2 mel-26BC
∅
positive control

MEI-1F interacted specifically with the N-terminal half of MEL-26 (MEL-26AB). A weak positive result was also obtained with MEI-1A and MEI-2A, suggesting that the N-terminal regions of both of these proteins may associate.

From genetic analysis, MEI-1(*ct46*gf) protein has normal activity during meiosis. Therefore, this altered protein may behave as MEI-1(+) with respect to its interaction with MEI-2. Indeed, the yeast 2-hybrid result suggests that these two proteins can interact like MEI-1(+)/MEI-2. Interestingly, MEI-1(+), but not MEI-1(*ct46*gf), interacted with MEL-26. This provides some insight into the nature of the *mei-1(ct46*gf) mutation. MEL-26 likely exerts negative regulation on MEI-1/MEI-2 during mitosis by physically associating with MEI-1; the *mei-1(ct46*gf) mutation probably abolishes this interaction and removes the negative effect of MEL-26 during mitosis.

## VI. Ectopic expression of MEI-1 and MEI-2 in touch neurons

The fact that *mei-2* was not rescued by a single cosmid suggests that *mei-2* expression from extrachromosomal arrays is not efficient in the female germline. Therefore, it probably is not feasible to exploit the methods of transgenesis to further investigate the role of this gene in early embryos.

For most zygotic genes, expression from extrachromosomal arrays is efficient (Kelly *et al.*, 1997). Therefore, one way to assay the function of MEI-1 and MEI-2 is to express each protein in a specific tissue later in development

and determine if the resultant phenotype is consistent with our predictions for how these proteins act. The touch neurons of *C. elegans* may be amenable to such an assay. Unlike the 11 protofilament microtubules found in most cells in *C. elegans*, the touch neurons are composed of 15 protofilament microtubules. Furthermore, mutations in a touch neuron-specific α-tubulin (*mec-12*; Chalfie and Au, 1989; Fukushige *et al.*, 1999) or β-tubulin (*mec-7*; Chalfie and Au, 1989; Savage *et al.*, 1989) result in mechanosensory defects (Mec phenotype). Therefore, if MEI-1 and MEI-2 function as microtubule-severing proteins, ectopic expression of both proteins in these cells would be expected to cause a Mec defect similar to the loss of α- or β-tubulin.

Both *mei-1* and *mei-2* cDNA sequences were placed downstream of a *mec-7* promoter, which is active almost exclusively in the touch neurons (Hamelin *et al.*, 1992). The vector pPD96.48 (a gift from Andy Fire; Baltimore, MD) was used for this purpose. A transgenic strain carrying both mec-7::*mei-1* and mec-7::*mei-2*, in addition to the dominant Rol marker *rol-6(su1006)* was assayed for a Mec phenotype. This was accomplished by lightly touching the head and tail of Rol worms with an eyelash. Mec worms will not respond to gentle stimulation. Non-Rol siblings were also examined for a Mec phenotype and served as a control. Only about 25% of the Rol worms displayed a Mec phenotype (data not shown). Rol worms immunostained with anti-MEI-1 and anti-MEI-2 sera indicated that both proteins were expressed in the touch

neurons (Fig. 35; data not shown). However, expression was not always observed in all touch neurons, suggesting that the incomplete penetrance of the Mec phenotype could be due to low expression or mosaicism associated with the transgenic array. Integrating this transgenic array into the genome may increase the penetrance of the Mec phenotype and allow a more thorough analysis of the effect of ectopic MEI-1/MEI-2 on these neurons.

Katanin microtubule severing has an essential role in neuronal function (Ahmad *et al.*, 1999). Therefore, this system may be useful not only for understanding how MEI-1 and MEI-2 function, but also may be used to identify components of the touch neuron that are important for katanin-mediated function in these cells. For example, one could screen for mutations that alleviate the Mec phenotype in this genetically-sensitive transgenic strain.

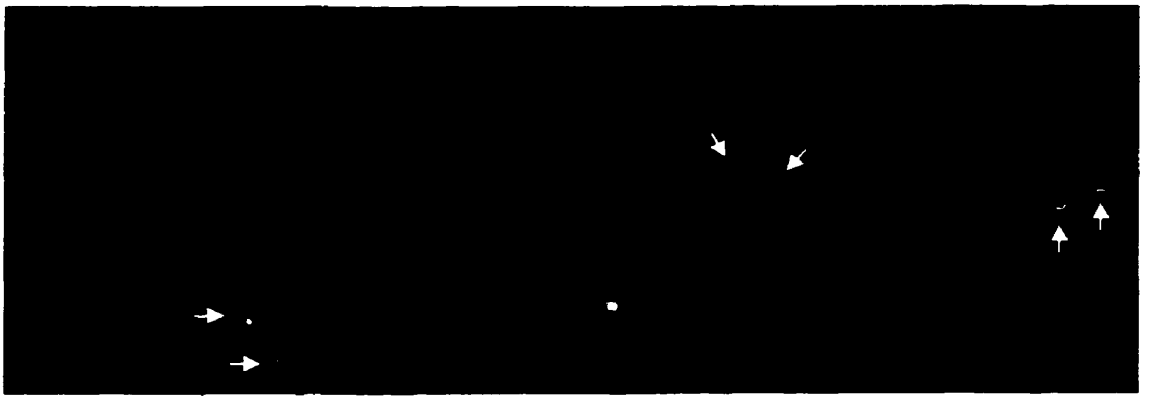

**Figure 35. The expression of MEI-2 in touch neurons of *C. elegans*.**

*mei-2* cDNA was fused to the touch neuron-specific *mec-7* promoter (see text). A transgenic worm stained with anti-MEI-2 serum (green colour) and DAPI to indicate nuclei (blue colour) is shown (merged image). The *mec-7* gene normally is expressed in six touch neurons (Hamelin, *et al.*, 1992). There are six cells clearly expressing ectopic MEI-2 (arrows). The bright spot in the centre represents endogenous MEI-2 at the meiotic spindle of an embryo. Other worms were stained for MEI-1 and these exhibited the same staining pattern (not shown).

# Discussion

*mei-2* was originally identified as a dominant suppressor of the mitotic-defective gain-of-function mutation *mei-1(ct46*gf*)* (Mains *et al.*, 1990). The homozygous recessive *mei-2(*lf*)* phenotype is identical to the *mei-1(*lf*)* phenotype: aneuploidy resulting from failure to assemble normal meiotic spindles (Mains *et al.*, 1990). Like *mei-1(*lf*)* embryos, the *mei-2(*lf*)* embryos either fail to extrude polar bodies or they form extremely large polar bodies (see Figure 3). Meiotic-defective mutations in *mei-1* and *mei-2* enhance each other with respect to these phenotypes, indicating that these two genes are required for the same process (Clandinin and Mains, 1993). The fact that decreased *mei-2* activity suppresses the mitotic defects caused by ectopic MEI-1 in both *mei-1(ct46*gf*)* and *mel-26(ct61)* mutants indicates that *mei-2* is required for *mei-1(+)* activity. In contrast, *mel-26* functions as a post-meiotic negative regulator of *mei-1* (Clark-Maguire and Mains, 1994b; Dow and Mains, 1998). *mel-26* encodes a novel protein, making predictions for a mechanism of action difficult. However, preliminary immunostaining experiments with crude MEL-26 antisera suggest that the MEL-26 protein locates to centrosomes (Dow, 1998). Therefore, MEL-26 may directly interfere with MEI-1/MEI-2 at the

centrosome in order to protect mitotic spindles from MEI-1/MEI-2 microtubule severing.

The *mei-2* gene was found by a combination of genetic mapping, positional cloning, and RNAi (Fig. 19). The generation of MEI-2-specific antiserum allowed a direct comparison of the staining patterns of MEI-1 and MEI-2. Consistent with the known genetic behaviour of these genes, both MEI-1 and MEI-2 reside at the chromatin and poles of meiotic spindles in wild-type embryos (Fig. 29). Both proteins seem dependent on each other for their localization because *mei-1(*lf*)* mutants abrogate the localization of MEI-2 (this work) and vice versa (Clark-Maguire and Mains, 1994b). From these results, it is not possible to know whether this colocalization is direct or indirect, because proper meiotic spindles do not form in either *mei-1* or *mei-2* mutant embryos. However, in mutant embryos that have an altered distribution of MEI-1 protein (as in *mei-1(ct46*gf*)* and *mel-26(ct61)*), ectopic MEI-2 also is present in an identical pattern (Figs. 28,29). In support of a direct-interaction model where MEI-1 and MEI-2 function as a complex during *C. elegans* meiosis, MEI-1 and MEI-2 associate in yeast (Fig. 34). Furthermore, expressed MEI-1 and MEI-2 copurify from HeLa cell extracts (Srayko *et al.*, 2000).

**A role for MEI-1/MEI-2 microtubule severing in *C. elegans*.**

The finding that co-expression of MEI-1 and MEI-2 in HeLa cells results in a microtubule-disassembly phenotype (Srayko *et al.*, 2000) identical to that observed for katanin (McNally *et al.*, 2000) indicates that MEI-1/MEI-2 has katanin-like microtubule-disassembly activity. The sea urchin protein katanin is a p60/p80 heterodimer that exhibits microtubule-severing activity *in vitro* (McNally and Vale, 1993). Although the biological role of katanin is not clear, its presence at spindle poles in sea urchins and mammalian cells suggests a role in disassembling microtubules near their minus ends during poleward flux (McNally *et al.*, 1996; McNally and Thomas, 1998). The catalytic p60 subunit of katanin is a member of the AAA family of ATPases that exhibits a high degree of similarity to MEI-1, although this similarity does not extend beyond the AAA domain (Clark-Maguire and Mains, 1994a; Hartman *et al.*, 1998). The p80 subunit of katanin contains a WD-40-rich N-terminus that has been implicated in targeting the katanin heterodimer to centrosomes (Hartman *et al.*, 1998) and may be involved in regulating severing activity (McNally *et al.*, 2000). I found that katanin p80 and MEI-2 share a conserved region in their carboxyl-termini (29% identity over 96 amino acids). This region of p80 has been implicated in physically interacting with p60 (Hartman *et al.*, 1998). The C-terminal similarity may represent conservation of a protein-protein

interaction domain between katanin p60/p80 and MEI-1/MEI-2 and, by implication, a conservation of function between these protein pairs.

Katanin is found in sea urchin embryos and cultured mammalian cells undergoing mitosis (McNally *et al.*, 1996; McNally and Thomas, 1998). Unlike katanin, MEI-1 and MEI-2 likely have no function during wild-type mitosis but they are essential for meiosis. In fact, MEI-1 and MEI-2 persistence into mitosis (as in *mei-1(ct46*gf) and *mel-26* mutants) is clearly disastrous. Despite these differences, the presence of MEI-1 and MEI-2 at mitotic centrosomes in *mei-1(ct46*gf) and *mel-26* mutants is strikingly reminiscent of katanin's *in vivo* mitotic location. Perhaps MEI-1/MEI-2 represents a specialized katanin that functions within the acentriolar environment of the meiotic spindle. Microtubule-disassembly exhibited by GFP-MEI-1 and either GST-F47G4.4 or GST-F47G4.5 raises the possibility that MEI-1 may associate with these *mei-2* homologues in the worm, possibly for developmental processes distinct from those involving MEI-2 (Srayko *et al.*, 2000; see below).

Does MEI-1/MEI-2 function to sever microtubules of the meiotic spindle, as suggested by their activity in HeLa cells? Observations of mutants that result in ectopic mitotic MEI-1 activity (*mei-1(ct46*gf) and *mel-26(ct61)*) suggest that MEI-1/MEI-2 can shorten microtubules in *C. elegans*. For instance, such mutants can be phenocopied by low doses of the microtubule-depolymerizing drug nocodazole (Strome and Wood, 1983), indicating that the persistence of MEI-1/MEI-2 into mitosis could result in shorter mitotic spindle microtubules.

Also, *mei-1(ct46*gf) and *mel-26(ct61)* mutants are enhanced by *lf* mutations in *zyg-9*, a gene that encodes a putative microtubule-stabilizing protein (Matthews *et al.*, 1998). Therefore, loss of a microtubule-stabilizing protein due to the *zyg-9* mutation would be expected to enhance renegade mitotic MEI-1/MEI-2 severing activity in the *mei-1(ct46*gf) mutant.

The cytoplasm of the early *C. elegans* embryo must support both meiotic and early mitotic spindle formation. Unlike the mitotic spindle, the female meiotic spindle is small and juxtaposed to the anterior cortex; polar body extrusion occurs rapidly and without loss of valuable cytoplasm. Meiotic-specific microtubule-severing activity may contribute to these morphological differences in several ways. One possibility is that MEI-1/MEI-2 present at the poles prevents astral microtubules from forming, thus allowing the meiotic spindle to remain in close proximity to the anterior cortex for polar body extrusion. MEI-1/MEI-2 at chromatin may also restrict the length of microtubules that form around the meiotic chromatin. Longer meiotic spindle microtubules may be unable to coalesce into focused spindle poles, explaining our observation that *mei-1(*lf) and *mei-2(*lf) mutant spindles lack bipolarity, but still exhibit microtubule staining around meiotic chromatin. In addition, microtubule persistence around extruded chromatin could cause the large polar body phenotype in *mei-1* and *mei-2* mutants. In cases where no polar body is extruded, the rudimentary meiotic spindles may be pushed too far away from the cortex. Another possibility is that microtubules nucleated by meiotic

chromatin may require a post-nucleation processing step prior to their incorporation into the spindle proper. An analogous katanin-mediated mechanism that allows the release of microtubules from neuronal centrosomes is required for proper axonal outgrowth (Ahmad *et al.*, 1999).

### *mel-45(sb51)* may result in an inappropriate splicing reaction

The identification of a sequence alteration in *mel-45(sb51)* indicated that this gene might be encoded by the MEI-2/katanin p80 homologue, F47G4.4. The sequence change was found within a splice-acceptor sequence of the ninth intron. Although the effect of this mutation on the splicing of F47G4.4 is not yet known, it may be possible to predict an effect by comparison to other *C. elegans* introns. A computer-based program called "The Intronerator" can be used for this purpose (Kent and Zahler, 2000). Although additional sequence information may be required in the *in vivo* splicing reaction, donor and acceptor site sequences show considerable conservation and are useful for predicting splicing patterns. For instance, the wild-type donor (5') and acceptor (3') sequence for the F47G4.4 intron in question is "GTAACC" and "TTCCAG", respectively. This combination is found in 102 introns in the entire *C. elegans* genome. When the same donor is paired with the *mel-45(sb51)* acceptor "TTCTAG", only 10 introns are found. Therefore, the *mel-45(sb51)* alteration may not completely eliminate splicing of this intron, but it may cause a

reduction in the efficiency of splicing, or an alternate splice to downstream exons. Based on the dominant *ts* nature of *mel-45(sb51)*, this mutation may result in a truncated protein that interferes with the wild-type product. Although F47G4.4 was found to physically interact with MEI-1 in HeLa cells (Srayko *et al.*, 2000), a simple model whereby the MEL-45(*sb51*) protein substitutes for MEI-2 and causes ectopic MEI-1 microtubule severing during mitosis is not likely, because ectopic mitotic MEI-1 staining is not observed in the *mel-45(sb51)* mutant. Alternatively, another MEI-1-like protein may normally associate with this MEI-2 homologue; the mutation may result in a deregulation of severing during mitosis that phenocopies the *mei-1(ct46*gf) mutant. At least one candidate for a MEI-1 homologue is the predicted gene, F32D1.1. Another possibility is that MEL-45(*sb51*) causes an increase in the activity of MEI-1 without affecting its distribution. The N-terminus of F47G4.4 contains a large region of similarity to katanin p80's N-terminus (Fig. 21, Results). This region of katanin (residues 1-304) has been implicated in negatively regulating the severing activity of the p60 subunit (McNally *et al.*, 2000). Perhaps MEL-45 normally complexes with MEI-1 (and possibly MEI-2) but functions to attenuate MEI-1 severing. *mel-45(sb51)* may remove this regulation, and even though MEI-1 may still be negatively regulated by MEL-26, the increased severing activity due to *mel-45(sb51)* may be sufficient to cause spindle defects. This may account for the lack of ectopic MEI-1 staining in the *mel-45(sb51)* background. Although additional experiments are

required, the *mel-45(sb51)* mutation may prove useful for examining the function of another katanin-like protein in *C. elegans*.

**MEI-1/MEI-2 and MEL-26 interactions during meiosis and mitosis.**

The yeast two-hybrid results indicated that MEI-1 can physically associate with both MEI-2 and MEL-26. This is consistent with the genetic and immunohistochemical data: MEI-1 and MEI-2 likely form a complex during meiosis that functions in meiotic spindle assembly. The MEI-1/MEL-26 interaction suggests a possible mechanism for the post-meiotic negative regulation of the MEI-1/MEI-2 complex.

The *mei-1(ct46gf)* mutation results in abnormal mitosis but meiotic spindles appear normal, suggesting that the mutant protein functions normally during meiosis (Mains *et al.*, 1990; Clark-Maguire and Mains, 1994b). MEI-1(*ct46*gf) interacted with MEI-2 in the yeast experiments, indicating that at least this aspect of MEI-1 function is not perturbed by the *mei-1(ct46gf)* mutation. Interestingly, MEL-26 associated with MEI-1(+), but not with MEI-1(*ct46*gf) in this assay. A model to explain the yeast two-hybrid results in the context of the meiosis to mitosis transition is presented in Figure 36. A MEI-1/MEI-2 complex forms during meiosis (perhaps after fertilization) to sever microtubules of the meiotic spindle. This complex is inactivated as a result of

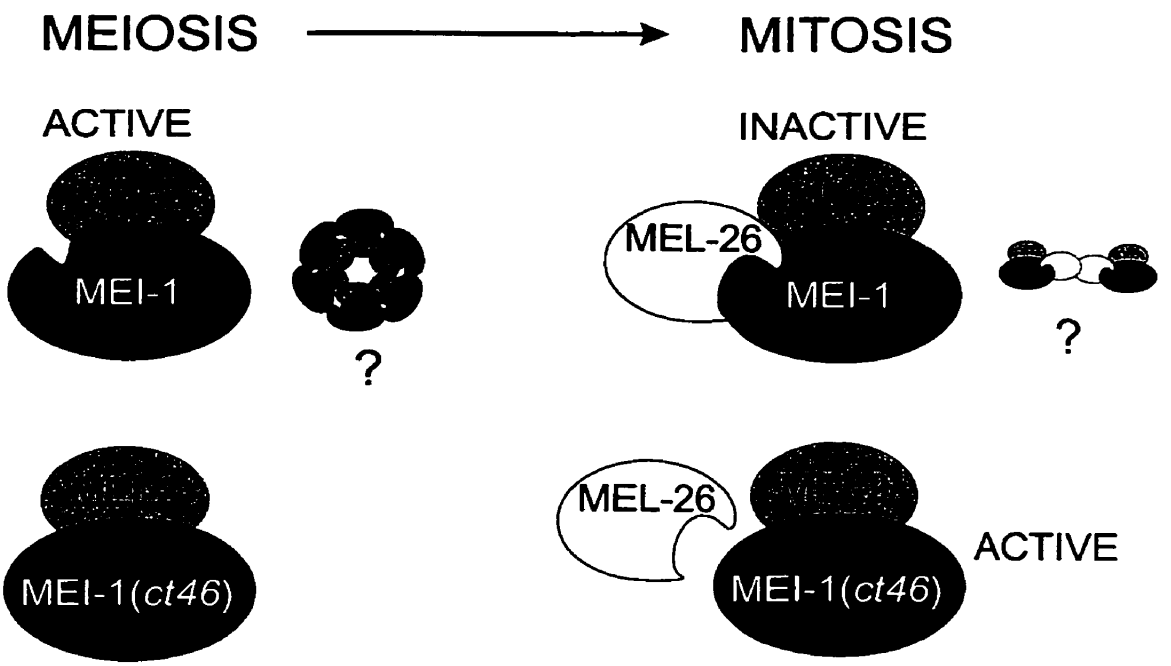


**Figure 36. The meiosis to mitosis transition: A model for MEI-1/MEI-2 and MEL-26 interactions.**

MEI-1 and MEI-2 are proposed to form a complex that is required to keep meiotic spindle microtubules short. MEI-1/MEI-2 may form oligomeric ring structures (a scaled-down version of this predicted structure is shown to the right). During mitosis, MEL-26 associates with MEI-1 to inactivate the MEI-1/MEI-2 complex. This interaction may also dissociate MEI-1 and MEI-2 (not shown). MEL-26 can associate with itself, suggesting that MEL-26 may also prevent the formation of the putative oligomeric structure (a scaled-down version of one possible outcome is shown to the right). The MEI-1(*ct46*gf) protein does not interact with MEL-26, allowing an active MEI-1/MEI-2 complex to persist into mitosis

MEL-26 interacting with MEI-1. The association between MEL-26 and MEI-1 also may uncouple MEI-1 and MEI-2, since MEI-2A was found to bind to MEI-1A (the same region that contains the *mei-1(ct46*gf) alteration). MEL-26 cannot associate with MEI-1(*ct46*gf), which results in a stable MEI-1/MEI-2 complex through many subsequent mitotic divisions.

MEL-26 is maternally provided and likely expressed very early in development, perhaps prior to fertilization. Why doesn't MEL-26 inactivate MEI-1/MEI-2 during meiotic spindle assembly? Preliminary evidence suggests MEL-26 is located at centrosomes (which are absent in meiotic spindles) (Dow, 1998). This could provide a physical barrier to the inactivation of MEI-1/MEI-2 during meiosis. Alternatively, MEL-26 may be present throughout the oocyte cytoplasm, but kept inactive by unknown mechanisms until after meiosis is complete.

The *mei-1(ct46*gf) mutation abolishes a predicted PEST sequence in the N-terminus of MEI-1. PEST sequences have been implicated in promoting rapid protein degradation via ubiquitin and the 26S proteosome (Rechsteiner and Rogers, 1996) or, in some cases via μ-calpain, a calcium-dependent protease (*e.g.*, IκBα; Shumway *et al.*, 1999). Therefore, the yeast two-hybrid results may reveal a requirement for the binding of MEL-26 to MEI-1 to promote degradation of the MEI-1/MEI-2 complex, perhaps analogous to

ubiquitin's role in targeting proteins to the 26S proteosome (reviewed in Ciechanover, 1994).

Ectopic MEI-1 and MEI-2 are observed in *mel-26* mutants, suggesting that the MEL-26 mutants may also fail to associate with MEI-1. At least three point mutations in *mel-26* are available to test this hypothesis. *mel-26(sb45)* and *mel-26(or184)* are located to the N-terminus and *mel-26(sb4)* is in the C-terminus. Yeast two-hybrid assays using these mutants may provide a way to further investigate the mechanism of negative regulation by MEL-26.

As with katanin p60, MEI-1 (and associated MEI-2) may form oligomeric ring structures. It has been suggested that an oligomeric ring of katanin may function within the hollow microtubule to allow simultaneous severing at each protofilament (McNally, 2000). This could explain the location of MEI-1 and MEI-2 at chromatin and spindle poles. Perhaps MEI-1/MEI-2 enters microtubules at one end, and exits the other end after the severing reaction. MEL-26 binding to MEI-1 could also sterically interfere with MEI-1/MEI-2's access to the microtubule core. In this model, MEL-26 need not dissociate the MEI-1/MEI-2 complex. At least one test of this model would be to perform co-immunoprecipitations from worm lysates of different mutant combinations. Unfortunately, previous attempts to co-immunoprecipitate MEI-1 and MEI-2 have not been successful. Only two embryos per hermaphrodite can undergo meiotic spindle assembly at any given time, therefore, complexed MEI-1/MEI-2 may represent a small fraction of the total proteins purified from a homogenous

worm lysate. Alternatives to this approach include co-immunopreciptiation of *in vitro* translated proteins. Although the MEI-1/MEI-2 complex may be very transient *in vivo*; conditions *in vitro* may allow a more stable complex.

The role of RAS-signaling in meiotic progression is well-established in *C. elegans* (Hubbard and Greenstein, 2000). Phosphorylation at tyrosine resides is an important component of many steps involved in transducing extracellular signals received by receptor tyrosine kinases. MEI-2 is not expected to have a role in signal transduction, but it may be phosphorylated by some component of this pathway. It could be that MEI-2 is translated in maturing oocytes but does not form a complex with MEI-1 until just before or after fertilization. Perhaps the phosphorylation of tyrosine in the C-terminus of MEI-2 induces structural changes that promote the formation of a MEI-1/MEI-2 complex. Of possible significance is that MEI-1, F47G4.4 and F47G4.5 also have a single tyrosine phosphorylation motif in their C-terminus. Future analysis with phospho-tyrosine-specific antibodies could provide a way to study this putative regulatory site.

One major structural difference between meiotic and mitotic spindles is that the former lack centrosomes. Whether all morphological distinctions between these two spindles can be accounted for by the presence or absence of centrosomes is not clear. MEI-1/MEI-2 are the first examples of meiotic-specific components that orchestrate meiotic spindle architecture. The existence of such genes implies that *in vivo* meiotic spindles do not simply form by default

in the absence of centrosomes. Further analysis of genes that genetically interact with *mei-1* and *mei-2* will likely reveal other factors that are involved in this important aspect of biology.

# References

Aamodt, E.J. and J.G. Culotti. 1986. Microtubules and microtubule-associated proteins from the nematode *Caenorhabditis elegans*: periodic cross-links connect microtubules in vitro. *J. Cell Biol.* **103**:23-31.

Afshar, K., N.R. Barton, R.S. Hawley, and L.S.B. Goldstein. 1995. DNA binding and meiotic chromosomal localization of the *Drosophila* nod kinesin-like protein. *Cell* 81:129-138.

Ahmad, F.J., W. Yu, F.J. McNally, and P.W. Baas. 1999. An essential role for katanin in severing microtubules in the neuron. *J. Cell Biol.* **145**:305-315.

Albertson, D.G. 1984. Formation of the first cleavage spindle in nematode embryos. *Dev. Biol.* **101**:61-72.

Albertson, D.G., A.M. Rose, and A.M. Villeneuve. 1997. Chromosome Organization, Mitosis, and Meiosis. In *C. elegans* II. D.L. Riddle, T. Blumenthal, B.J. Meyer, and J.R. Priess, editors. Cold Spring Harbor Press, Cold Spring Harbor. 47-78.

Albertson, D.G. and J.N. Thomson. 1993. Segregation of holocentric chromosomes at meiosis in the nematode, *Caenorhabditis elegans*. *Chromosome Research* **1**:15-26.

Alphey, L., J. Jimenez, H. White-Cooper, I. Dawson, P. Nurse, and D.M. Glover. 1992. *twine*, a *cdc25* homolog that functions in the male and female germline of *Drosophila*. *Cell* **69**:977-988.

Altschul, S.F., W. Gish, W. Miller, E.W. Myers, and D.J. Lipman. 1990. Basic local alignment search tool. *J. Mol. Biol.* **215**:403-410.

Altschul, S.F., T.L. Madden, A.A. Schaffer, J. Zhang, Z. Zhang, W. Miller, and D.J. Lipman. 1997. Gapped BLAST and PSI-BLAST: a new generation of protein database search programs. *Nucleic Acids Research* **25**:3389-3402.

Amos, L.A. and K. Hirose. 1997. The structure of microtubule motor complexes. *Curr. Opin. Cell Biol.* **9**:4-11.

Andersen, S.S.L. 1999. Balanced regulation of microtubule dynamics during the cell cycle: a contemporary view. *BioEssays* **21**:53-60.

Andersen, S.S.L., A.J. Ashford, R. Tournebize, O. Gavet, A. Sobel, A.A. Hyman, and E. Karsenti. 1997. Mitotic chromatin regulates phosphorylation of Stathmin/Op18. *Nature* **389**:640-643.

Anderson, P. 1995. Mutagenesis. In *Caenorhabditis elegans*: Modern Biological Analysis of an Organism. H.F. Epstein and D.C. Shakes, editors. Academic Press, Inc., San Diego, CA. 31-54.

Arnal, I., E. Karsenti, and A.A. Hyman. 2000. Structural transitions at microtubule ends correlate with their dynamic properties in *Xenopus* egg extracts. *J. Cell Biol.* **149**:767-774.

Ashcroft, N.R., M.E. Kosinski, D. Wickramasinghe, P.J. Donovan, and A. Golden. 1998. The four *cdc25* genes from the nematode *Caenorhabditis elegans*. *Gene* **214**:59-66.

Ashcroft, N.R., M. Srayko, M.E. Kosinski, P.E. Mains, and A. Golden. 1999. RNA-mediated interference of a *cdc25* homolog in *Caenorhabditis elegans* results in defects in the embryonic cortical membrane, meiosis, and mitosis. *Dev. Biol.* **206**:15-32.

Austin, J. and J. Kimble. 1987. *glp-1* is required in the germ line for regulation of the decision between mitosis and meiosis in *C. elegans*. *Cell* **51**:589-599.

Barnes, T.M., Y. Kohara, A. Coulson, and S. Hekimi. 1995. Meiotic recombination, noncoding DNA and genomic organization in *Caenorhabditis elegans*. *Genetics* **141**:159-179.

Barton, M.K., T. Schedl, and J. Kimble. 1987. Gain-of-function mutations of *fem-3*, a sex-determination gene in *Caenorhabditis elegans*. *Genetics* **115**:107-119.

Barton, N.R., A.J. Pereira, and L.S. Goldstein. 1995. Motor activity and mitotic spindle localization of the *Drosophila* kinesin-like protin KLP61F. *Mol. Biol. Cell* **6**:1563-1574.

Blangy, A., H.A. Lane, P. d'Herin, M. Harper, M. Kress, and E.A. Nigg. 1995. Phosphorylation by $p34^{cdc2}$ regulates spindle association of human Eg5, a kinesin-related motor essential for bipolar spindle formation *in vivo*. *Cell* **83**:1159-1169.

Block, S.M. 1996. Fifty ways to love your lever: Myosin motors. *Cell* **87**:151-157.

Blumenthal, T. and K. Steward. 1997. RNA Processing and Gene Structure. In *C. elegans* II. D.L. Riddle, T. Blumenthal, B.J. Meyer, and J.R. Priess, editors. Cold Spring Harbor Laboratory Press, Cold Spring Harbor. 117-145.

Breeden, L. and K. Nasmyth. 1985. Regulation of the yeast HO gene. *Cold Spring Harbor Symposium Quant. Biol.* **50**:643-650.

Brenner, S. 1974. The genetics of *Caenorhabditis elegans*. *Genetics* **77**:71-94.

Brunet, S., Z. Polanski, M.-H. Verlhac, J.Z. Kubiak, and B. Maro. 1998. Bipolar meiotic spindle formation without chromatin. *Curr. Biol* 8:1231-1234.

*C.elegans* Sequencing Consortium. 1998. Genome sequence of the nematode *C. elegans*: a platform for investigating biology. *Science* **282**:2012-2018.

Chalfie, M. and M. Au. 1989. Genetic control of differentiation of the *Caenorhabditis elegans* touch receptor neurons. *Science* **243**:1027-1033.

Chalfie, M. and J.N. Thomson. 1982. Structural and functional diversity in the neuronal microtubules of *Caenorhabditis elegans*. *J. Cell Biol.* **93**:15-23.

Charrasse, S., M. Schroeder, C. Gauthier-Rouviere, F. Ango, L. Cassimeris, D.L. Gard, and C. Larroque. 1998. The TOGp protein is a new human microtubule associated protein homologous to the *Xenopus* XMAP215. *J. Cell Sci.* **111**:1371-1383.

Church, D.L., K.-L. Guan, and E.J. Lambie. 1995. Three genes of the MAP kinase cascade, *mek-2*, *mpk-1/sur-1* and *let-60 ras*, are required for meiotic cell cycle progression in *Caenorhabditis elegans*. *Development* **121**:2525-2535.

Ciechanover, A. 1994. The ubiquitin-proteasome proteolytic pathway. *Cell* **79**:13-21.

Clandinin, T.R. and P.E. Mains. 1993. Genetic studies of *mei-1* gene activity during the transition from meiosis to mitosis in *Caenorhabditis elegans*. *Genetics* **134**:199-210.

Clark-Maguire, S. and P.E. Mains. 1994a. *mei-1*, a gene required for meiotic spindle formation in *Caenorhabditis elegans*, is a member of a family of ATPases. *Genetics* **136**:533-546.

Clark-Maguire, S. and P.E. Mains. 1994b. Localization of the *mei-1* gene product of *Caenorhabditis elegans*, a meiotic-specific spindle component. *J. Cell Biol.* **126**:199-209.

Compton, D.A. 1998. Focusing on spindle poles. *J. Cell Sci.* 111:1477-1481.

Courtot, C., C. Fankhauser, V. Simanis, and C.F. Lehner. 1992. The *Drosophila* cdc25 homolog *twine* is required for meiosis. *Development* **116**:405-416.

Crétien, D., S.D. Fuller, and E. Karsenti. 1995. Structure of growing microtubule ends: two-dimensional sheets close into tubes at variable rates. *J. Cell Biol.* **129**:1311-1328.

Crittenden, S.L., E.R. Troeml, T.C. Evans, and J. Kimble. 1994. GLP-1 is localized to the mitotic region of the *C. elegans* germ line. *Development* **120**:2901-2911.

Desai, A., S. Verma, T.J. Mitchison, and C.E. Walczak. 1999. Kin I kinesins are microtubule-destabilizing enzymes. *Cell* **96**:69-78.

Dogterom, M., M.-A. Félix, C.C. Guet, and S. Leibler. 1996. Influence of M-phase chromatin on the anisotropy of microtubule asters. *J. Cell Biol.* **133**:125-140.

Dow, M. R. 1998. The cloning and characterization of the *mel-26* gene of *Caenorhabditis elegans*. Ph.D. Thesis, University of Calgary, Calgary, AB, Canada.

Dow, M.R. and P.E. Mains. 1998. Genetic and molecular characterization of the *Caenorhabditis elegans* gene, *mel-26*, a post-meiotic negative regulator of MEI-1, a meiotic-specific spindle component. *Genetics* **150**:119-128.

Doxsey, S.J., P. Stein, L. Evans, P.D. Calarco, and M. Kirschner. 1994. Pericentrin, a highly conserved centrosome protein involved in microtubule organization. *Cell* **76**:639-650.

Edgar, B.A. and P.H. O'Farrell. 1989. Genetic control of cell division patterns in the *Drosophila* embryo. *Cell* **57**:177-187.

Edgar, B.A. and P.H. O'Farrell. 1990. The three postblastoderm cell cycles of *Drosophila* embryogenesis are regulated in G2 by *string*. *Cell* **62**:469-480.

Edgar, L.G. 1995. Blastomere culture and analysis. In *Caenorhabditis elegans*: Modern Biological Analysis of an Organism. H.F. Epstein and D.C. Shakes, editors. Academic Press, Inc., San Diego, CA. 303-321.

Endow, S.A., R. Chandra, D.J. Komma, A.H. Yamamato, and E.D. Salmon. 1994. Mutants of the *Drosophila* ncd microtubule motor protein cause centrosomal and spindle pole defects in mitosis. *J. Cell Sci.* **107**:859-867.

Enos, A.P. and N.R. Morris. 1990. Mutation of a gene that encodes a kinesin-like protein blocks nuclear division in *A. nidulans*. *Cell* **60**:1019-1027.

Finst, R.J., P.J. Kim, E.R. Griffis, and L.M. Quarmby. 2000. Fa1p is a 171 kDa protein essential for axonemal microtubule severing in *Chlamydomonas*. *J. Cell Sci.* **113**:1963-1971.

Fire, A., D.G. Albertson, S.W. Harrison, and D.G. Moerman. 1991. Production of antisense RNA leads to effective and specific inhibition of gene expression in *C. elegans*. *Development* **113**:503-514.

Fire, A., S. Xu, M.K. Montgomery, S.A. Kostas, S.E. Driver, and C.C. Mello. 1998. Potent and specific genetic interference by double-stranded RNA in *Caenorhabditis elegans*. *Nature* **391**:806-811.

Francis, R., M.K. Barton, J. Kimble, and T. Schedl. 1995a. *gld-1*, a tumor-suppressor gene required for oocyte development in *Caenorhabditis elegans*. *Genetics* **139**:579-606.

Francis, R., E. Maine, and T. Schedl. 1995b. Analysis of the multiple roles of *gld-1* in germline development: interactions with the sex determination cascade and the *glp-1* signaling pathway. *Genetics* **139**:607-630.

Fukushige, T., Z.K. Siddiqui, M. Chou, J.G. Culotti, C.B. Gogonea, S.S. Siddiqui, and M. Hamelin. 1999. MEC-12, an α-tubulin required for touch sensitivity in *C. elegans*. *J. Cell Sci.* **112**:395-403.

Gaglio, T., A. Saredi, J.B. Bingham, M.J. Hasbani, S.R. Gill, T.A. Schroer, and D.A. Compton. 1996. Opposing motor activities are required for the organization of the mammalian mitotic spindle pole. *J. Cell Biol.* **135**:399-414.

Gaglio, T., A. Saredi, and D.A. Compton. 1995. NuMA is required for the organization of the microtubules into aster-like mitotic arrays. *J. Cell Biol.* **131**:693-708.

Gard, D.L. 1992. Microtubule organization during maturation of *Xenopus* oocytes: assembly and rotation of the meiotic spindle. *Dev. Biol.* **151**:516-530.

Gard, D.L. and M.W. Kirschner. 1987. A microtubule-associated protein from *Xenopus* eggs that specifically promotes assembly at the plus-end. *J. Cell Biol.* **105**:2203-2215.

Goldstein, B. and S.N. Hird. 1996. Specification of the anteroposterior axis in *C. elegans*. *Development* **122**:1467-1474.

Gönczy, P., S. Pichler, M. Kirkham, and A.A. Hyman. 1999. Cytoplasmic dynein is required for distinct aspects of MTOC positioning, including centrosome separation, in the one cell stage *Caenorhabditis elegans* embryo. *J. Cell Biol.* **147**:135-150.

Green, P. 1995. Genefinder Documentation. http://www.ibc.wustl.edu/bio_data/genefinder.html.

Greenwald, I. and H. Horvitz. 1980. *unc-93(e1500)*: A behavior mutant of *Caenorhabditis elegans* that defines a gene with a wild-type null phenotype. *Genetics* **96**:147-164.

Guo, S. and K.J. Kemphues. 1995. *par-1*, a gene required for establishing polarity in *C. elegans* embryos, encodes a putative Ser/Thr kinase that is asymmetrically distributed. *Cell* **81**:611-620.

Hamelin, M., I.M. Scott, J.C. Way, and J.G. Culotti. 1992. The *mec-7* β-tubulin gene of *Caenorhabditis elegans* is expressed primarily in the touch receptor neurons. *EMBO J* **11**:2885-2893.

Harlow, E. and D. Lane. 1988. Antibodies: a Laboratory Manual. Cold Spring Harbor Laboratory, Cold Spring Harbor, New York. 726 pp.

Hartman, J.J., J. Mahr, K. McNally, K. Okawa, A. Iwamatsu, S. Thomas, S. Cheesman, J. Heuser, R.D. Vale, and F.J. McNally. 1998. Katanin, a microtubule-severing protein, is a novel AAA ATPase that targets to the centrosome using a WD40-containing subunit. *Cell* **93**:277-287.

Hartman, J.J. and R.D. Vale. 1999. Microtubule disassembly by ATP-dependent oligomerization of the AAA enzyme katanin. *Science* **286**:782-785.

Hayashi, S. and H.C. Wu. 1990. Lipoproteins in bacteria. *J. Bioenerg. Biomembr.* **22**:451-471.

Heald, R., R. Tournebize, T. Blank, R. Sandaltzopoulos, P. Becker, A.A. Hyman, and E. Karsenti. 1996. Self-organization of microtubules into bipolar spindles around artificial chromosomes in *Xenopus* egg extracts. *Nature* **382**:420-425.

Henderson, S.T., D. Gao, E.J. Lambie, and J. Kimble. 1994. *lag-2* may encode a signaling ligand for the GLP-1 and LIN-12 receptors of *C. elegans*. *Development* **120**:2913-2924.

Herman, R.K., J.E. Madl, and C.K. Kari. 1979. Duplications in *Caenorhabditis elegans*. *Dev. Biol.* **49**:200-219.

Hoffmann, I. and E. Karsenti. 1994. The role of cdc25 in checkpoints and feedback controls in the eukaryotic cell cycle. *J. Cell Sci.* 18:75-79.

Horvitz, H.B., S. Brenner, J. Hodgkin, and R.K. Herman. 1979. A uniform genetic nomenclature for for the nematode *Caenorhabditis elegans*. *Molecular and General Genetics* **175**:129-133.

Howell, B., N. Larsson, M. Gullberg, and L. Cassimeris. 1999. Dissociation of the tubulin-sequestering and microtubule catastrophe-promoting activities of oncoprotein 18/stathmin. *Mol. Biol. Cell* **10**:105-118.

Hoyt, M.A., L. He, K.K. Loo, and W.S. Saunders. 1992. Two *Saccharomyces cerevisiae* kinesin-related gene products required for mitotic spindle assembly. *J. Cell Biol.* **118**:109-120.

Hoyt, M.A., H. Ling, L. Totis, and W.S. Saunders. 1993. Loss of function of *Saccharomyces cerevisiae* kinesin-related *CIN8* and *KIP1* is suppressed by *KAR3* motor domain mutations. *Genetics* **135**:35-44.

Huang, X.Y. and D. Hirsh. 1989. A second trans-spliced RNA leader sequence in the nematode *Caenorhabditis elegans*. *Proc. Natl. Acad. Sci. USA* **86**:8640-8644.

Hubbard, E.J.A. and D. Greenstein. 2000. The *Caenorhabditis elegans* gonad: A test tube for cell and developmental biology. *Developmental Dynamics* **218**:2-22.

Hunter, T. 1982. Synthetic peptide substrates for a tyrosine protein kinase. *J. Biol. Chem.* **257**:4843-4848.

Hyman, A.A., D. Crétien, I. Arnal, and R.H. Wade. 1995. Structural changes accompanying GTP hydrolysis in microtubules: information from a slowly hydrolyzable analogue guanylyl-(α,β )-methylene-diphosphonate. *J. Cell Biol.* **128**:117-125.

Hyman, A.A. and E. Karsenti. 1996. Morphogenetic properties of microtubules and mitotic spindle assembly. *Cell* **84**:401-410.

Inou'e, S. 1997. The role of microtubule assembly dynamics in mitotic force generation and functional organization of living cells. *J. Struct. Biol* **118**:87-93.

Jones, A.R. and T. Schedl. 1995. Mutations in *gld-1*, a female germ cell-specific tumor suppressor gene in *Caenorhabditis elegans*, affect a conserved domain also found in Src-associated protein Sam68. *Genes Dev.* **9**:1491-1504.

Joshi, H.C., M.J. Palacios, L. McNamara, and D.W. Cleveland. 1992. γ -tubulin is a centrosomal protein required for cell cycle-dependent microtubule nucleation. *Nature* **356**:80-83.

Kadyk, L.C. and J. Kimble. 1998. Genetic regulation of entry into meiosis in *Caenorhabditis elegans. Development* **125**:1803-1813.

Kelly, W.G., S. Xu, M.K. Montgomery, and A. Fire. 1997. Distinct requirements for somatic and germline expression of a generally expressed *Caenorhabditis elegans* gene. *Genetics* **146**:227-238.

Kemphues, K.J., N. Wolf, W.B. Wood, and D. Hirsh. 1986. Two loci required for cytoplasmic organization in early embryos of *Caenorhabditis elegans. Dev. Biol.* **113**:449-460.

Kent, W.J. and A.M. Zahler. 2000. The Intronerator: exploring introns and alternative splicing in *C. elegans. Nucleic Acids Research* **28**:91-93.

Kornfeld, K. 1997. Vulval development in *Caenorhabditis elegans. Trends Genet.* **13**:55-61.

Krause, M. 1995. Transcription and Translation. In *Caenorhabditis elegans*: Modern Biological Analysis of an Organism. H.F. Epstein and D.C. Shakes, editors. Academic Press, Inc., San Diego, CA. 483-512.

Krause, M. and D. Hirsh. 1987. A trans-spliced leader sequence on actin mRNA in *C. elegans. Cell* **49**:753-761.

Kubiak, J.Z., M. Weber, and B. Maro. 1992. Cell cycle modification during the transition between meiotic M-phases in mouse oocytes. *J. Cell Sci.* **1992**:102-457.

Lockhart, A. and R.A. Cross. 1996. Kinetics and motility of the Eg5 microtubule motor. *Biochemistry* **35**:2365-2373.

Lohret, T.A., F.J. McNally, and L.M. Quarmby. 1998. A role for katanin-mediated axonemal severing during *Chlamydomonas* deflagellation. *Mol. Biol. Cell* **9**:1195-1207.

Lohret, T.A. and L.M. Quarmby. 1999. Microtubule severing. *Cell Motil. & Cytoskeleton* **43**:1-9.

Lombillo, V.A., R.J. Stewart, and J.R. McIntosh. 1995. Minus-end-directed motion of kinesin-coated microspheres driven by microtubule depolymerization. *Nature* **373**:161-164.

Mains, P.E., K.J. Kemphues, S.A. Sprunger, I.A. Sulston, and W.B. Wood. 1990. Mutations affecting the meiotic and mitotic divisions of the early *Caenorhabditis elegans* embryo. *Genetics* **126**:593-605.

Manning, B.D., J.G. Barrett, J.A. Wallace, H. Granok, and M. Snyder. 1999. Differential regulation of the Kar3p kinesin-related protein by two associated proteins, Cik1p and Vik1p. *J. Cell Biol.* **144**:1219-1233.

Matthews, L.R., P. Carter, D. Thierry-Mieg, and K. Kemphues. 1998. ZYG-9, a *Caenorhabditis elegans* protein required for microtubule organization and function, is a component of meiotic and mitotic spindle poles. *J. Cell Biol.* **141**:1159-1168.

Matthies, H.J.G., R. McDonald, L.S.B. Goldstein, and W.E. Theurkauf. 1996. Anastral meiotic spindle morphogenesis: role of the non-claret disjunctional kinesin-like protein. *J. Cell Biol.* **134**:455-464.

McKim, K.S. and A.M. Rose. 1990. Chromosome I duplications in *Caenorhabditis elegans*. *Genetics* **124**:115-132.

McNally, F.J. 1999. Microtubule dynamics: controlling split ends. *Curr. Biol* **9**:R274-R276

McNally, F.J. 2000. Capturing a ring of samurai. *Nature Cell Biology* **2**:4-7.

McNally, F.J., K. Okawa, A. Iwamatsu, and R.D. Vale. 1996. Katanin, the microtubule-severing ATPase, is concentrated at centrosomes. *J. Cell Sci.* **109**:561-567.

McNally, F.J. and S. Thomas. 1998. Katanin is responsible for the M-phase microtubule-severing activity in *Xenopus* eggs. *Molecular Biology of the Cell* **9**:1847-1861.

McNally, F.J. and R.D. Vale. 1993. Identification of katanin, an ATPase that severs and disassembles stable microtubules. *Cell* **75**:419-429.

McNally, K.P., O.A. Bazirgan, and F.J. McNally. 2000. Two domains of p80 katanin regulate microtubule severing and spindle pole targeting by p60 katanin. *J. Cell Sci.* **113**:1623-1633.

Mello, C.C., J.M. Kramer, D. Stinchcomb, and V. Ambros. 1991. Efficient gene transfer in *C. elegans*: extrachromosomal maintenance and integration of transforming sequences. *EMBO J.* **10**:3959-3970.

Meluh, P.B. and M.D. Rose. 1990. KAR3, a kinesin-related gene required for yeast nuclear fusion. *Cell* **60**:1029-1041.

Merdes, A. and D.W. Cleveland. 1997. Pathways of spindle pole formation: different mechanisms; conserved components. *J. Biol. Chem.* **138**:953-956.

Meuwissen, R.L.J., H.H. Offenberg, A.J.J. Dietrich, A. Riesewijk, M. van Iersel, and C. Heyting. 1992. A coiled-coil related protein specific for synapsed regions of meiotic prophase chromosomes. *EMBO J.* **11**:5091-5100.

Mitchison, T.J. and M. Kirschner. 1984. Dynamic instability of microtubule growth. *Nature* **312**:237-242.

Mitenko, N.L., J.R. Eisner, J.R. Swiston, and P.E. Mains. 1997. A limited number of *Caenorhabditis elegans* genes are readily mutable to dominant, temperature-sensitive maternal-effect embryonic lethality. *Genetics* **147**:1665-1674.

Montgomery, M.K., S. Xu, and A. Fire. 1998. RNA as a target of double-stranded RNA-mediated genetic interference in *Caenorhabditis elegans*. *Proc. Natl. Acad. Sci. USA* **95**:15502-15507.

Muller, H.J. 1932. Further studies on the nature and causes of gene mutations. *Proc. 6th Int. Congr. Genet.* 1:213-255.

Müller-Reichert, T., D. Crétien, F. Severin, and A.A. Hyman. 1998. Structural changes at microtubule ends accompanying GTP hydrolysis: information from a slowly hydrolyzable analogue of GTP, guanylyl(alpha,beta)methylenediphosphonate. *Proc. Natl. Acad. Sci. USA* **95**:3661-3666.

Nelson, G.A., K.K. Lew, and S. Ward. 1978. Intersex, a temperature-sensitive mutant of the nematode *C. elegans*. *Dev. Biol.* 66:386-409.

Nigon, V. and J. Brun. 1955. L'évolution des structures nucléares dans l'ovogenése de *Caenorhabditis elegans* Maupas 1900. *Chromosoma* 7:129-169.

Page, B.D., L.L. Satterwhite, M.D. Rose, and M. Snyder. 1994. Localization of the Kar3 kinesin heavy chain-related protein requires the Cik1 interacting protein. *J. Cell Biol.* **124**:507-519.

Patel, S. and M. Latterich. 1998. The AAA team: related ATPases with diverse functions. *Trends Cell Biol.* 8:65-71.

Patschinsky, T., T. Hunter, F.S. Esch, J.A. Cooper, and B.M. Sefton. 1982. Analysis of the sequence of amino acids surrounding sites of tyrosine phosphorylation. *Proc. Natl. Acad. Sci. USA* **79**:973-977.

Piperno, G. and M.T. Fuller. 1985. Monoclonal antibodies specific for an acetylated form of α-tubulin recognize the antigen in cilia and flagella from a variety of organisms. *J. Cell Biol.* **101**:2085-2094.

Rechsteiner, M. and S.W. Rogers. 1996. PEST sequences and regulation by proteolysis. *Trends in Biochemical Sciences* **21**:267-271.

Rice, S., A.W. Lin, D. Safer, C.L. Hart, N. Naber, B.O. Carragher, S.M. Cain, E. Pechatnikova, E.M. Wilson-Kubalek, M. Whittaker, E. Pate, R. Cooke, E.W. Taylor, R.A. Milligan, and R.D. Vale. 1999. A structural change in the kinesin motor protein that drives motility. *Nature* **402**:778-784.

Riddle, D.L., T. Blumenthal, B.J. Meyer, and J.R. Priess. 1997. *C. elegans* II. Cold Spring Harbor Laboratory Press, Cold Spring Harbor. 1222 pp.

Robinson, J.T., E.J. Wojcik, M.A. Sanders, M. McGrail, and T.S. Hays. 1999. Cytoplasmic dynein is required for the nuclear attachment and migration of centrosomes during mitosis in *Drosophila*. *J. Cell Biol.* **146**:597-608.

Roof, D.M., P.B. Meluh, and M.D. Rose. 1992. Kinesin-related proteins required for assembly of the mitotic spindle. *J. Cell Biol.* **118**:95-108.

Rosenbluth, R.E., C. Cuddeford, and D.L. Baillie. 1985. Mutagenesis in *Caenorhabditis elegans*. II. A spectrum of mutational events induced with 1500 R of gamma-radiation. *Genetics* **109**:493-511.

Russell, P. and P. Nurse. 1986. *cdc25*$^{+}$ functions as an inducer in the mitotic control of fission yeast. *Cell* **45**:145-153.

Sambrook, J., E.F. Fritsch, and T. Maniatis. 1989. Molecular Cloning: A Laboratory Manual. Cold Spring Harbor Laboratory Press, Cold Spring Harbor, NY.

Saunders, W.S. and M.A. Hoyt. 1992. Kinesin-related proteins required for structural integrity of the mitotic spindle. *Cell* **70**:451-458.

Savage, C., M. Hamelin, J.G. Culotti, A. Coulson, D.G. Albertson, and M. Chalfie. 1989. *mec-7* is a β-tubulin gene required for the production of 15-protofilament microtubules. *Genes Dev.* **3**:870-881.

Sawada, T. and G. Schatten. 1988. Microtubules in ascidian eggs during meiosis, fertilization, and mitosis. *Cell Motil. & Cytoskeleton* **9**:219-230.

Sawin, K.E., K. LeGuellec, M. Philippe, and T.J. Mitchison. 1992. Mitotic spindle organization by a plus-end-directed microtubule motor. *Nature* **359**:540-542.

Sawin, K.E. and T.J. Mitchison. 1991. Poleward microtubule flux in mitotic spindles assembled *in vitro*. *J. Cell Biol.* **112**:941-954.

Sawin, K.E. and T.J. Mitchison. 1995. Mutations in the kinesin-like protein Eg5 disrupting localization to the mitotic spindle. *Proc. Natl. Acad. Sci. USA* 92:4289-4293.

Schatten, G. 1994. The centrosome and its mode of inheritance: The reduction of the centrosome during gametogenesis and its restoration during fertilization. *Dev. Biol.* **165**:299-335.

Schedl, T. 1997. Developmental genetics of the germ line. In *C. elegans* II. D.L. Riddle, T. Blumenthal, B.J. Meyer, and J.R. Priess, editors. Cold Spring Harbor Press, Cold Spring Harbor. 241-269.

Sharp, D.J., K.L. McDonald, H.M. Brown, H.J. Matthies, C.E. Walczak, R.D. Vale, T.J. Mitchison, and J.M. Scholey. 1999. The bipolar kinesin, KLP61F, cross-links microtubules within interpolar microtubule bundles of *Drosophila* embryonic mitotic spindles. *J. Cell Biol.* **144**:125-138.

Shumway, S.D., M. Maki, and S. Miyamoto. 1999. The PEST domain of IκBα is necessary and sufficient for *in vitro* degradation by μ-calpain. *J. Biol. Chem.* **274**:30874-30881.

Simon, J.R. and E.D. Salmon. 1990. The structure of microtubule ends during the elongation and shortening phases of dynamic instability examined by negative-stain electron microscopy. *J. Cell Sci.* **96**:571-582.

Smirnov, M.N., V.N. Smirnov, E.I. Budowsky, S.G. Inge-Vechtomov, and N.G. Serebrjakov. 1967. Red pigment of adenine-deficient yeast *Saccharomyces cerevisiae. Biochem. Biophys. Res. Commun.* **27**:299-304.

Srayko, M., D.W. Buster, O.A. Bazirgan, F.J. McNally, and P.E. Mains. 2000. MEI-1/MEI-2 katanin-like microtubule severing activity is required for *Caenorhabditis elegans* meiosis. *Genes Dev.* **14**:1072-1084.

Stearns, T. and M. Kirschner. 1994. *In vitro* reconstitution of centrosome assembly and function: The central role of γ-tubulin. *Cell* **76**:623-637.

Steuer, E.R., L. Wordeman, T.A. Schroer, and M.P. Sheetz. 1990. Localization of cytoplasmic dynein to mitotic spindles and kinetchores. *Nature* **345**:266-268.

Strome, S. and W.B. Wood. 1983. Generation of asymmetry and segregation of germ-line granules in early *C. elegans* embryos. *Cell* **35**:15-25.

Tabara, H., A. Grishok, and C.C. Mello. 1998. RNAi in C. elegans: soaking in the genomic sequence. *Science* **282**:430-431.

Theurkauf, W.E. and R.S. Hawley. 1992. Meiotic spindle assembly in *Drosophila* females: behaviour of nonexchange chromosomes and the effects of mutations in the *nod* kinesin-like protein. *J. Cell Biol.* **116**:1167-1180.

Tilney, L.G., J. Bryan, D.J. Bush, K. Fujiwara, M.S. Mooseker, D.B. Murphy, and D.H. Snyder. 1973. Microtubules: evidence for 13 protofilaments. *J. Cell Biol.* **59**:267-275.

Tournebize, R., R. Heald, and A.A. Hyman. 1997. Role of chromosomes in assembly of meiotic and mitotic spindles. *Progress in Cell Cycle Research* **3**:271-284.

Tran, P.T., P. Joshi, and E.D. Salmon. 1997. How tubulin subunits are lost from the shortening ends of microtubules. *J. Struct. Biol* **118**:107-118.

Vale, R.D. 1991. Severing of stable microtubules by a mitotically activated protein in *Xenopus* egg extracts. *Cell* **64**:827-839.

Vernos, I. and E. Karsenti. 1996. Motors involved in spindle assembly and chromosome segregation. *Curr. Biol* **8**:4-9.

Vernos, I., J. Raats, T. Hirano, J. Heasman, E. Karsenti, and C. Wylie. 1995. Xklp1, a chromosomal *Xenopus* kinesin-like protein essential for spindle organization and chromosome positioning. *Cell* **81**:117-127.

Villeneuve, A.M. 1994. A *cis*-acting locus that promotes crossing over between X chromosomes in *Caenorhabditis elegans*. *Genetics* **136**:887-902.

Walczak, C.E. 2000. Microtubule dynamics and tubulin interacting proteins. *Curr. Opin. Cell Biol.* **12**:52-56.

Walczak, C.E. and T.J. Mitchison. 1996a. Kinesin-related proteins at mitotic spindle poles: Function and regulation. *Cell* **85**:943-946.

Walczak, C.E., T.J. Mitchison, and A. Desai. 1996b. XKCM1: A *Xenopus* kinesin-related protein that regulates microtubule dynamics during mitotic spindle assembly. *Cell* **84**:37-47.

Walczak, C.E., I. Vernos, T.J. Mitchison, E. Karsenti, and R. Heald. 1998. A model for the proposed roles of different microtubule-based motor proteins in establishing spindle bipolarity. *Curr. Biol* **8**:903-913.

Walker, R.A., E.D. Salmon, and S.A. Endow. 1990. The *Drosophila claret* segregation protein is a minus-end directed motor molecule. *Nature* **347**:780-782.

Wallon, G., J. Rappsilber, M. Mann, and L. Serrano. 2000. Model for stathmin/Op18 binding to tubulin. *EMBO J* **19**:213-222.

Wang, S.Z. and R. Adler. 1995. Chromokinesin: a DNA-binding, kinesin-like nuclear protein. *J. Cell Biol.* **128**:761-768.

Weisman, L.S., R. Bacallao, and W. Wickner. 1987. Multiple methods of visualizing the yeast vacuole permit evaluation of its morphology and inheritance during the cell cycle. *J. Cell Biol.* **105**:1539-1547.

White-Cooper, H., L. Alphey, and D.M. Glover. 1993. The *cdc25* homologue *twine* is required for only some aspects of the entry into meiosis in *Drosophila*. *J. Cell Sci.* **110**:1035-1044.

Williams, B.D. 1995. Genetic Mapping. In *Caenorhabditis elegans*: Modern Biological Analysis of an Organism. H.F. Epstein and D.C. Shakes, editors. Academic Press, Inc., San Diego, CA. 659

Winey, M. and B. Byers. 1993. Assembly and functions of the spindle pole body in budding yeast. *Trends Genet.* **9**:300-304.

Wolf, S.G., E. Nogales, M. Kikkawa, D. Gratzinger, N. Hirokawa, and K.H. Downing. 1996. Interpreting a medium resolution model of tubulin: Comparison of zinc sheet and microtubule structure. *J. Mol. Biol.* **262**:485-501.

Wood, W.B. 1988. The Nematode *Caenorhabditis elegans*. Cold Spring Harbor Laboratory Press, Cold Spring Harbor, NY. 667 pp.

Yen, T.J., G. Li, B.T. Schaar, I. Szilak, and D.W. Cleveland. 1992. CENP-E is a putative kinetochore motor that accumulates just before mitosis. *Nature* **359**:536-539.

Zetka, M.C., I. Kawasaki, S. Strome, and F. Müller. 1999. Synapsis and chiasma formation in *Caenorhabditis elegans* require HIM-3, a meiotic chromosome core component that functions in chromosome segregation. *Genes Dev.* **13**:2258-2270.

Zollman, S., D. Godt, G.G. Prive, J.L. Couderc, and F.A. Laski. 1994. The BTB domain, found primarily in zinc finger proteins, defines an evolutionarily conserved family that includes several developmentally regulated genes in *Drosophila*. *Proc. Natl. Acad. Sci. USA* **91**:10717-10721.